

ANNUAL REPORT 2015

理论有机化学与功能分子

教育部重点实验室

工作年报

**Key Laboratory of Theoretical Organic Chemistry
and Functional Molecule, Ministry of Education**

理论有机化学与功能分子
教育部重点实验室工作年报
(2015年)

通讯地址：湖南科技大学理论有机化学与功能分子教育部重点
实验室，411201

联系电话：0731-58290097

目 录

一、实验室概况	1
二、学术交流情况	8
三、开放基金评审	11
四、科普传播	12
五、2015 年发表的主要研究论文	12
1. 代表性论文目录	12
2. 代表性论文首页	20

一、实验室概况

湖南科技大学理论化学与分子模拟省部共建教育部重点实验室，于 2008 年 11 月经教育部批准立项建设（教育部科技函 [2008]153 号），于 2013 年 7 月通过教育部验收。

实验室主要以《国家中长期科学和技术发展规划纲要》为指导，面向《国家优先发展与重点支持领域》中的环保、新材料与药物等重大战略需求，聚焦环境治理、功能分子材料、药物创制与开发及其分子构效关系的研究，将合成的功能分子材料及药物重点用于环境治理，助推湖南医药产业升级。坚持理论与应用相结合，注重学科交叉，立足地方，瞄准学科前沿，形成四个稳定并具特色的研究方向：分子构效关系，资源环境功能分子材料，光电功能分子材料，生物活性分子与药物。注重微观与宏观相结合、理论与实践相结合，在提升知识创新能力和学术水平的同时，为地方经济建设服务。

通过近 6 年来的建设与发展，实验室已形成一支结构比较合理、团结协作、具有多学科研究背景的学术队伍。现有研究人员 51 人，其中教授 22 人，副高职称人员 13 人，博士 49 人，博士生导师 4 人，硕士生导师 38 人，国务院政府特殊津贴专家 2 人，教育部新世纪人才 1 人，湖南省跨世纪学术和技术带头人 1 人，湖南省 121 人才工程入选者 3 人，湖南省普通高校学科带头人 2 人。外聘湖南科技大学“湘江学者计划”特聘教授 2 人。

6年来实验室新增科研项目 173 项，其中国家级项目 49 项（国家自然科学基金项目 47 项、国际合作重点项目 1 项、国家科技支持计划子课题 1 项）、省部级项目 52 项、横向项目 26 项，累计科研经费 6700 余万元。在 *Biomaterials*, *Biosens. Bioelectron.*, *Anal. Chem.*, *Chem. Comm.*, *J. Phys. Chem. B*, *Org. Lett.*, *J.*

*Org. Chem.*等期刊上共发表论文 564 篇,其中被SCI、EI、ISTP等收录的论文 321 篇,出版专著 4 部、教材 2 部。获发明专利 45 项(授权),省部级科研奖励 18 项。获湖南省高校科技创新团队 1 个。

实验室面积达 5000 平方米,拥有液质联用仪、核磁共振波谱仪(500 MHz)、X-射线单晶衍射仪、扫描电镜、微量热仪、原子力显微镜、X-粉末衍射仪、圆二色光谱仪、气质联用仪、液相色谱仪等一批先进大型仪器,总值达 4500 余万元。

在实验室的大力支撑下,获批矿业工程博士点和博士后科研流动站。实验室依托化学一级硕士学位授权点、应用化学和化学工艺二级硕士学位授权点进行研究生招生与培养,6 年来共招收硕士研究生 291 人,240 人获得硕士学位。同时还与厦门大学、中南大学、湘潭大学等联合培养研究生,招收博士生 2 人,与中南大学联合博士生 1 人。实验室共有 8 个相关本科专业:化学、无机非金属材料化学、材料化学、应用化学、化工工艺、环境工程、制药工程、能源化工程等,其中化学为国家第一类特色专业,材料化学为省级特色专业。拥有有机化学省级优秀教学团队 1 个,省级精品课程 3 门(有机化学、物理化学和量子化学)。形成了“夯实基础,接触前沿,以培养创新能力为目标”的人才培养模式,确保人才培养质量,获省级教学成果奖 2 项。

1. 实验室各研究单元的构成

理论化学与功能分子教育部重点实验室由分子构效关系，资源环境功能分子材料，光电功能分子材料，生物活性分子与药物4个研究方向构成，重点实验室学术带头人和学术骨干名单见下表

实验室学术带头人和学术骨干一览表

研究方向	姓名	出生年	获最高学位时间	专业技术职务
分子构效关系	曹晨忠	1957	2004.07(博士)	教授/博士生导师
	易平贵	1961	2000.03(博士)	教授/博士生导师
	曾荣今	1963	2006.12(硕士)	教授/硕士生导师
	周再春	1974	2007.07(博士)	副教授/硕士生导师
	袁华	1976	2007.07(博士)	副教授/硕士生导师
资源环境功能分子材料	刘立华	1969	2006.07(博士)	教授/硕士生导师
	冯涛	1957	1999.07(博士)	教授/博士生导师
	戴财胜	1964	2000.07(博士)	教授/硕士生导师
	曾坚贤	1970	2008.07(博士)	教授/硕士生导师
	周虎	1981	2009.07(博士)	副教授/硕士生导师
光电功能分子材料	黄昊文	1969	2004.08(博士)	教授/硕士生导师
	田俐	1973	2009.07(博士)	教授/硕士生导师
	易清风	1963	2001.07(博士)	教授/硕士生导师
	龙云飞	1969	2007.12(博士)	教授/硕士生导师
	陈建	1980	2009.06(博士)	副教授/硕士生导师
生物活性分子与药物	唐子龙	1967	2004.08(博士)	教授/硕士生导师
	谢文林	1967	2003.06(博士)	教授/硕士生导师
	李筱芳	1972	2003.06(博士)	教授/硕士生导师
	周智华	1973	2007.06(博士)	教授/硕士生导师
	于贤勇	1975	2005.07(博士)	教授/硕士生导师

2. 实验室主任及管理人员

实验室主任：曹晨忠

实验室常务副主任：唐子龙

学术秘书：于贤勇，周再春

室务会成员：曹晨忠，易平贵，唐子龙，曾荣今，易清风，曾云龙，于贤勇

3. 实验室学术委员会组成人员

学术委员会主任：郭庆祥

学术委员会副主任：易平贵

学术委员会委员(按姓氏拼音排序):

曹晨忠，方维海，郭庆祥，胡常伟，黄培强，刘又年，潘远江，唐子龙，吴海龙，吴水珠，肖文精，杨楚罗，杨松，杨新玲，易平贵，易清风，朱晓晴。

4. 实验室2015年取得成绩

4.1 获得的科研项目

新增各类科研项目 23 项，其中国家自然科学基金课题 12 项、省部级课题 7 项、横向课题 4 项；累计经费 838 万元，学校配套经费 331.6，合计 1169.6 万元。

序号	项目下达编号	项目、课题名称	项目来源	项目起讫时间	科研经费(万元)	负责人
1	21472040	有机化合物液态导热率定量构效关系研究	国家自然科学基金面上项目	2015.01-2018.12	82(+35.4)	刘万强
2	21471052	可控制备还原氧化石墨烯-咔咯纳米复合材料及电化学传感应用	国家自然科学基金面上项目	2015.01-2018.12	80(+35)	邓克勤
3	41472328	锰矿区土-水界面重金属污染流迁移转化机理及其过程数学模型研究	国家自然科学基金面上项目	2015.01-2018.12	92(+37.4)	任伯帜
4	21475040	基于近红外量子点复合物的高灵敏度真菌毒素生物传感器	国家自然科学基金面上项目	2015.01-2018.12	85(+36)	曾云龙
5	51478182	基于半焦的城市污泥调质与深度脱水机理及污泥煤浆制备方法的研究	国家自然科学基金面上项目	2015.01-2018.12	84(+35.8)	戴财胜
6	21406058	纳米金/多级孔磷酸铝-氧化硅(APO-SiO ₂)复合材料制备及催化环己烷选择氧化研究	国家自然科学基金青年项目	2015.01-2017.12	25(+19)	陈丽娟
7	21402047	嘧啶环偶极两端取代基交换对嘧啶类化合物物理化学性能的影响规律研究	国家自然科学基金青年项目	2015.01-2017.12	25(+19)	袁华
8	51443002	吸热与润滑功能树脂的设计、制备及其性能调控	国家自然科学基金主任基金项目	2015.01-2015.12	15(+15)	周虎
9	21445008	新型易功能化金纳米簇的设计合成及多元重金属离子检测	国家自然科学基金主任基金项目	2015.01-2015.12	10(+10)	陈述
10	21402048	芳基格氏试剂与 N-烯基酰胺的 N-芳基化反应及其机理研究	国家自然科学基金青年项目	2015.01-2017.12	25(+19)	焦银春

11	21401055	多孔功能 MOFs 材料的设计合成与氢气、二氧化碳气体吸附性能研究	国家自然科学基金青年项目	2015.01-2017.12	30 (+21)	汪朝旭
12	51408215	DON 荧光组分与 DON 含量、N-DBPs 的相关性分析及优化混凝过程研究	国家自然科学基金青年项目	2015.01-2017.12	25 (+19)	朱国成
13	2015JJ4026	以拓扑异构酶为靶含噻唑环的吡啶酮新型衍生物的合成及抗肿瘤活性研究	湖南省自然科学基金项目	2015.01-2017.12	5 (+2)	谢文林
14	2015JJ6035	YBCO 复合体系的温室铁磁控	湖南省自然科学基金项目	2015.01-2017.12	5 (+2)	朱中华
15	2015RS4044	湖湘青年人才项目	湖南省科技厅项目	2015.05-2017.12	10	周虎
16	湘团联 [2015]13 号	湖湘青年英才项目	湖南省委组织部项目	2015.05-2018.05	10	周虎
17	15A061	印迹聚合物/陶瓷复合膜的制备、表征及其对稀有金属离子的识别行为与机理	湖南省教育厅重点项目	2015.09-2018.12	6 (+2)	曾圣贤
18	15B081	荧光金纳米簇智能杂化材料的可控制备与荧光调控	湖南省教育厅优秀青年项目	2015.09-2017.12	4 (+2)	廖博
19	15B080	富钙铝矿物蠕虫状橄榄石集合体和球粒的氧同位素组成特征研究	湖南省教育厅优秀青年项目	2015.09-2017.12	4 (+2)	戴德求
20	D11518	聚乙烯醇缩醛基苯胺席夫碱的合成研究	湖南省湘维有限公司	2015.03-2017.03	150	唐子龙
21	D11554	电石渣/粉煤灰协同资源化利用技术开发研究	湖南省湘维有限公司	2015.05-2016.05	45	伍泽广
22	D11574	氧化聚乙烯蜡微乳液的产业化研究	南雄市连邦化工石油科技有限公司	2015.09-2016.09	16	刘清泉
23	D115B8	一种优化的依达拉奉合成方法	吉林省博大制药有限公司	2015.12-2031.09	5	于贤勇

4.2 发表论文

2015年本实验室共发表论文 64 篇，其中被SCI、EI收录 51 篇。

4.3 专利授权或申请

2015年本实验室共授权 5 项发明专利，申请 3 项发明专利。

序号	专利名称	专利号	专利类型	授权或申请时间	第一完成人
1	一种检测汞离子的两亲性聚合物纳米粒子、制备方法及应用	ZL201410061992.9	发明专利	2015-12-30	陈建
2	具有杀菌活性的 2, 3-二芳基-1, 3-萘并噁嗪类化合物	ZL201410251185.3	发明专利	2015-12-02	唐子龙
3	一种无膜的直接硼氢化钠燃料电池及其制造	ZL201410010905.7	发明专利	2015-08-19	易清风
4	一种无膜的直接肼燃料电池及其制造方法	ZL201410010906.1	发明专利	2015-11-04	易清风
5	利用含铁废水制备冰晶石并产氯化硫酸铝铁的方法	ZL201310076561.5	发明专利	2015-04-01	曾荣今
6	一种水热制备钒酸铈纳米线束的方法	201510956562.8	发明专利	2015-12-17	田俐
7	一种电石渣与废硫酸制备硫酸钙晶须的方法	201510941518.X	发明专利	2015-12-15	伍泽广
8	异相成核水热法制备碳量子点及用于去除水中重金属离子的方法	2015108112743	发明专利	2015-11-23	曾云龙

4.4 学科建设与人才培养

2015年本实验室共招收 41 名硕士研究生，33 名研究生获得硕士学位。

4.5 获奖情况

2015获省部级以上科研成果奖 2 项。

序号	项目名称	完成人	单位	获奖时间	获奖名称、等级	发证机关
1	高效水处理材料及新型高级氧化技术研究基础	郑怀礼、李风亭、赵纯、张冰如、张智、吴胜举、张鹏、吴一楠、朱国成	湖南科技大学	2015.02	教育部高等学校自然科学二等奖	教育部
2	基于能力培养的化工类专业大学生创新训练体系的构建与实践	申少华、周虎、胡忠于、李国斌、谢文林、岳明	湖南科技大学	2015.12	全国煤炭行业教育教学成果二等奖	中国煤炭教育协会

二、学术交流情况

2015 年主办学术会议 1 次。

学术会议名称	时间	参加总人数
功能分子高层论坛以及 2015 年湖南精细化学品生产及应用研讨会	2015-10-24	100

2015 年实验室人员参加国内外学术会议统计情况如下

参会人	时间	地点	会议名称	主（承）办单位
龙云飞	2015-05-08	华中师范大学	第十二届全国分析化学年会	中国化学会和国家自然科学基金委、华中师范大学
周再春	2015-07-28	东北师范大学	第九届全国有机化学学术会议	中国化学会、东北师范大学、中国科学院长春应用化学研究所
唐子龙	2015-07-28	东北师范大学	第九届全国有机化学学术会议	中国化学会、东北师范大学、中国科学院长春应用化学研究所
谢文林	2015-07-28	东北师范大学	第九届全国有机化学学术会议	中国化学会、东北师范大学、中国科学院长春应用化学研究所
赵云辉	2015-07-28	东北师范大学	第九届全国有机化学学术会议	中国化学会、东北师范大学、中国科学院长春应用化学研究所

刘立华	2015-08-26	北京五洲大酒店	The International Conference on Clean Water and Air & Soil	The international Water,Air, and Soil Conservation society
黄昊文	2015-10-24	湖南科技大学	功能分子高层论坛以及 2015 年湖南精细化学品生产及应用研讨会	湖南省化学化工学会精细化专业委员会、理论有机化学与功能分子教育部重点实验室
周再春	2015-10-24	湖南科技大学	功能分子高层论坛以及 2015 年湖南精细化学品生产及应用研讨会	湖南省化学化工学会精细化专业委员会、理论有机化学与功能分子教育部重点实验室
张少伟	2015-10-24	湖南科技大学	功能分子高层论坛以及 2015 年湖南精细化学品生产及应用研讨会	湖南省化学化工学会精细化专业委员会、理论有机化学与功能分子教育部重点实验室
唐子龙	2015-10-24	湖南科技大学	功能分子高层论坛以及 2015 年湖南精细化学品生产及应用研讨会	湖南省化学化工学会精细化专业委员会、理论有机化学与功能分子教育部重点实验室
易平贵	2015-10-24	湖南科技大学	功能分子高层论坛以及 2015 年湖南精细化学品生产及应用研讨会	湖南省化学化工学会精细化专业委员会、理论有机化学与功能分子教育部重点实验室
曹晨忠	2015-10-24	湖南科技大学	功能分子高层论坛以及 2015 年湖南精细化学品生产及应用研讨会	湖南省化学化工学会精细化专业委员会、理论有机化学与功能分子教育部重点实验室

于贤勇	2015-10-24	湖南科技大学	功能分子高层论坛以及 2015 年湖南精细化学品生产及应用研讨会	湖南省化学化工学会精细化专业委员会、理论有机化学与功能分子教育部重点实验室
谢文林	2015-10-24	湖南科技大学	功能分子高层论坛以及 2015 年湖南精细化学品生产及应用研讨会	湖南省化学化工学会精细化专业委员会、理论有机化学与功能分子教育部重点实验室
汤建庭	2015-10-24	湖南科技大学	功能分子高层论坛以及 2015 年湖南精细化学品生产及应用研讨会	湖南省化学化工学会精细化专业委员会、理论有机化学与功能分子教育部重点实验室
焦银春	2015-10-24	湖南科技大学	功能分子高层论坛以及 2015 年湖南精细化学品生产及应用研讨会	湖南省化学化工学会精细化专业委员会、理论有机化学与功能分子教育部重点实验室
曹佳民	2015-10-24	湖南科技大学	功能分子高层论坛以及 2015 年湖南精细化学品生产及应用研讨会	湖南省化学化工学会精细化专业委员会、理论有机化学与功能分子教育部重点实验室

2015 年来访人员学术报告情况

姓名	职称	单位	报告题目	时间
肖文精	教授	华中师范大学化学学院	含氮杂环合成中的硫叶立德化学	2015-01-22
唐少华	教授	国家知识产权局专利局化学发明审查部	专利申请与答复方面	2015-03-19
裴勇	教授	湘潭大学	原子团簇结构和性质的模拟理论	2015-04-02
尹笃林	教授	湖南师范大学	湖南石化产业发展的现状与展望——基于新四化到五化的点	2015-04-03

			滴体会	
欧晓明	教授	湖南省化工研究院	从农药代谢降解论新农药创制	2015-04-03
张少伟	博士	南开大学	基于有机多羧酸配体构筑的金属-有机框架的合成、结构及性质研究	2015-04-23
邓泽平	博士	湖南华腾公司、美国休斯敦大学	生物医药 CRO 产业的经济规模及产业模式	2015-04-24
丁黎明	研究员	国家纳米科学中心	第三代太阳电池	2015-06-02
陈仕国	教授	深圳大学	安全持久抗菌整理剂及其在纺织品上的应用	2015-06-16
刘又年	教授	中南大学	分子自组装及功能化	2015-06-24
朱卫国	教授	湘潭大学	有机光伏材料及其太阳能电池	2015-06-24
彭丽芬	博士	日本冈山理科大学	多官能团化的炔化合物的合成及其在有机材料中的应用: 双消除反应和 Ph ₂ P(O)保护基方法	2015-07-03
Andrew Hursthouse	教授	英国西苏格兰大学	Water Treatment in the Management of Contaminated Land and Industrial Wastes	2015-10-12
曾程初	教授	北京工业大学	Electrochemically catalytic oxidation: Fundamental and Application in Organic Synthesis	2015-11-10
马於光	教授	华南理工大学发光材料与器件国家重点实验室	“热激子”材料原理与进展	2015-11-13
徐昕	教授	厦门大学	金属苯为什么是非平面的	2015-12-25

三、开放基金评审

2015年度共评审开放基金课题 9 项, 累计经费 10 万元。

2015年度理论化学与功能分子教育部重点实验室开放基金

序号	姓名	题 目	经费/万元	申报人所在单位
1	谭华	单核及双核环金属铂(II)配合物近红外发光材料的合成及性能研究	1	湘潭大学

2	许志峰	2-(2-羟甲基苯基氨基)乙酰芳胺及其金属配合物的合成与性能研究	1.5	衡阳师范学院
3	刘秋华	单氧杂核修饰卟啉对低价铜(I)离子的电荷效应	1.5	中南大学
4	石顺存	污水生化处理有机物去除率与动力学参数间关系的研究	1	湖南科技大学
5	曹朝曦	取代基电子效应对含羟基席夫碱衍生物及其配合物的性质研究	1	湖南科技大学
6	李筱芳	基于 N-错位卟啉的大 π 共轭体系的合成及其性质研究	1	湖南科技大学
7	于贤勇	抗肿瘤糖肽基过氧化钒配合物合成与性质研究	1	湖南科技大学
8	陈建	基于 FRET 的聚合物量子点构建与硫离子比率荧光检测	1	湖南科技大学
9	汤建庭	高效介孔 TiO ₂ 光催化剂的可控合成	1	湖南科技大学

四、科普传播

2015.06.05 - 2015.06.07 (3天) 和 2015.10.10 - 2015.10.12 (3天) 作为实验室科普固定开放日, 共接收 100 余人来实验室参观学习。本年度科普宣讲, 累计参与公众 100 余人次; 发表科普文章 1 篇。

五、2015年发表的主要研究论文

理论化学与功能分子教育部重点实验室2015年所发代表性论文目录

1. Chunxiang Li, Xiyang Qiu, Zhaohui Hou, Keqin Deng. A dumbbell probe-mediated rolling circle amplification strategy for highly sensitive transcription factor detection. *Biosensors & Bioelectronics*, 2015, 64, 505-510.
2. Shu Chen, JianTang, Yangfang Kuang, Lili Fu, Fangfang Ma, Yuanyuan Yang, Guanfan Chen, Yunfei Long. Selective deposition of HgS at the corner sites of triangular silver nanoprism and its tunable LSPR for colorimetric Hg²⁺ detection. *Sensors & Actuators B Chemical*, 2015, 221, 1182-1187.

3. Shenna Chen, Qian Zhao, Lingyang Zhang, Linqian Wang, Yunlong Zeng, Haowen Huang. Combined detection of breast cancer biomarkers based on plasmonic sensor of gold nanorods. *Sensors & Actuators B Chemical*, 2015, 221, 1391-1397.
4. Jian Chen, Ya Li, Weibang Zhong, Qingyang Hou, Hong Wang, Xiang Sun, Pinggui Yi. Novel fluorescent polymeric nanoparticles for highly selective recognition of copper ion and sulfide anion in water. *Sensors & Actuators B Chemical*, 2015, 206, 230-238.
5. Zaichun Zhou, Xiaochun Zhou, Qiuhua Liu, Xi Zhang, Haomin Liu. Fixation of Zinc (II) Ion to dioxygen in a highly deformed porphyrin: implications for the oxygen carrier mechanism of distorted heme. *Organic Letters*, 2015, 17, 4078-4081.
6. Anping Tang, Donghua He, Zeqiang He, Guorong Xu, Haishen Song, Ronghua Peng. Electrochemical performance of LiMnBO₃/C composite synthesized by a combination of impregnation and precipitation followed by annealing. *Journal of Power Sources*, 2015, 275, 888-892.
7. Huiyan Kuang, Xiaoyun Yuan, Lei Feng, Haowen Huang, Chunran Tang, Keqin Deng, Yunlong Zeng. Simple and sensitive detection for trace chromium (VI) using albumin as fluorescence probes. *Journal of the Chilean Chemical Society*, 2015, 60, 2840-2842.
8. Lingyang Zhang, Shenna Chen, Qian Zhao, Haowen Huang. Carbon dots as a fluorescent probe for label-free detection of physiological potassium level in human serum and red blood cells. *Analytica Chimica Acta*, 2015, 880, 130-135.
9. Jingai Zhang, Xiaojing Ma, Wenqian Yang, Ying Zhou, Xufu Tang, Yan Zou, Hui Li, Jingjing He, Shimin Xie, Yunhui Zhao, Fengping Liu, Wenlin Xie. Synthesis and Biological Evaluation of Kojic Acid Derivatives Containing 1, 2, 4-Triazole As Potent Tyrosinase inhibitors. *Chemical Biology and Drug Design*, 2015, 86, 1087-1092.
10. Bin Liu, Xiaofang Li, Marcin Stepień, Piotr J. Chmielewski. Towards norcorrin: hydrogenation chemistry and the heterodimerization of nickel (II) norcorrole. *Chemistry - A European Journal*, 2015, 21, 7790-7797.
11. Zhihua Zhou, Siliang He, Tianlong Huang, Cheng Peng, Hu Zhou, Qingquan Liu, Wennan Zeng, Lihua Liu, Huihua Huang, Liujiào Xiang, Hua Yan. Preparation of gelatin/hyaluronic

- acid microspheres with different morphologies for drug delivery. *Polymer Bulletin*, 2015, 72, 713-723.
12. Zihua Zhou, Huihua Huang, Tianlong Huang, Cheng Peng, Hu Zhou, Qingquan Liu, Wennan Zeng, Lihua Liu, Dafu Cao, Siliang He, Liujiào Xiang, Hua Yan. Synthesis and characterization of novel maleated poly (D, L-lactide-co-glycolide) by direct melt copolymerization. *Polymer Bulletin*, 2015, 72, 1531-1543.
 13. Chaotun Cao, Baiying Wei, Chenzhong Cao. Effect of substituents on the NMR and UV spectra of N-(4-substituted benzylidene) anilines and N-(4-substituted benzylidene) cyclohexylamines. *Acta Physico-Chimica Sinica*, 2015, 31, 204-210.
 14. Jianting Tang, Datang Li, Zhaoxia Feng, Chengyun Long. HgI₂: A novel photocatalyst with high performance in degradation of rhodamine B dyes under visible-light irradiation. *Journal of Alloys & Compounds*, 2015, 653, 310-314.
 15. Qingquan Liu, Mingda Wu, Yinxiang Duan, Baoli Ou, Bo Liao, Shaohua Shen, Hu Zhou. Functional block copolymers from controlled radical and ring opening polymerization. *Polymer Science*, 2015, 57, 387-394.
 16. Jianxian Zeng, Huajun Chen, Xinke Yuan, Xie Yu. A ion-imprinted chitosan/Al₂O₃ composite material for selective separation of copper(II). *Desalination & Water Treatment*, 2015, 55, 1229-1239.
 17. Chenzhong Cao, Yakun Bi, Chaotun Cao. Effect of substituents on reduction potential of para-disubstituted N-benzylidenebenzenamine derivatives. *Chinese Journal of Organic Chemistry*, 2015, 35, 1302-1309.
 18. Leilei Yang, XiaoLian Hu, Zhenqiang Tang, Xiaofang Li. Synthesis of tetrahydrothiophene and thiophene-fused porphyrin. *Chemistry Letters*, 2015, 44, 1515-1517.
 19. Jian Chen, Fuhua Huang, Hong Wang, Ya Li, Shengli Liu, Pinggui Yi. One-pot preparation of multicolor polymeric nanoparticles with high brightness by single wavelength excitation. *Journal of Applied Polymer Science*, 2015, 132, 41492.

20. Bin Liu, Jie zhang, MengTing Wang, Rongjin Zeng, Xiaofang Li. Synthesis of Novel Spiro[Cyclopropane-Pyrrolizin] Derivatives via Mg-Mediated Conjugate Addition of Bromoform. *Research on Chemical Intermediates*, 2015, 41, 2345-2352.
21. Jian Chen, Weibang Zhong, Ying Tang, Zhan Wu, Ya Li, Pinggui Yi, Jianhui Jiang. Amphiphilic BODIPY-based photoswitchable fluorescent polymeric nanoparticles for rewritable patterning and dual-color cell imaging. *Macromolecules*, 2015, 48, 3500-3508.
22. Jianting Tang, Beibei Song, Qian Deng, Hongchuan Xin. Facile hydrothermal-carbonization approach to carbon-modified BiVO₄ composites with enhanced photocatalytic activity. *Materials Science in Semiconductor Processing*, 2015, 35, 90-95.
23. Zhongzhong Cao, Chaotun Cao, Chenzhong Cao. Comparison of the ¹³C (C=N) chemical shifts of substituted N-(phenyl-ethylene)-anilines and substituted N-(benzylidene)-anilines. *Journal of Physical Organic Chemistry*, 2015, 28, 564-569.
24. Guanfan Chen, Mengzhuo Tang, Rongjin Zeng, Wanqiang Liu, Chenzhong Cao. Group effect on ionization potential for mono-substituted aliphatic compounds. *Journal of Physical Organic Chemistry*, 2015, 28, 612-616.
25. Guorong Xu, Jinjin Shi, Wenhao Dong, Ya Wen, Xiangping Min, AnpingTang. One-pot synthesis of a Ni-Mn₃O₄ nanocomposite for supercapacitors. *Journal of Alloys & Compounds*, 2015, 630, 266-271.
26. Zilong Tang, Zanwen Xia, Shuhong Chang, Zhaoxu Wang. Synthesis and fungicidal activity of novel 2-aryl-3-(1,3,4-thiadiazolyl)-6(8)-methyl-1,3-benzoxazines. *Bioorganic & Medicinal Chemistry Letters*, 2015, 25, 3378-3381.
27. Hu Zhou, Ruiping Xun, Kejian Wu, Zhihua Zhou, Bin Yu, Youxin Tang, Ning Li. Polyurethane membrane with temperature- and pH-Controllable permeability. *Macromolecular Research*, 2015, 23, 94-99.
28. Keqin Deng, Chunxiang Li, Xiyang Qiu, Jianhong Zhou, Zhaohui Hou. Electrochemical Preparation, Characterization and Application of Electrodes Modified with Nickel–Cobalt Hexacyanoferrate/Graphene Oxide–Carbon Nanotubes. *Journal of Electroanalytical Chemistry*, 2015, 755, 197-202.

29. Lili Fu, Yuan Xiong, Shu Chen and Yunfei Long. Trace Copper Ion Detection by The Suppressed Decolorization of Chromotrope 2R Complex. *Analytical Methods*, 2015, 7, 266-270.
30. Guanfan Chen, Xiangsi Wu, Chenzhong Cao, Fengping Liu, Rongjin Zeng, Wanqiang Liu. A QSPR correlation on the ^{13}C NMR chemical shifts of bridge carbons for different series of aromatic Schiff bases. *Magnetic Resonance in Chemistry*, 2015, 53, 172-177.
31. Guorong Xu, Ya Wen, Xiangping Min, Wenhao Dong, Anping Tang, Haishen Song. Construction of MnO_2 /3-dimensional porous crack N_i for high-performance supercapacitors. *Electrochimica Acta*, 2015, 186, 133-141.
32. Keqin Deng, Chunxiang Li, Xiyang Qiu, Jianhong Zhou, Zhaohui Hou. Synthesis of cobalt hexacyanoferrate decorated graphene oxide/carbon nanotubes-COOH hybrid and their application for sensitive detection of hydrazine. *Electrochimica Acta*, 2015, 174, 1096-1103.
33. Jiayin Li, Min Yang, Zhaoxia Feng, Fujun Lan, Chunlin Teng, Datang Li, Jianting Tang. A new HgSe photocatalyst for degradation of organic dyes under visible light irradiation. *Materials Letters*, 2015, 161, 591-594.
34. Qian Zhao, Shenna Chen, Lingyang Zhang, Haowen Huang. Detection of Fe(III) and Bio-Copper in Human Serum Based on Fluorescent AuAg Nanoclusters. *Analytical Methods*, 2015, 7, 296-300.
35. Qihua Liu, Xiaochun Zhou, Haomin Liu, Xi Zhang, Zaichun Zhou. Fractional transfer of a free unpaired electron to overcome energy barriers in the formation of Fe^{4+} from Fe^{3+} during core contraction of macrocycles: implication for heme distortion. *Organic & Biomolecular Chemistry*, 2015, 13, 2939-2946.
36. Xianyong Yu, Zhixi Liao, Bingfei Jiang, Xiaolian Hu, Xiaofang Li. Spectroscopic analyses on interaction of bovine serum albumin with novel spiro[cyclopropane-pyrrolizin]. *Spectrochimica Acta Part A Molecular & Biomolecular Spectroscopy*, 2015, 137, 129-136.
37. Shenna Chen, Qian Zhao, Lingyang Zhang, Xiaodong Xia, Haowen Huang. Successive detection of glucose and bio-copper in human serum based on a multiplex biosensor of gold nanorods. *Analytical Methods*, 2015, 7, 1018-1025.

38. Jianting Tang, Jiayin Li, Yang Cheng, Peng Huang, Qian Deng. Facile hydrothermal-carbonization preparation of carbon-modified Sb₂S₃ composites for photocatalytic degradation of methyl orange dyes. *Vacuum*, 2015, 120, 96-100.
39. Xianyong Yu, Bingfei Jiang, Zhixi Liao, Yue Jiao, Pinggui Yi. Study on the interaction between besifloxacin and bovine serum albumin by spectroscopic techniques. *Spectrochimica Acta Part A Molecular & Biomolecular Spectroscopy*, 2015, 149, 116-121.
40. Qingquan Liu, Zhe Tang, Minda Wu, Xiaojuan Li. Novel ferrocene-based nanoporous organic polymers for clean energy application. *RSC Advances*, 2015, 5, 8933-8937.
41. Bin Liu, Hongyun Fang, Xiaofang Li, Wenting Cai, Lipiao Bao, Marc Rudolf, Fabian Plass, Louzhen Fan, Xing Lu, and Dirk M. Guldi. Synthesis and photophysical properties of a Sc₃N@C₈₀-corrole electron donor-acceptor conjugate. *Chemistry - A European Journal*, 2015, 21, 746-752.
42. Xinyan Hou, Shu Chen, Lianju Shun, Yini Zhao, Zhiwu Zhang, Yunfei Long, Li Zhu. Visual detection of trace copper ions based on copper-catalyzed reaction of ascorbic acid with oxygen. *Spectrochimica Acta Part A Molecular & Biomolecular Spectroscopy*, 2015, 149, 103-108.
43. Linyan Wang, Chaotun Cao, Chenzhong Cao. Comparison of the substituent effects on the ¹³C NMR with the ¹H NMR chemical shifts of CH=N in substituted benzyldeneanilines. *Magnetic Resonance in Chemistry*, 2015, 53, 520-525.
44. Qiuhua Liu, Xi Zhang, Wennan Zeng, Jianxiu Wang, Zaichun Zhou. Fine-tuning of electronic structure of cobalt (II) ion in nonplanar porphyrins and tracking of a cross-hybrid stage: implications for the distortion of natural tetrapyrrole macrocycles. *Journal of Physical Chemistry B*, 2015, 119, 14102-14110.
45. Xinyan Hou, Shu Chen, Jian Tang, Yunfei Long, Li Zhu. Visual detection of trace copper (II) ion based on its catalytic action in the dissociation of thiosulfate. *Analytical Methods*, 2015, 7, 2542-2546.

46. Datang Li, Jianting Tang, Jing li. $\text{Fe}_4\text{I}_3\text{O}_{24}\text{H}_{15}$: A novel semiconductor with high performance in photodegradation of rhodamine B dyes under visible light irradiation. *Journal of Alloys and Compounds*, 2015, 633, 296-299.
47. Junfeng Xiang, Pinggui Yi, Xianyong Yu, Jian Chen, Yanlei Hao, Zhiyong Ren. Excited-state proton transfer of 2-(2-Hydroxyphenyl)benzothiazole in confined nanocavity. *Chemical Journal of Chinese Universities*, 2015, 36, 654-659.
48. Xianyong Yu, Bingfei Jiang, Zhixi Liao, Xiaofang Li. Study on the interaction between 21-(Ph-N@N)-NCTPP and bovine serum albumin by spectroscopic techniques. *Spectrochimica Acta Part A Molecular & Biomolecular Spectroscopy*, 2015, 142, 260-265.
49. Qingfeng Yi, Qinghua Chen, Zheng Yang. A novel membrane-less direct alcohol fuel cell. *Journal of Power Sources*, 2015, 298, 171-176.
50. Qingfeng Yi, Qinghua Chen. In situ preparation and high electrocatalytic activity of binary Pd-Ni nanocatalysts with low Pd-loadings. *Electrochimica Acta*, 2015, 182, 96-103.
51. 周虎, 吴科建, 余斌, 李宁, 周智华, 孙汉洲. 聚氨酯基合成纸的制备及性能. *高分子材料科学与工程*, 2015, 31, 176-180.
52. 唐子龙, 王恋, 马红伟, 王宏清. 新型N-(1,3,4-噻二唑基)噻唑甲酰胺的合成及其杀菌活性. *化学试剂*, 2015, 37, 298-330.
53. 唐子龙, 夏赞稳, 王宏清, 王恋, 焦银春, 陈金文. 2,3-二芳基-1,3-苯并噁嗪的合成及杀菌活性. *应用化学*, 2015, 32, 143-150.
54. 黄康利, 石顺存, 胡薇, 刘蓓, 闫东. 含双键酰胺咪唑啉季铵盐缓蚀性能研究. *工业水处理*, 2015, 35, 40-43.
55. 刘立华, 刘星, 李艳红, 杨刚刚, 周智华, 徐国荣. 两性高分子重金属螯合絮凝剂的合成及其对Cu(II)的去除性能. *环境工程学报*, 2015, 9, 1049-1056.
56. 李宁, 蒋敏, 罗小阳, 唐甲林, 秦先志, 周虎. 光致抗蚀剂的制备及其性能研究. *印制电路信息*, 2015, 9, 10-13.
57. 石顺存, 黄康利, 潘 蕾, 焦银春. 酰胺咪唑啉季铵盐合成及其缓蚀性能. *石油学报(石油加工)*, 2015, 4, 912-919.
58. 唐安平, 钟倩雯, 胡拥军, 刘立华, 徐国荣. 锂离子电池正极材料 LiMBO_3 研究进展. *电源技术*, 2015, 39, 1533-1535.

59. 陈冠凡, 罗青青, 曹晨忠, 曾荣今, 刘万强. 取代苯甲酸苯酯羰基化学位移中的取代基相互作用. *计算机与应用化学*, 2015, 32, 43-46.
60. 李宁, 余斌, 郭家旺, 孙汉洲, 吴科建, 周虎. 桐酸单甘酯改性水性聚氨酯的制备及其性能. *聚氨酯工业*, 2015, 30, 29-32.
61. 申洁, 唐安平, 贺冬华, 刘立华, 徐国荣. LiFeBO_3 / LBO复合材料的制备及其电化学性能. *湖南科技大学学报(自然科学版)*, 2015, 30, 110-115.
62. 向柳姣, 严画, 张金枝, 黄惠华, 何思良, 周智华. PCL/MDI/DEG体系聚氨酯水凝胶的制备及其亲水性能. *粉末冶金材料科学与工程*, 2015, 20, 788-794.
63. 李春香, 邱喜阳, 周建红, 令玉林, 邓克勤. 电还原氧化石墨烯-铁氰化钴修饰电极对肼的测定. *分析科学学报*, 2015, 31, 475-478.
64. 曾荣今, 刘传磊, 沈鹏飞, 唐沙, 熊春刚, 吴湘思. 一锅法合成N1, N3-二烷基取代3, 4-二氢嘧啶-2 (1H) 酮及其抗菌活性研究. *化学研究与应用*, 2015, 10, 1531-1538.



A dumbbell probe-mediated rolling circle amplification strategy for highly sensitive transcription factor detection



Chunxiang Li^a, Xiyang Qiu^a, Zhaohui Hou^{b,*}, Keqin Deng^{a,*}

^a Key Laboratory of Theoretical Organic Chemistry and Function Molecule, Ministry of Education, School of Chemistry and Chemical Engineering, Hunan University of Science and Technology, Xiangtan 411201, PR China

^b School of Chemistry and Chemical Engineering, Hunan Institute of Science and Technology, Yueyang 414006, PR China

ARTICLE INFO

Article history:

Received 9 August 2014

Received in revised form

21 September 2014

Accepted 23 September 2014

Available online 26 September 2014

Keywords:

Transcription factor detection

Rolling circle amplification

TATA-binding protein

ABSTRACT

Highly sensitive detection of transcription factors (TF) is essential to proteome and genomics research as well as clinical diagnosis. We describe herein a novel fluorescent-amplified strategy for ultrasensitive, quantitative, and inexpensive detection of TF. The strategy consists of a hairpin DNA probe containing a TF binding sequence for target TF, a dumbbell-shaped probe, a primer DNA probe designed partly complementary to hairpin DNA probe, and a dumbbell probe. In the presence of target TF, the binding of the TF with hairpin DNA probe will prohibit the hybridization of the primer DNA probe with the “stem” and “loop” region of the hairpin DNA probe, then the unhybridized region of the primer DNA will hybridize with dumbbell probe, subsequently promote the ligation reaction and the rolling circle amplification (RCA), finally, the RCA products are quantified via the fluorescent intensity of SYBR Green I (SG). Using TATA-binding protein (TBP) as a model transcription factor, the proposed assay system can specifically detect TBP with a detection limit as low as 40.7 fM, and with a linear range from 100 fM to 1 nM. Moreover, this assay related DNA probe does not involve any modification and the whole assay proceeds in one tube, which makes the assay simple and low cost. It is expected to become a powerful tool for bioanalysis and clinic diagnostic application.

© 2014 Elsevier B.V. All rights reserved.

1. Introduction

Transcription factors are proteins that bind to specific DNA sequences, thereby control the transcription of genetic information from DNA to messenger RNA (Latchman, 1997). Transcription factors are essential for the regulation of gene expression and confirmed to be the largest family of human proteins. There are approximately 2600 proteins in the human genome (approximately 10% of genes in the genome) that contain DNA-binding domains, and most of them are presumed to function as transcription factors (Babu et al., 2004).

Transcription factors play critical roles in the regulation of a variety of essential cellular processes, such as cell development, differentiation, and growth (Lee and Young, 2000). Furthermore, the changes in expression level of some transcription factors has been confirmed to closely connect with multiple aspects of oncogenesis (Baldwin, 2001; Libermann and Zerbini, 2006; Wolf et al., 2005). Therefore, quantitative protein detection of

transcription factors plays an important part in clinical diagnosis and biomedical research. Many powerful traditional techniques have been developed for transcription factors detection. They include DNase footprinting assay (Galas and Schmitz, 1978), electrophoretic mobility shift assay (EMSA) (Garner and Revzin, 1981), Western blots, and enzyme-linked immunosorbent assay (ELISA) (Burnette, 1981; Engvall and Perlmann, 1971). However, these methods such as DNase footprinting assay, EMSA, Western blots are usually time-consuming and laborious with the involvement of either radioisotopes or fluorescence labels and are not adaptable to assays requiring high throughput (Zhang et al., 2012). Furthermore, they cannot achieve quantitative analysis of protein expression. ELISA is a widely used quantitative detection method for protein and other analytes. While it needs expensive antibodies against each target protein, which elevates the analysis cost. Therefore, it is highly desirable to develop robust methods for simple, cost-effective, and sensitive detection of transcription factors.

Recent years, a broad class of fluorescence-based approaches have emerged, including fluorescence polarization assays, “molecular beacon” based assays, protein–DNA FRET assays (Giannetti et al., 2006; Liu et al., 2012; Lundblad et al., 1996; Moellering et al., 2009). In comparison to conventional methods, fluorescence

* Corresponding authors.

E-mail addresses: zhqh96@163.com (Z. Hou), keqindeng@hnust.edu.cn (K. Deng).



Selective deposition of HgS at the corner sites of triangular silver nanoprism and its tunable LSPR for colorimetric Hg²⁺ detection



Shu Chen*, Jian Tang, Yangfang Kuang, Lili Fu, Fangfang Ma, Yuanyuan Yang, Guanfan Chen, Yunfei Long*

Key Laboratory of Theoretical Organic Chemistry and Function Molecule, Ministry of Education, School of Chemistry and Chemical Engineering, Hunan University of Science and Technology, Xiangtan, 411201, China

ARTICLE INFO

Article history:

Received 18 March 2015

Received in revised form 7 July 2015

Accepted 19 July 2015

Available online 22 July 2015

Keywords:

Triangular silver nanoprism

Hg²⁺

LSPR

HgS

Colorimetric detection

ABSTRACT

This paper developed a novel colorimetric strategy for the detection of Hg²⁺ based on the apical activation and passivation of unmodified triangular silver nanoprism (AgNPR). Triangular AgNPR can be rapidly etched into round nanodiscs by thiosulfate anion (S₂O₃²⁻), leading to a change in colloid color from blue to yellow. However, if Hg²⁺ is introduced into the system together with S₂O₃²⁻, changes in the shape and color of the AgNPR can be effectively prevented by the specific precipitation reaction between Hg²⁺ and S₂O₃²⁻. The shape evolution of AgNPR was clearly revealed by the TEM measurements, including apical corrosion at the three corner sites and selectively HgS deposited over the etched zones. The spectroscopic changes in localized surface plasmon resonance (LSPR) wavelength of the AgNPR were used as the analytical signal, and a novel colorimetric platform for Hg²⁺ detection was established in a label-free fashion. It provides reliable and sensitive quantification with a detection limit as low as 0.2 nM and a dynamic range of 5.0 nM to 10.0 μM. Furthermore, this method has been successfully implemented for the determination of Hg²⁺ in wastewater samples.

© 2015 Elsevier B.V. All rights reserved.

1. Introduction

Mercury is a notoriously toxic environmental pollutants that can accumulate in the human body and severely disrupt the central nervous and endocrine systems [1,2]. Water-soluble divalent mercuric ion (Hg²⁺) is the most usual and stable form of mercury pollution [3]. Accordingly, designing simple method with high selectivity and sensitivity for monitoring of Hg²⁺ becomes an increasing demand. Traditional techniques have been developed for detecting Hg²⁺ in water samples, such as atomic absorption spectrometry [4], inductively coupled plasma mass spectrometry [5], atomic fluorescence spectrometry [6], high-performance liquid chromatography [7], and surface-enhanced Raman scattering [8]. Most of these techniques feature excellent performance but at the expense of sophisticated equipment, time-consuming sample processing protocols, or the need for well-trained operators.

Alternatively, colorimetric assays have attracted particular interest because of their simplicity, practicality, fast response times, and use of a relatively simple apparatus [9]. In addition, the

obvious color change afforded by such assays can be read out by the naked eye, which allows for the identification of Hg²⁺ without using special equipment [10]. In particular, gold or silver nanoparticles-based colorimetric sensors have been extensively studied for Hg²⁺ detection in recent years [11,12]. Their characteristic optical property, known as localized surface plasmon resonance (LSPR), offers excellent platform for the development of novel sensing strategies [13,14]. The application in Hg²⁺ detection typically relies on the functionalization of mercury-specific mediators or chromophoric probes, such as oligonucleotides [15–18], oligopeptide [19,20], thiol compounds [21,22], and other chemodosimeters [23–27]. Although these approaches provide low detection limits and fast response times, they still require complicated procedures for precise probe synthesis and surface modification. In this regard, it still remains a great challenge to realize label-free sensing in colorimetric Hg²⁺ detection with high selectivity and sensitivity.

Recently, anisotropic silver nanostructures with well-defined shapes and colors have been attracted prominent attention due to their unique optical properties [28,29]. For example, triangular silver nanoprism (AgNPR) exhibits particularly high refractive index sensitivities due to the intensification of electromagnetic fields at three corner sites. Their LSPR absorption peak, which is tunable over a broad vis-NIR region, is highly sensitive to the size, shape, and composition as well as the surrounding medium [30]. For example,

* Corresponding authors. Tel.: +86 731 58388503; fax: +86 731 58372324.

E-mail addresses: chenshumail@gmail.com (S. Chen), lyunfei927@163.com (Y. Long).



Combined detection of breast cancer biomarkers based on plasmonic sensor of gold nanorods



Shenna Chen^a, Qian Zhao^a, Lingyang Zhang^a, Linqian Wang^b, Yunlong Zeng^a,
Haowen Huang^{a,*}

^a Key Laboratory of Theoretical Organic Chemistry and Function Molecule, Ministry of Education, Hunan Provincial University Key Laboratory of QSAR/QSPR, School of Chemistry and Chemical Engineering, Hunan University of Science and Technology, Xiangtan, China

^b Department of Laboratory, Hunan Provincial Tumor Hospital, The Affiliated Tumor Hospital of Xiangya Medical School of Central South University, Changsha, Hunan Province, China

ARTICLE INFO

Article history:

Received 22 May 2015

Received in revised form 7 August 2015

Accepted 7 August 2015

Available online 9 August 2015

Keywords:

Gold nanorods

Breast cancer

Biomarker

Cancer antigen 15-3

Combined detection

ABSTRACT

In this study, a combined detection assay for determination of cancer antigen 15-3 (CA15-3) and copper level in breast cancer serum was developed by use of gold nanorod (GNR)-based plasmonic sensor. Rapid detection of tumor marker (CA15-3) can be accomplished through a simple transduction of optical signal induced by immune-reaction between CA15-3 and GNR@CA15-3 antibody. On the other hand, the copper-induced change of localized surface plasmon resonance of GNRs results in a direct readout of optical signal. Therefore, practical application for combined determination of CA15-3 and copper levels of human serum samples of breast cancer was performed. The results are close agreement with those given by the hospital or other standard approach, confirming this assay with high accuracy. The combined detection strategy provides potential applications for early diagnosing and monitoring the progress of malignant tumor.

© 2015 Elsevier B.V. All rights reserved.

1. Introduction

Breast cancer is a common cancer and the leading cause of cancer related deaths in women throughout the world. In spite of recent advanced and developed modern medicine technology, there is not a satisfactory way to overcome by far. Early diagnosis and treatment can effectively lower the cancer mortality rate, and many researchers are making a considerable effort to exploit the sophisticated diagnosis and therapeutic actions to improve treatment efficacy [1–3]. Cancer-associated protein markers which are present in the blood have significance for early diagnosis of cancer [4]. For example, cancer antigen 15-3 (CA15-3) is one of the most accepted markers among the various breast cancer markers for the diagnosis of breast cancer, which can monitor the patients' status after surgical operation and supply the reliable assurance for the rational use of clinical medicine [5–10]. Recently, a variety of methods have been developed for detection of CA15-3 based on immunoreactions, such as enzyme-linked immunosorbent assay, radio immunoassay, enzyme immunoassay, chemiluminescence immunoassay [11]. However, these methods usually suffer from problems of complicated label processing and time-consuming

separations. To meet the increasing clinical demands for the rapid detection of CA15-3 with high sensitivity, new methods capable of rapid and sensitive detection of CA15-3 are required.

Copper is an essential trace element responsible for maintaining homeostasis in the human body. Excess copper has greater carcinogenic potential by producing free radical that can bring about lipid peroxidation [12]. Furthermore, previous studies demonstrated that trace element might be relevant to malignant tumors [13–15]. Elevated copper levels have been found in sera from patients with various malignant tumors and the variation of copper levels may correlate to cancer progression. The determination of copper level may help to elucidate the relation of copper to breast cancer and to decide whether the element could be used as additional biochemical marker for diagnosis or prognosis of tumour development. Therefore, it is very significant to develop combined detection of CA15-3 and copper level in serum sample for early diagnosing and monitoring the progress of breast cancer. Many analytical methods were usually adopted for detection of copper. For example, atomic absorption spectrometry [16,17], atomic emission spectrometry [18], inductively coupled plasma mass spectrometry [19], can reliably determine the total concentration of copper including their insoluble forms, but they are costly and time-consuming and require expensive specialized equipment and highly qualified staff. Other methods, such as electrochemical methods and nanosensors [20,21], neither require sophisticated equipment nor complicated

* Corresponding author. Tel.: +86 731 58290045; fax: +86 731 58290509.
E-mail address: hhwn09@163.com (H. Huang).



Novel fluorescent polymeric nanoparticles for highly selective recognition of copper ion and sulfide anion in water



Jian Chen^{a,b,*}, Ya Li^a, Weibang Zhong^a, Qingyang Hou^a, Hong Wang^a, Xiang Sun^a, Pinggui Yi^a

^a Key Laboratory of Theoretical Organic Chemistry and Functional Molecule of Ministry of Education, Hunan Province College Key Laboratory of QSAR/QSPR, School of Chemistry and Chemical Engineering, Hunan University of Science and Technology, Xiangtan 411201, PR China

^b State Key Laboratory of Chemo/Biosensing and Chemometrics, Hunan University, Changsha 410082, PR China

ARTICLE INFO

Article history:

Received 11 May 2014

Received in revised form 15 August 2014

Accepted 11 September 2014

Available online 20 September 2014

Keywords:

Sensor

FRET

Polymeric nanoparticle

Copper ion

Sulfide anion

ABSTRACT

In the present study, a fluorescence resonance energy transfer (FRET)-mediated multifunctional sensor based on fluorescent polymeric nanoparticles was synthesized via a combination of a facile one-pot miniemulsion polymerization and subsequently by surface modification technology. Firstly, fluorescent polymeric nanoparticles were obtained by copolymerization of styrene, vinylbenzylchloride and the fluorescent vinylic crosslinking monomer (fluorescein-O,O-bis-propene: FBP) in oil-in-water miniemulsion stabilized with a cationic surfactant (dodecyltrimethyl ammonium bromide: DTAB). Then, 1,4,7,10-tetraazacyclododecane (Cyclen) was selected as ligand to graft onto the surface of nanoparticles. Due to the specific FRET effect between FBP and the Cu²⁺-Cyclen complex, the as-prepared nanoparticles display highly sensitive (detection limit: 340 nM) on-off-type fluorescence change with high selectivity toward Cu²⁺ among 11 metal ions (such as K⁺, Na⁺, Co²⁺, Ni²⁺, Zn²⁺, Hg²⁺, Mn²⁺, Ca²⁺, Mg²⁺, Fe²⁺ and Pb²⁺) in 100% aqueous solution. Moreover, it is worth to note that the in situ generated nanoparticle-Cu²⁺ ensemble could recover the quenched fluorescence upon addition of sulfide anion resulting in an off-on-type sensing with a detection limit of 2.1 μM in the same medium. No obvious interference was observed from other familiar anions such as Cl⁻, NO₃⁻, SO₄²⁻, HCO₃⁻, CO₃²⁻, Br⁻, F⁻, S₂O₃²⁻, ClO₄⁻ and HPO₄²⁻. Furthermore, the nanoparticle-based dual-ion sensor can be reversibly switched for multi-times by alternative addition of adequate Cu²⁺ or S²⁻, was also applicable in a relatively wide pH range (pH 4–10), and exhibited excellent long-term photostability for Cu²⁺ detection (≥40 days) in aqueous media. Thus, this approach may reveal a new pathway for selective detection of multiplex analyst in environmental and biological applications.

© 2014 Elsevier B.V. All rights reserved.

1. Introduction

The development of fluorescent sensors for selective detection of a chemical and biological analyst has attained increasing attentions because of their potential applications in chemistry, life sciences, medicine and environmental monitoring [1–5]. As one of the candidates, sulfide anion is widespread in the environment via generation from industrial processes and biological metabolism [6]. As a well-known toxic pollutant, sulfide anion can cause gradual and cumulative damage to life, such as loss of consciousness and irritation of mucous membranes [7]. Once protonated, sulfide becomes even more toxic as it turns into HS⁻, and further converts to H₂S under acidic pH [8]. Recent studies have shown that

protonated sulfide is linked to diseases like Alzheimer's disease [9], Down's syndrome [10], diabetes [11], and liver cirrhosis [12]. Thus, developing a strategy for sulfide anion measurement is very important for treatments and environmental requirements.

Compared with other traditional detection techniques including titration [13], inductively coupled plasma atomic emission spectroscopy [14], ion chromatography [15] and electrochemical method [16] etc., usage of fluorescent sensor to detect sulfide anion reveals a more promising strategy for its easy detection together with high sensitivity and selectivity. To date, some of the talented fluorescent sensors have been fabricated for sulfide anion detection [6,14,17–42]. However, most of the sensors often involve time-consuming organic synthesis or need harmful organic co-solvent system, which strongly limits their commercial applications in many fields like water quality monitoring and in vitro or in vivo detection of sulfide anion. Nevertheless, among these sensing platforms, a unique strategy like utilization of copper sulfide affinity

* Corresponding author. Tel.: +86 731 58290045; fax: +86 731 58290045.
E-mail address: cj0066@gmail.com (J. Chen).

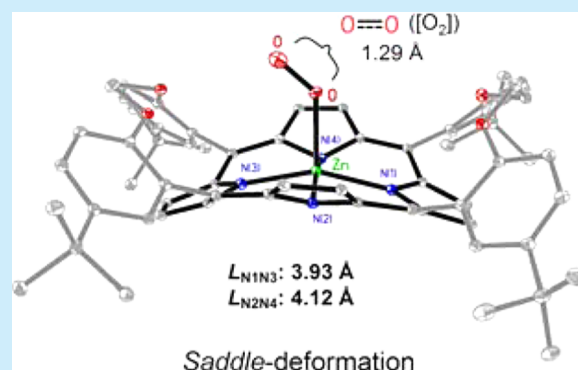
Fixation of Zinc(II) Ion to Dioxygen in a Highly Deformed Porphyrin: Implications for the Oxygen Carrier Mechanism of Distorted Heme

Zaichun Zhou,* Xiaochun Zhou, Qihua Liu,* Xi Zhang, and Haomin Liu

Key Laboratory of Theoretical Organic Chemistry and Functional Molecule of the Ministry of Education, School of Chemistry and Chemical Engineering, Hunan University of Science and Technology, Xiangtan 411201, China

S Supporting Information

ABSTRACT: Three saddle-type nonplanar zinc porphyrins strapped by two short alkyl linkers have been synthesized. The deformation induced by the linkers can cause a spectral red shift of >30 nm compared with the absorption maxima of regular porphyrins and can also regulate the electronic structure of the central zinc(II) ion. The zinc(II) ion then complexes and activates a free dioxygen to form a superoxide group ligand by enlarging the splitting of energy levels of d orbitals under strong core deformation. The fixation of dioxygen can be reasonably explained by the Dewar–Chatt–Duncanson model. These results indicate that this type of saddle porphyrin has the potential to be used as a new model system of heme.



The use of dioxygen in oxidation reactions catalyzed by transition metals is relatively rare despite its enormous potential.¹ Indeed, the addition and activation of dioxygen by metallic compounds remains a largely immature field despite extensive literature on the subject, particularly regarding iron– O_2 and copper– O_2 systems.^{4,5} Porphyrinoids play a vital role in the oxidation processes of biological systems, e.g., the well-known heme, a porphyrin complex containing Fe.^{6,7} Heme is sufficiently active to weaken the O–O bond of dioxygen and catalyze hydroxylation of inactivated C–H bonds.⁸ The macrocyclic distortion of porphyrin in heme has been recognized as a conserved structural feature of particular proteins.^{9,10}

Nonplanarity is universal to all heme proteins that bind NO or O_2 .¹¹ Distorted heme can both stabilize the lower-valent Fe(II) oxidation state of the central iron species¹² and generate its higher-valent iron(IV, V)-oxo complex.¹³ This distortion is energetically unfavorable, so its universality suggests that such conformational variation is crucial to the functions of metalloporphyrins and heme.^{7,14} Nonplanar metalloporphyrins show many interesting properties, including potent catalytic ability,¹⁵ variable coordination,¹⁶ large spectral red shift,¹⁷ tunable spin densities,¹⁸ and other unusual physical properties.¹⁹

In heme chemistry, the electronic structure of the metal ion in a complex can undergo marked changes induced by a slight variation of the macrocycle.²⁰ One advantage of porphyrin macrocycles is that they are highly flexible and can adopt a range of nonplanar conformations that are needed for a variety of biological functions.²¹ Recently, we demonstrated that the core contraction derived from a ruffling deformation of the porphyrin macrocycle can induce a conversion of the electronic

structure of coordinated Fe(III).^{22,23} Reports have also shown that zinc(II) species can be used as a catalyst in many oxidation reactions involving molecular oxygen²⁴ as well as in organic reactions.²⁵ These facts indicate that the activation of a metal to dioxygen possibly depends on its size but not necessarily on the presence of an odd electron. We developed an interest in what will occur in the filled d orbital of a Zn(II) ion under full contraction (strong deformation) of a macrocycle with an N_4 core. In the current report, three 5,10-15,20-distrapped zinc porphyrins 1-Zn to 3-Zn with saddle-type distortion are synthesized and characterized to determine the effect of this macrocyclic deformation on the electronic structure of the central zinc ion.

Distrapped materials 1-Zn to 3-Zn were obtained from the condensation of dialdehyde with pyrrole with a molar ratio of 1:2 in yields of 0.8–6.0% in refluxing propionic acid (Scheme 1).^{26,27} The formation of this type of highly deformed macrocycle involves tandem reactions including condensation and oxidation and includes a pyrrole-containing intermediate bridged by straps $\text{O}(\text{CH}_2)_x\text{O}$ ($x = 2, 3, \text{ and } 4$) at the two phenyl groups of the pyrrolyl α -positions (see Supporting Information p S6). The model compounds were directly characterized by X-ray diffraction, UV–vis and NMR spectral methods, and high-resolution mass spectrometry.

Macrocyclic distortion in porphyrins results in a spectral red shift, and the degree of distortion roughly depends on the magnitude of the shift.²⁸ For models 1-Zn to 3-Zn, as the degree of distortion increased, the maxima of the Soret band red-shifted from 429.5 to 450.0 nm (3-Zn \rightarrow 1-Zn), as shown

Received: July 15, 2015

Published: August 13, 2015



Electrochemical performance of LiMnBO₃/C composite synthesized by a combination of impregnation and precipitation followed by annealing



Anping Tang^{a,*}, Donghua He^a, Zeqiang He^b, Guorong Xu^a, Haishen Song^a, Ronghua Peng^a

^a Key Laboratory of Theoretical Chemistry and Molecular Simulation of Ministry of Education, School of Chemistry and Chemical Engineering, Hunan University of Science and Technology, Xiangtan 411201, China

^b College of Biology and Environmental Science, Jishou University, Jishou 416000, China

HIGHLIGHTS

- Monoclinic/hexagonal mixed-phase LiMnBO₃/C composites were synthesized by a novel impregnation-precipitation method.
- The discharge specific capacity for LiMnBO₃ has a very substantial improvement.
- The LiMnBO₃/C composite shows good cyclability at the four rates of C/20, C/10, C/5 and C/2, respectively.

ARTICLE INFO

Article history:

Received 14 August 2014

Received in revised form

15 November 2014

Accepted 18 November 2014

Available online 20 November 2014

Keywords:

LiMnBO₃

Cathode material

Lithium ion batteries

ABSTRACT

Monoclinic/hexagonal mixed-phase LiMnBO₃/C composites have been prepared by the impregnation-precipitation method using ketjen black (KB) with 3D conductive network as both template and conductive framework. The synthesized products are characterized by means of X-ray diffraction (XRD), scanning electron microscopy (SEM), nitrogen sorption and electrochemical tests. Morphology studied by SEM and nitrogen sorption shows that LiMnBO₃ particles are embedded in the nanostructured carbon networks. The LiMnBO₃/C electrodes deliver an initial discharge specific capacity of 150, 137, 121 and 85 mAh g⁻¹ at C/20, C/10, C/5 and C/2 rate, respectively. Although the capacity for the LiMnBO₃/C electrode decreases considerably with increasing rate, stable cycling performance is obtained for all the four rates.

© 2014 Elsevier B.V. All rights reserved.

1. Introduction

Polyanion-type cathode materials for lithium ion batteries have attracted great attention due to a lot of advantages since the first discovery of the electrochemical properties of the olivine LiFePO₄ by Padhi et al. [1]. However, polyanions also bring some inactive mass into the polyanion-type cathode materials, which impedes both the specific capacity and the specific energy, and it is necessary to minimize this drawback. Considering this, a new family of lithium transition metal borates, namely LiMBO₃ (M = Mn, Fe or Co), has generated recent excitement in the battery community because the higher charge/mass ratio of the BO₃³⁻ group leads to a

larger theoretical specific capacity of ~220 mAh g⁻¹, about 30% larger than that of PO₄³⁻-based LiMPO₄ [2–9].

Among the LiMBO₃ borates, LiMnBO₃ exists in two different phases: the low-temperature monoclinic form and the high-temperature hexagonal form. As a result of their structural differences, the two materials display different average potential (3.7 V for monoclinic phase and 4.1 V for hexagonal phase versus Li/Li⁺) and different electrochemical property (e.g. the former displays better electrochemical property than the latter [5]). Additionally, one recent report claimed that monoclinic/hexagonal mixed phased LiMnBO₃ displays better lithium electrochemical performance than the pure phased LiMnBO₃ [10]. Like LiFePO₄, the LiMBO₃ borates suffer from poor electronic and ionic conductivity, although there have been considerable developments in the electrochemical performance [2,11,12]. Recently, these obstacles have been overcome for LiFeBO₃ by employing conductive carbon

* Corresponding author.

E-mail address: anpingxt@126.com (A. Tang).

SIMPLE AND SENSITIVE DETECTION FOR TRACE CHROMIUM (VI) USING ALBUMIN AS FLUORESCENCE PROBES

HUI-YAN KUANG, XIAO-YUN YUAN, LEI FENG, HAO-WEN HUANG, CHUN-RAN TANG, KE-QIN DENG, YUN-LONG ZENG*

(School of Chemistry and Chemical Engineering, Hunan University of Science and Technology, Key Laboratory of Theoretical Chemistry and Molecular Simulation of Ministry of Education of China, Xiangtan 411201, PR China)

ABSTRACT

We have developed a novel method for fast determination of chromium(VI) using egg albumin(EAB) as fluorescence probe. The influence factors, including pH, reaction time, concentration of EAB, were investigated on the performance of the method and the optimum experimental conditions were determined. Under the optimum conditions, the relative fluorescence intensity of albumin was linearly proportional to Cr(VI) over a concentration range from 1.0×10^{-7} to 6.0×10^{-5} mol L⁻¹ with a correlation coefficient of 0.9936 and a detection limit of 5.2 nmol L⁻¹. This is a fast, simple, high selective and environment-friendly method, which has been employed to detect trace Cr(VI) in drinking water samples with satisfactory. The infrared spectral information indicated that the possible mechanism of fluorescence quenched may be the change of the secondary structures of EAB in the presence of Cr(VI).

Key words: Trace chromium(VI); fast analysis; egg albumin; fluorescence probe; drinking water

1. INTRODUCTION

In recent years, significant progress has been realized on the impact of pollution on the environment and human health. Water, food and medicine are the possible sources of contaminants such as chromium. Chromium exists in two oxidation states, Cr(III) and Cr(VI) in solution, which have contrasting physiological effects. Cr(III) is known as an essential trace element for maintaining normal physiological function. However, Cr(VI) is highly carcinogenic and mutagenic [1-3], and can cause various of clinical problems, such as immediate cardiovascular shock, negative effects on kidney, liver, and other organs [4]. Hence, the research has drawn much attention in detection of trace Cr(VI) in drinking water recently. Many new methods to detect trace Cr(VI) have been developed, including spectrophotometric method [5,6], fluorescence probe method [7-9], electrochemical method [10,11], ion chromatography [12], inductively coupled plasma mass spectrometry [13], inductively coupled plasma-optical emission spectrometry [14], atomic absorption spectrometry [15]. These methods need either expensive instruments or long analysis time, or consumption of a great deal of reagents [16]. Therefore, developing simple and environment-friendly method for selective, sensitive and rapid determination of trace chromium is still a great challenge.

Protein is a biodegradable and environment-friendly reagent and has widely used in biochemistry and analytical chemistry [17-19]. Egg albumin (EAB) is a cheap, environment-friendly, and egg resources are very rich (available in abundance in egg). But the research of this reagent in analytical chemistry was seldom reported. In this work, we find that EAB shows high selective for Cr(VI), and then have developed a novel method for fast determination of trace chromium(VI) based on the fluorescence quenched of EAB by Cr(VI).

2. EXPERIMENTAL

2.1 Apparatus

Fluorescence measurements were performed using Hitachi F-4500 fluorescence spectrophotometer (Tokyo, Japan) with a xenon discharge lamp, 1cm quartz cells at room temperature. Infrared spectra and UV-visible spectra were recorded using Spectrum One Spectrophotometer and Lamaba 35 UV-Vis Spectrophotometer (Perkin-Elmer, American), respectively.

2.2 Reagents

Egg albumin and K₂Cr₂O₇ (Standard Reagent) were purchased from China Pharmaceutical Group (Shanghai, China). Stock standard aqueous solution of K₂Cr₂O₇ was prepared at concentration of 0.0050 M, and the other concentration of K₂Cr₂O₇ was prepared by diluting the stock standard solution with double distilled water. All other chemicals used were of analytical grade without further purification. Doubly distilled water was used for all chemical procedures.

2.3 Detection of chromium(VI)

Chromium(VI) determination was carried out by successively adding 100 ml varying concentration of Cr(VI) or sample solution into 10 ml 0.40 mg EAB KH₂PO₄-Na₂HPO₄ buffer solution (PBS) solution (pH 9.18). The fluorescence

intensity of the solution was recorded at the peak wavelength (about 345 nm). All measurements were made under room temperature.

3. RESULTS AND DISCUSSION

3.1 Selection of excitation wavelength

Emission and excitation spectra of EAB (a,b) and UV-vis absorption spectra of EAB and K₂Cr₂O₇ (c,d) are shown in figure 1, respectively. There is continuous excitation spectrum of EAB (see Fig. 1 curve b) with a maximum peak locates at 295 nm. When the excitation is set at 295 nm, the albumin has a broad, strong and symmetric emission (curve a in Fig.1) with the maximum fluorescence at 345 nm. As known, potassium dichromate absorbs UV light, which may cause the inner filter and can appear error. Hence, the characteristic of UV-vis absorption spectrum of potassium dichromate was investigated. As seen from Fig.1 (curve d), there are UV-vis absorption peaks of potassium dichromate locating at about 255 nm and 354 nm. Fortunately, the absorption is very weak at the wavelength range from 295 nm to 315 nm. So the fluorescence emission at 345 nm was used for quantitative analysis, and the excitation was set at 295 nm in the following experiments.

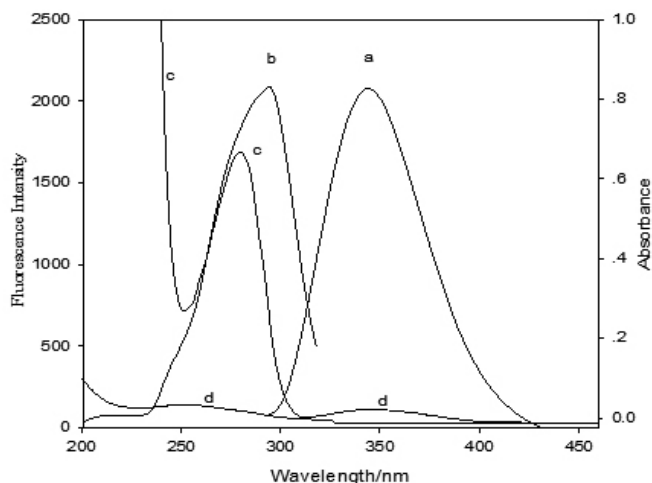


Fig. 1. Emission and excitation spectra of EAB (a,b) and UV-vis absorption spectra of EAB and K₂Cr₂O₇ (c,d).

Concentration, egg albumin: 50 mg L⁻¹, potassium dichromate: 3.0 mg L⁻¹.

3.2 Influence of ions on the fluorescence of the albumin

The effect of ions on the fluorescence intensity of EAB was studied and



Carbon dots as a fluorescent probe for label-free detection of physiological potassium level in human serum and red blood cells



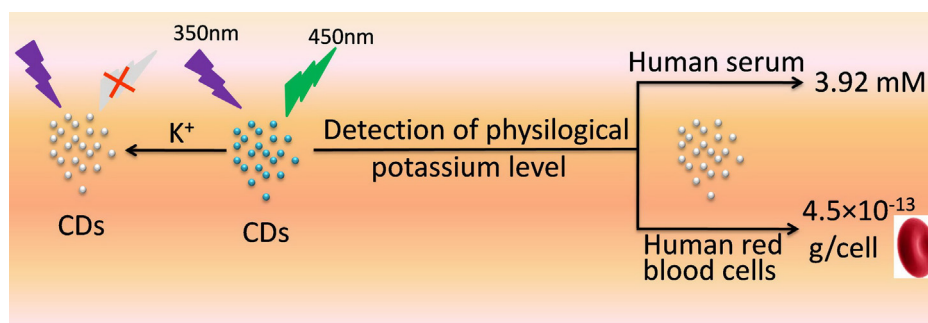
Linyang Zhang, Shenna Chen, Qian Zhao, Haowen Huang*

School of Chemistry and Chemical Engineering, Hunan University of Science and Technology, Hunan Provincial University Key Laboratory of QSAR/QSPR, Key Laboratory of Theoretical Organic Chemistry and Function Molecule, Ministry of Education, Xiangtan, China

HIGHLIGHTS

- A unique photoluminescence carbon dots with larger size were prepared by microwave-assisted method.
- A highly sensitive CD-based fluorescence probe for label-free detection of K^+ was established.
- Physiological potassium levels of human serum and red blood cells may be directly and rapidly detected.

GRAPHICAL ABSTRACT



ARTICLE INFO

Article history:

Received 11 March 2015

Received in revised form 21 April 2015

Accepted 25 April 2015

Available online 2 May 2015

Keywords:

Carbon dots
Potassium ion
Label free
Human serum
Human red blood cells

ABSTRACT

A unique photoluminescence carbon dots (CDs) with larger size were prepared by microwave-assisted method. Complex functional groups on the surface of the CDs facilitate the nanoparticles to form affinity with some metal ions. Taking advantage of the effective fluorescence quenching effect of K^+ , a highly sensitive CD-based fluorescence analytical system for label-free detection of K^+ with limit of detection (LOD) 1.0×10^{-12} M was established. The concentrations of potassium ion in biological samples such as human serum are usually found at millimolar levels or even higher. The proposed method begins with a substantial dilution of the sample to place the K^+ concentration in the dynamic range for quantification, which covers 3 orders of magnitude. This offers some advantages: the detection of K^+ only needs very small quantities of biological samples, and the dilution of samples such as serum may effectively eliminate the potential interferences that often originate from the background matrix. The determined potassium levels were satisfactory and closely comparable with the results given by the hospital, indicating that this fluorescent probe is applicable to detection of physiological potassium level with high accuracy. Compared with other relative biosensors requiring modified design, bio-molecular modification or/and sophisticated instruments, this CD-based sensor is very simple, cost-effective and easy detection, suggesting great potential applications for successively monitoring physiological potassium level and the change in biological system.

© 2015 Elsevier B.V. All rights reserved.

1. Introduction

Carbon-based nonmaterials have attracted much attention due to their unique properties. Owing to the robust chemical inertness, size dependent photoluminescence, high photostability against photo bleaching and blinking, low cytotoxicity and excellent

* Corresponding author. Tel.: +86 731 58290045.
E-mail address: hhwn09@163.com (H. Huang).



Synthesis and Biological Evaluation of Kojic Acid Derivatives Containing 1,2,4-triazole as Potent Tyrosinase Inhibitors

Wenlin Xie^{1,2,3,*}, Jingai Zhang^{1,2,3}, Xiaojing Ma^{1,2,3}, Wenqian Yang^{1,2,3}, Ying Zhou^{1,2,3}, Xufu Tang^{1,2,3}, Yan Zou^{1,2,3}, Hui Li^{1,2,3}, Jingjing He^{1,2,3}, Shimin Xie⁴, Yunhui Zhao^{1,2,3} and Fengping Liu^{1,2,3}

¹School of Chemistry and Chemical Engineering, Hunan University of Science and Technology, Xiangtan 411201, China

²Key Laboratory of Theoretical Chemistry and Molecular Simulation of Ministry of Education, Hunan University of Science and Technology, Xiangtan 411201, China

³Hunan Provincial University Key Laboratory of QSAR/QSPR, Xiangtan, 411201, China

⁴Hunan University of Humanities, Science and Technology, Loudi 417000, China

*Corresponding author: Wenlin Xie, xwl99zsu@163.com

A series of 5-substituted-3-[5-hydroxy-4-pyrone-2-yl-methylmercapto]-4-amino-1,2,4-triazole derivatives were synthesized by nucleophilic substitution reaction of 5-hydroxy-2-chloromethyl-4H-pyran-4-one with 5-substituted-3-mercapto-4-amino-1,2,4-triazole, and their inhibitory effects on mushroom tyrosinase were evaluated. The results indicated that most of the synthesized compounds exhibited significant inhibitory activity. Specifically, 5-(4-chlorophenyl)-3-[5-hydroxy-4-pyrone-2-yl-methylmercapto]-4-amino-1,2,4-triazole (**6j**) exhibited the most potent tyrosinase inhibitory activity with IC₅₀ value of 4.50 ± 0.34 μM. The kinetic studies of the compound (**6j**) demonstrated that the inhibitory effects of the compound on the tyrosinase were belonging to competitive inhibitors. Meanwhile, the structure–activity relationship was also discussed.

Key words: 1,2,4-triazole, kojic acid derivatives, mushroom tyrosinase, tyrosinase inhibitors

Received 12 January 2015, revised 12 April 2015 and accepted for publication 13 April 2015

Melanogenesis is a physiological process resulting in the production of melanin pigment, which plays an important role in the prevention of sun-induced skin injury (1). Although the melanin production in human skin is a major defense mechanism against UV light, excessive accumulations of

epidermal pigmentation can cause various hyperpigmentation disorders, such as freckle, senile lentigines, and melasma. Tyrosinase (polyphenol oxidase, EC 1.14.18.1) is a multifunctional copper-containing enzyme that is widely distributed in micro-organisms, animals, and plants (2). It can catalyze two distinct reactions during the biosynthesis of melanin, involving the hydroxylation of L-tyrosine to L-dopa and the oxidation of L-dopa to dopaquinone, which is highly reactive and can polymerize spontaneously to form melanin (3). Therefore, the regulation of melanin synthesis via the inhibition of tyrosinase is an important research topic (4). In clinical usage, tyrosinase inhibitors are used for treatments of dermatological disorders related to melanin hyperaccumulation and are essential in cosmetics for depigmentation (5,6), such as age spots and freckle, caused by the accumulation of an excessive level of epidermal pigmentation (7). Inhibition of tyrosinase is equally important commercially. In most fruits and vegetables, the enzyme is responsible for undesired browning that takes place during senescence or damage during postharvest handling, leading to faster degradation and shorter shelf life (8). Therefore, inhibition of tyrosinase is desirable to control browning and reduce economic losses. Accordingly, the development of safe and effective tyrosinase inhibitors is of great concern in clinical medicine and cosmetic industries.

Kojic acid (**1**) is produced by various bacteria and fungi, such as *Penicillium* and *Aspergillus*, and is widely used as a skin-whitening agent because it can inhibit tyrosinase (9). However, its inhibiting effect and storage properties are inadequate for use in cosmetics. Thus, many kojic acid derivatives have been synthesized, usually by modifying the C-7 hydroxyl group to form a variety of new derivatives. Triazole is the core structural motif in a variety of different compounds in medicinal chemistry and has been reported to exhibit a broad range of biological properties, including enzyme inhibition (10,11), antimicrobial (12), antinociceptive (13), and anti-inflammatory activities (14). Studies by Usman Ghani *et al.* (15) have demonstrated that 5-substituted-3-mercapto-4-amino-1,2,4-triazole (**4**) derivatives have promising inhibitory activities of tyrosinase. Therefore, in view of exploring new, potent, and safer inhibitors of tyrosinase, we designed a novel compounds by combining structures of two putative tyrosinase inhibitors, kojic acid (**1**) and 5-substituted-3-mercapto-4-amino-1,2,4-triazole (**4**), to

■ Porphyrinoid Hydrogenation

Towards Norcorrin: Hydrogenation Chemistry and the Heterodimerization of Nickel(II) Norcorrole

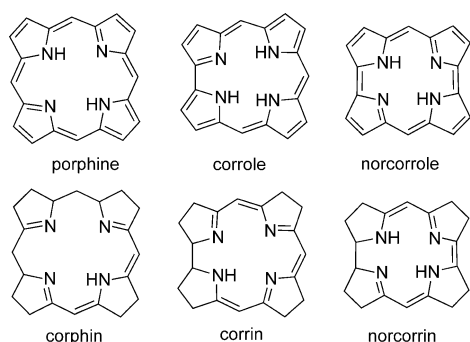
Bin Liu,^[a] Xiaofang Li,^{*[a]} Marcin Stępień,^[b] and Piotr J. Chmielewski^{*[b]}

Abstract: 5,14-Dimesitylnorcorrolatonickel(II) was hydrogenated under mild conditions (room temperature, 1 atm H₂, THF solution, 5 min.) in the presence of Raney nickel to yield nonaromatic derivatives that were isolated and characterized by NMR spectroscopy, UV/Vis spectrophotometry, HRMS, cyclic voltammetry, and X-ray diffraction analysis. The major

hydrogenation product, 1,2,3,7,8,9-hexahydronorcorrolatonickel(II), underwent dimerization in the presence of *p*-chloranil to give a nonsymmetrically linked 2,3'-bis(norcorrole) system that can adopt eight different oxidation states over a redox potential window of 3 V and has a HOMO–LUMO gap of 0.92 V.

Introduction

Macrocyclic tetrapyrroles are widespread in nature, occurring mostly in the forms of porphine- or corrole-type rings (Scheme 1). Although these macrocycles can be aromatic, for example, porphine in haem-containing proteins, chlorin in chlorophyll, or bacteriochlorin in bacteriochlorophyll, it appears that aromaticity is not a prerequisite for their hydrolytic or redox stability, particularly when they contain a metal ion



Scheme 1. Schematic structures of selected cyclic tetrapyrroles.

[a] B. Liu, Prof. X. Li

Key Laboratory of Theoretical Organic Chemistry and Functional Molecules, Ministry of Education School of Chemistry and Chemical Engineering Hunan University of Science and Technology Xiangtan, Hunan 411201 (P. R. China)
E-mail: lixiaofang@iccas.ac.cn

[b] Prof. M. Stępień, Prof. P. J. Chmielewski

Department of Chemistry, University of Wrocław F. Joliot-Curie 14, 50 383 Wrocław (Poland)
E-mail: piotr.chmielewski@chem.uni.wroc.pl

Supporting information for this article is available on the WWW under <http://dx.doi.org/10.1002/chem.201500736>.

within the coordination core. For example, the nickel-containing coenzyme F430 of methanogenic bacteria consists of the corphin ring in which there are only five double bonds within the macrocycle and the system is capable of the stabilization of three different metal oxidation states.^[1–3] Vitamin B₁₂ (cobalamin) comprises the corrin ligand, which is formally an octahydrogenated corrole.^[4,5] In fact, contracted porphyrins, that is, tetrapyrroles of reduced macrocyclic ring size, are represented in nature solely by this nonaromatic porphyrinoid.

Hydrogenated porphyrinoids are typically obtained by the condensation of saturated oligopyrrole precursors or by the direct reduction of aromatic macrocycles either by catalytic hydrogenation or by the use of chemical reductants. Such reductions usually result in mixtures of differently hydrogenated products and show low regio- and stereoselectivity.^[6–9] In addition, no direct hydrogenation of corroles has been reported to date.

The addition of hydrogen to the *meso* positions^[10,11] or to a bridging carbon of the bipyrrrole moiety^[12] of porphyrinoids leads to a disruption of the π -electron delocalization path, invariably producing nonaromatic macrocycles.

Norcorrole, a contracted tetrapyrrolic porphyrin macrocycle that comprises two *meso* bridges was first synthesized in the form of an iron(III) complex, as reported by Bröring et al. in 2008.^[13] The alternative synthetic approach of Kobayashi and Shinokubo and their co-workers allowed the efficient preparation of the stable diamagnetic norcorrole–nickel(II) complex **1** (see Scheme 2), which has been shown to be antiaromatic, in line with the presence of a 16 π -electron conjugation in its structure.^[14–16] Compound **1** is readily obtainable, and its symmetric structure makes it an attractive object for studying paratropic ring-current effects as well as the spectroscopic and redox properties of antiaromatic complexes. Because of the structural rigidity of this norcorrole complex, its magnetic properties are affected only by the oxidation state and not by conformational changes, in contrast to several antiaromatic expanded porphyrins.^[17] The purpose of this study was to ex-

Preparation of gelatin/hyaluronic acid microspheres with different morphologies for drug delivery

Zhihua Zhou · Siliang He · Tianlong Huang · Cheng Peng ·
Hu Zhou · Qingquan Liu · Wennan Zeng · Lihua Liu ·
Huihua Huang · Liujiao Xiang · Hua Yan

Received: 27 July 2014/Revised: 24 October 2014/Accepted: 2 January 2015/
Published online: 13 January 2015
© Springer-Verlag Berlin Heidelberg 2015

Abstract Gelatin/hyaluronic acid (Gel/HA) microspheres were prepared by emulsion–coagulation method using glutaraldehyde as cross-linker. The influence of treatment methods, including removing water by different concentrations of acetone/water solution and freeze drying, on surface morphology was also investigated. The *in vitro* release behaviors of icariin from smooth Gel/HA microspheres were also studied. The results indicated that the smooth and wrinkled Gel/HA microspheres were obtained when treated by pure acetone/water solution (volume ratio of 3:1) and pure acetone, respectively. More wrinkled microcracks could be observed when the Gel/HA microspheres were washed by pure acetone for longer time. The microspheres with porous structure were prepared when the obtained smooth Gel/HA microspheres were treated by freeze-drying method at $-45\text{ }^{\circ}\text{C}$. The size of Gel/HA microspheres increased with increasing immersion time in distilled water and

Z. Zhou (✉) · S. He · H. Zhou · Q. Liu · W. Zeng · L. Liu · H. Huang · L. Xiang · H. Yan
School of Chemistry and Chemical Engineering, Hunan University of Science and Technology,
Xiangtan, People's Republic of China
e-mail: zhou7381@126.com

Z. Zhou
Key Laboratory of Theoretical Chemistry and Molecular Simulation of Ministry of Education,
Hunan University of Science and Technology, Xiangtan, People's Republic of China

Z. Zhou
Hunan Province College Key Laboratory of QSAR/QSPR, Hunan University of Science and
Technology, Xiangtan, People's Republic of China

T. Huang
Department of Orthopedics, The Second Xiangya Hospital, Central South University,
Changsha, People's Republic of China

C. Peng
Department of Burns and Plastic Surgery, The Third Xiangya Hospital, Central South University,
Changsha, People's Republic of China

Synthesis and characterization of novel maleated poly(D,L-lactide-*co*-glycolide) by direct melt copolymerization

Zhihua Zhou^{1,2,3} · Huihua Huang¹ · Tianlong Huang⁴ · Cheng Peng⁵ · Hu Zhou¹ · Qingquan Liu¹ · Wennan Zeng¹ · Lihua Liu¹ · Dafu Cao¹ · Siliang He¹ · Liujiào Xiang¹ · Hua Yan¹

Received: 12 November 2014 / Revised: 5 March 2015 / Accepted: 10 March 2015 /

Published online: 17 March 2015

© Springer-Verlag Berlin Heidelberg 2015

Abstract Novel maleated poly(D,L-lactide-*co*-glycolide) (MPLGA) was melt copolymerized directly from maleic anhydride, D,L-lactide and glycolide monomers with stannous octoate as catalyst and benzoyl peroxide as initiator. FTIR, ¹H NMR, GPC and maleation content were employed to qualitatively characterize the synthesized MPLGA. The effects of the catalyst dosage, reaction time and reaction temperature on weight average molecular mass, polydispersity index and maleation content of MPLGA were also investigated. The results indicated that the novel MPLGA was successfully obtained using melting-copolymerization method. MPLGA, with a weight average molecular mass of about 5.39×10^4 Da, a polydispersity index of 1.51 and a maleation content of 7.1 wt%, was obtained when polymerization was conducted with catalyst dosage of 0.03 wt% for 36 h at 140 °C. The results indicated that the introduction of maleic anhydride into PLGA may offer new and important options for biomaterial applications.

Keywords D,L-Lactide · Glycolide · Maleic anhydride · Poly(D,L-lactide-*co*-glycolide) · Modification

✉ Zhihua Zhou
zhou7381@126.com

¹ School of Chemistry and Chemical Engineering, Hunan University of Science and Technology, Xiangtan, People's Republic of China

² Key Laboratory of Theoretical Chemistry and Molecular Simulation of Ministry of Education, Hunan University of Science and Technology, Xiangtan, People's Republic of China

³ Hunan Province College Key Laboratory of QSAR/QSPR, Hunan University of Science and Technology, Xiangtan, People's Republic of China

⁴ Department of Orthopedics, The Second Xiangya Hospital, Central South University, Changsha, People's Republic of China

⁵ Department of Burns and Plastic Surgery, The Third Xiangya Hospital, Central South University, Changsha, People's Republic of China

[Article]

doi: 10.3866/PKU.WHXB201412191

www.whxb.pku.edu.cn

取代基效应对 *N*-4-取代苯亚甲基苯胺与 *N*-4-取代苯亚甲基环己胺 NMR 和 UV 光谱影响的差异性

曹朝瞰 魏佰影 曹晨忠*

(湖南科技大学化学化工学院, 理论有机化学与功能分子教育部重点实验室,
分子构效关系湖南省普通高等学校重点实验室, 湖南 湘潭 411201)

摘要: 合成了 *N*-4-取代苯亚甲基苯胺(1)与 *N*-4-取代苯亚甲基环己胺(2)两个系列化合物, 测定其 ^{13}C 和 ^1H 核磁共振(NMR)化学位移以及紫外(UV)吸收光谱. 定量对比了取代基效应对两个系列化合物 $\text{CH}=\text{N}$ 键的 ^{13}C NMR 化学位移 $\delta_{\text{C}(\text{C}=\text{N})}$ 和 ^1H NMR 化学位移 δ_{H} 以及 UV 吸收光谱最大波长能量(ν_{max})的影响差异. 研究表明, 对于分子骨架相似的化合物(1)和(2), 取代基效应的作用方式存在多样性: (i)化合物(1)的 $\delta_{\text{C}(\text{C}=\text{N})}$ 、 δ_{H} 以及 ν_{max} 受到基团的特殊交叉相互作用($\Delta\sigma^2$)的影响显著, 而 $\Delta\sigma^2$ 对化合物(2)相应性能的影响很小; (ii)无论化合物(1)还是化合物(2), 取代基/诱导效应 σ_{F} 和共轭效应 σ_{R} 对 $\delta_{\text{C}(\text{C}=\text{N})}$ 的影响为负相关, 而对 δ_{H} 的影响为正相关, 它们对 $\delta_{\text{C}(\text{C}=\text{N})}$ 和 δ_{H} 的影响正好相反. 另一方面, 场/诱导效应 σ_{F} 对(1)和(2)的 $\delta_{\text{C}(\text{C}=\text{N})}$ 影响重要, 而对它们的 δ_{H} 影响很小; (iii)化合物(1)和(2)的 $\delta_{\text{C}(\text{C}=\text{N})}$ 、 δ_{H} 以及 ν_{max} 的变化规律, 可分别建立通用方程表达, 其中与 $\text{CH}=\text{N}$ 的 N 原子键连苯基的影响可由指示变量(I)表示, 该苯基对三种性能分别有固定的贡献.

关键词: 苯亚甲基胺; 取代基效应; 核磁共振; 紫外吸收; 基团特殊交叉作用

中图分类号: O641

Effect of Substituents on the NMR and UV Spectra of *N*-(4-substituted benzylidene) Anilines and *N*-(4-substituted benzylidene) Cyclohexylamines

CAO Chao-Tun WEI Bai-Ying CAO Chen-Zhong*

(Hunan Provincial University Key Laboratory of QSAR/QSPR, Key Laboratory of Theoretical Organic Chemistry and Function Molecule of Ministry of Education, School of Chemistry and Chemical Engineering, Hunan University of Science and Technology, Xiangtan 411201, Hunan Province, P. R. China)

Abstract: Two series of compounds: *N*-(4-substituted benzylidene) anilines (1) and *N*-(4-substituted benzylidene) cyclohexylamines (2) were synthesized. Their ^{13}C NMR and ^1H NMR chemical shifts and their UV absorption spectra were obtained. Compounds (1) and (2) were compared quantitatively to determine the effect of the substituents on the ^{13}C NMR chemical shifts $\delta_{\text{C}(\text{C}=\text{N})}$ and the ^1H NMR chemical shifts δ_{H} of the $\text{CH}=\text{N}$ bond, and the UV absorption maximum wavelength energies ν_{max} . Our results show that the substituents affect compounds (1) and (2) differently despite them having a similar molecular skeleton. These effects are: (i) a substituent specific cross-interaction effect ($\Delta\sigma^2$) that significantly affects the $\delta_{\text{C}(\text{C}=\text{N})}$, δ_{H} , and ν_{max} of compounds (1) while its effect on the corresponding properties of compounds (2) is limited, (ii) for compounds (1) and compounds (2) the field/induced effect σ_{F} and the conjugation effect σ_{R} of the substituents negatively affect $\delta_{\text{C}(\text{C}=\text{N})}$. However, they positively influence δ_{H} and thus both σ_{F} and σ_{R} show opposite behavior toward $\delta_{\text{C}(\text{C}=\text{N})}$ compared

Received: September 24, 2014; Revised: December 19, 2014; Published on Web: December 19, 2014.

*Corresponding author. Email: czcao@hnust.edu.cn; Tel: +86-731-58291336.

The project was supported by the National Natural Science Foundation of China (21272063, 21072053) and Natural Science Foundation of Hunan Province, China (14JJ3112).

国家自然科学基金(21272063, 21072053)和湖南省自然科学基金(14JJ3112)项目资助

© Editorial office of Acta Physico-Chimica Sinica



HgI₂: A novel photocatalyst with high performance in degradation of rhodamine B dyes under visible-light irradiation



Jianting Tang^{*}, Datang Li^{**}, Zhaoxia Feng, Chengyun Long

Key Laboratory of Theoretical Organic Chemistry and Functional Molecule for Ministry of Education, School of Chemistry and Chemical Engineering, Hunan University of Science and Technology, Xiangtan, 411201, China

ARTICLE INFO

Article history:

Received 1 June 2015

Received in revised form

7 August 2015

Accepted 2 September 2015

Available online 9 September 2015

Keywords:

Mercuric iodide

Photocatalysis

Degradation

ABSTRACT

A new photocatalyst, HgI₂, was successfully developed. The HgI₂ sample was characterized by scanning electron microscopy (SEM), X-ray diffraction (XRD), ultraviolet–visible diffuse reflectance spectrum (UV–vis DRS) and photoluminescence (PL) techniques. Its activity is as high as that of the highly efficient photocatalyst Ag₃PO₄ in degradation of rhodamine B (RhB) dyes under irradiation of visible light. It can be reused for at least three cycles without obvious loss of its activity in the degradation experiments. The main active species of HgI₂ for the RhB degradation are superoxide anion radicals. The high photocatalytic activity of HgI₂ may be attributed to its low recombination rate of the photogenerated carriers.

© 2015 Elsevier B.V. All rights reserved.

1. Introduction

In the past decades, semiconductor photocatalysis was widely studied due to its application in environmental pollution treatment [1–8]. The key issue to utilize solar energy through photocatalysis is the utilization of visible light in the process. Thus, many efforts have been dedicated to develop visible-light-responsive photocatalysts to deal with the problem of environmental pollution [9]. A general problem with photocatalysis is the rapid recombination rate of photogenerated carriers of photocatalysts, which leads to low photocatalytic activity [9]. Therefore, it is still desirable but difficult to prepare visible-light-responsive photocatalysts, especially with high performance, to fully utilize solar energy in photocatalysis.

Ag₃PO₄, as a highly efficient visible-light-responsive photocatalyst, is already an important research topic because of its higher photocatalytic activity than the currently known photocatalysts including BiVO₄, N-doped TiO₂, etc., in water oxidation and degradation of organic compounds [10,11]. We successfully prepared some new semiconductors Ag@(Ag₂S/Ag₃PO₄) [12], Ag₃AsO₄ [13] and AgIO₄ [14], which achieved higher photodegradation activity than that of Ag₃PO₄ photocatalyst. Very recently, we developed a new Fe₄I₃O₂₄H₁₅ semiconductor with activity close to that of

Ag₃PO₄ in photodegradation of RhB under visible light irradiation, and it can be reused for at least five times without obvious loss of activity [15]. In this study, we report another new visible-light-responsive photocatalyst, HgI₂. Its photocatalytic activity is as high as that of Ag₃PO₄, and is much higher than that of AgI [16]. The factors accounting for the excellent photocatalytic performance of HgI₂ was also proposed.

2. Experimental

2.1. Preparation

At room temperature, 1 mmol of Hg(NO₃)₂·2H₂O, 2 mmol of KI and 0.2 mL of NH₃·H₂O (10 mol L⁻¹) were mixed with 100 mL of deionized water in the dark. The brown red precipitate was separated by centrifuging, washing with deionized water for several times, and drying at 60 °C. Thus, the HgI₂ sample was obtained. The Ag₃PO₄ and AgI samples were prepared according to the previously reported procedure [9,13].

2.2. Characterization

SEM experiment was undertaken on a FEI Quanta-200 microscope at an accelerating voltage of 20 kV. XRD patterns were recorded on a D/MAX-2500/PC powder diffractometer under Cu-K_α radiation at a scanning rate of 2θ min⁻¹ = 4° min⁻¹. The accelerating voltage and applied current were 40 kV and 250 mA,

^{*} Corresponding author.

^{**} Corresponding author.

E-mail addresses: jttang1103@126.com (J. Tang), dlihx@163.com (D. Li).

Functional Block Copolymers from Controlled Radical and Ring Opening Polymerization¹

Qingquan Liu, Mingda Wu, Yinxiang Duan, Baoli Ou, Bo Liao, Shaohua Shen, and Hu Zhou

School of Chemistry and Chemical Engineering, Key Laboratory of Theoretical Chemistry and Molecular Simulation of Ministry of Education, Hunan University of Science and Technology, Xiangtan 411201, China

e-mail: qqliu@hnust.edu.cn, hzhou@hnust.edu.cn

Received November 18, 2014;

Revised Manuscript Received March 1, 2015

Abstract—Three techniques of controlled radical polymerization, namely nitroxide-mediated radical polymerization (NMRP), atom transfer radical polymerization (ATRP), and reversible addition-fragmentation chain transfer (RAFT) polymerization in combination with ring opening polymerization (ROP) were employed to prepare functional block-copolymers with controllable molecular weight and narrow molecular weight distribution. The structure, molecular weight, and PDI of block-copolymers were characterized by various techniques. The synthesis routes of NMRP-ROP, ROP-ATRP, and ROP-RAFT exhibited excellent controllable features in the preparation of functional block-copolymers.

DOI: 10.1134/S1560090415050097

INTRODUCTION

Recent development of controlled radical polymerization resulted in the preparation of a great deal of well-defined polymers with predictable molecular weights [1, 2]. The most important methods reported include nitroxide-mediated polymerization (NMP), atom transfer radical polymerization (ATRP), and reversible addition-fragmentation chain transfer (RAFT) polymerization. In general, controlled radical polymerization in combination with ring opening polymerization (ROP) has been employed to synthesize numerous functional block copolymers [3–5].

Functional block copolymers including amphiphilic one have huge application prospects due to their special properties. For example, polystyrene-*b*-polylactide (PS-*b*-PLA) had been extensively used in the field of optical active materials [6], ordered nanoporous membrane [7], polymer monoliths with ordered nanoporous channels [8], template materials for nanomaterials growth [9], etc. In the application of ordered nanoporous monoliths, PS-*b*-PLA forms ordered microstructure by solution casting and anneal inducing microphase separation, and ordered porous monoliths will be generated with etching process of PLA block [8]. The molecular weight of the blocks and their molar ratio are the key factors for governing the pore size of monoliths. Poor control over the molecular weight and the block ratio of the copolymers will result in defects of

pore structure [8, 9]. Therefore, the precise control over molecular weight of each block is significantly important for the application of PS-*b*-PLA copolymers.

In order to synthesize PS-*b*-PLA with well-defined architectures, we have combined controlled radical polymerization with ROP applying two synthetic strategies. In the first case, PS macroinitiator was used for PS-*b*-PLA synthesis. In the second one, PLA macroinitiator was generated by ROP, and then PLA-*b*-PS was synthesized by controlled radical polymerization. In the present study controllability, experimental feasibility and convenience of these strategies are analyzed.

EXPERIMENTAL

Materials

2,2'-Azo-bis-isobutyronitrile (AIBN) was purchased from Linfeng Chem Co. Ltd, China; it was recrystallized from methanol before use. Styrene was purified from inhibitor, dried over anhydrous magnesium sulfate, and distilled under vacuum. 4-Hydroxy-2,2,6,6-tetramethyl piperidinyloxy (HTEMPO), stannous octoate (Sn(Oct)₂), 2-bromoisobutyrate bromide, CuBr, *N,N,N',N''*-pentamethyldiethylenetriamine (PMDETA), dicyclohexylcarbodiimide (DCCD), 4-dimethylaminopyridine (DMAP) and *D,L*-lactide were purchased from the Aldrich Chemicals and used without further purification. *S*-1-Dode-

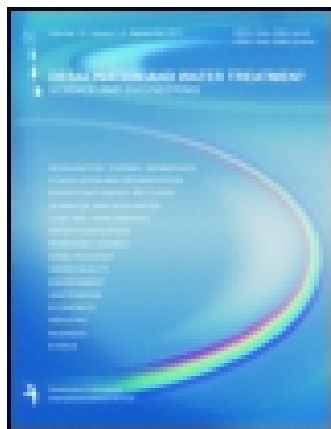
¹ The article is published in the original.

This article was downloaded by: [University of Arizona]

On: 06 July 2014, At: 06:02

Publisher: Taylor & Francis

Informa Ltd Registered in England and Wales Registered Number: 1072954 Registered office: Mortimer House, 37-41 Mortimer Street, London W1T 3JH, UK



Desalination and Water Treatment

Publication details, including instructions for authors and subscription information:

<http://www.tandfonline.com/loi/tdwt20>

A ion-imprinted chitosan/ Al_2O_3 composite material for selective separation of copper(II)

Jianxian Zeng^a, Huajun Chen^a, Xinke Yuan^b, Qiannan Guo^a & Xie Yu^a

^a Key Laboratory of Theoretical Chemistry and Molecular Simulation of Ministry of Education, School of Chemistry and Chemical Engineering, Hunan Province College Key Laboratory of QSAR/QSPR, Hunan University of Science and Technology, Xiangtan 411201, China, Tel. +86 731 58290045; Fax: +86 731 58290509

^b Technology Center of China Tobacco Hunan Industrial Co., Ltd., Changsha 410007, P.R. China, Tel. +86 015907367824

Published online: 06 Jun 2014.

To cite this article: Jianxian Zeng, Huajun Chen, Xinke Yuan, Qiannan Guo & Xie Yu (2014): A ion-imprinted chitosan/ Al_2O_3 composite material for selective separation of copper(II), *Desalination and Water Treatment*, DOI: [10.1080/19443994.2014.923332](https://doi.org/10.1080/19443994.2014.923332)

To link to this article: <http://dx.doi.org/10.1080/19443994.2014.923332>

PLEASE SCROLL DOWN FOR ARTICLE

Taylor & Francis makes every effort to ensure the accuracy of all the information (the "Content") contained in the publications on our platform. However, Taylor & Francis, our agents, and our licensors make no representations or warranties whatsoever as to the accuracy, completeness, or suitability for any purpose of the Content. Any opinions and views expressed in this publication are the opinions and views of the authors, and are not the views of or endorsed by Taylor & Francis. The accuracy of the Content should not be relied upon and should be independently verified with primary sources of information. Taylor and Francis shall not be liable for any losses, actions, claims, proceedings, demands, costs, expenses, damages, and other liabilities whatsoever or howsoever caused arising directly or indirectly in connection with, in relation to or arising out of the use of the Content.

This article may be used for research, teaching, and private study purposes. Any substantial or systematic reproduction, redistribution, reselling, loan, sub-licensing, systematic supply, or distribution in any form to anyone is expressly forbidden. Terms & Conditions of access and use can be found at <http://www.tandfonline.com/page/terms-and-conditions>

对位-二取代氮苄叉苯胺还原电位的取代基效应

曹晨忠* 毕亚坤 曹朝暉

(湖南科技大学化学化工学院 理论有机化学与功能分子教育部重点实验室
分子构效关系湖南省普通高校重点实验室 湘潭 411201)

摘要 合成 52 种 4,4'-二取代氮苄叉苯胺衍生物 p -XPhCH=NC₆H₄Y- p 作为模型化合物, 系统地研究了取代基效应对其还原电位 E_{Red} 的影响规律. 通过研究表明该类化合物的 E_{Red} 与桥连键 C=N 的 ¹³C NMR 化学位移 $\delta_{\text{C}}(\text{C}=\text{N})$ 没有线性关系, E_{Red} 和 $\delta_{\text{C}}(\text{C}=\text{N})$ 两者的影响因素有较大差别, 仅用 Hammett 取代基常数不能很好地表达 E_{Red} 的变化规律. 影响 E_{Red} 的主要因素有: 取代基 X 的场/诱导效应、取代基 X 和 Y 的共轭效应, 此外取代基 X 的激发态取代基参数也有重要影响. 上述 4 个参数与 52 种化合物的 E_{Red} 有良好的相关性, 相关系数为 0.9756, 标准偏差为 0.052 V. 在这 4 个影响因素中, 基团 X 的场/诱导效应、共轭效应和激发态取代基效应对 E_{Red} 改变的贡献都比较大, 而基团 Y 的共轭效应对还原电位 E_{Red} 改变的贡献相对较小, 但不能忽略它.

关键词 取代氮苄叉苯胺; 还原电位; 取代基效应; 激发态取代基参数; 化学位移

Effect of Substituents on Reduction Potential of Para-disubstituted N-Benzylidenebenzenamine Derivatives

Cao, Chenzhong* Bi, Yakun Cao, Chaotun

(Key Laboratory of Theoretical Organic Chemistry and Function Molecule, Ministry of Education, Hunan Provincial University Key Laboratory of QSAR/QSPR, School of Chemistry and Chemical Engineering, Hunan University of Science and Technology, Xiangtan 411201)

Abstract 52 samples of 4,4'-disubstituted *N*-benzylidenebenzenamine (p -XPhCH=NC₆H₄Y- p) derivatives were synthesized, the effect of substituents on the reduction potential E_{Red} of these compounds was systematically investigated. The result shows that there is not linear relation between their E_{Red} and the chemical shift $\delta_{\text{C}}(\text{C}=\text{N})$ of the ¹³C NMR of C=N bridge bond in the molecules. The factors affecting E_{Red} are obvious different from that affecting on $\delta_{\text{C}}(\text{C}=\text{N})$, and the change regularity of E_{Red} can not be expressed well by only employing Hammett substituent constant. The main factors affecting the E_{Red} are the field/inductive effect of substituent X, the conjugative effects of substituents X and Y, and the excited-state substituent constant of substituent X plays an important role of influence on E_{Red} . Above four parameters have good correlations with the E_{Red} of the 52 samples of compounds, the correlation coefficient of the correlation equation is 0.9756, and the standard derivation is 0.052 V. Among the four factors, the contributions of the field/inductive effect, the conjugative effect and the excited-state substituent constant of group X to the changes of E_{Red} are relative large, while the contribution of the conjugative effect of group Y is relative small, and can not be ignored.

Keywords substituted *N*-benzylidenebenzenamine; reduction potential; substituent effect; excited-state substituent parameter; chemical shift

席夫碱是一类常见的有机化合物, 在多方面有重要的用途. 例如, 席夫碱的 C=N 双键是一个极性键, 易于被还原成 CHNH 键, 该反应在有机合成中具有广泛的应用. 而取代氮苄叉苯胺衍生物 XC₆H₄CH=NC₆H₄Y

是一类含有 π 电子共轭体系的席夫碱类衍生物, 当两端苯环连接不同取代基时, 会改变整个分子内的电子云分布, 从而影响该化合物的物理化学性质. 近年来, 曹晨忠等^[1-4]研究了取代基效应对取代氮苄叉苯胺衍生物

* E-mail: czcao@hnust.edu.cn

Received November 25, 2014; revised December 16, 2014; published online February 2, 2015.

Project supported by the National Natural Science Foundation of China (No. 21272063), the Scientific Research Fund of Hunan Provincial Education Department (No. 14C0466), and the Natural Science Foundation of Hunan Province (No. 14JJ3112).

国家自然科学基金(No. 21272063)、湖南省教育厅科研(No. 14C0466)及湖南省自然科学基金(No. 14JJ3112)资助项目.

Synthesis of Tetrahydrothiophene and Thiophene-fused Porphyrin

Lei-Lei Yang, Xiao-Lian Hu, Zhen-Qiang Tang, and Xiao-Fang Li*

Key Laboratory of Theoretical Organic Chemistry and Functional Molecules, Ministry of Education, School of Chemistry and Chemical Engineering, Hunan University of Science and Technology, Xiangtan, Hunan 411201, P. R. China

(E-mail: lixiaofang@iccas.ac.cn)

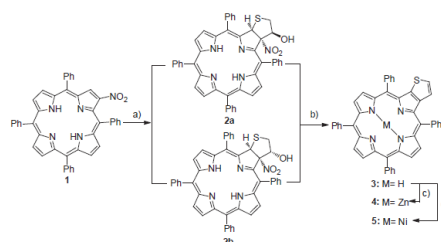
The sulfa-Michael/aldol cascade reaction of 1,4-dithiane-2,5-diol to 2-NO₂-porphyrin has been developed, and this method provides a new facile approach to tetrahydrothiophene-fused porphyrin. Thermal methodologies drive dehydration and aromatization of tetrahydrothiophene-fused porphyrin to form thiophene-fused porphyrin in high yield. The peripheral fused-thiophene did not change the coordination properties of the porphyrin to Zn(II) and Ni(II).

Porphyrins have attracted considerable attention in recent years because of their potential applications in catalysts, molecular sensing, artificial photosynthesis, nonlinear optical materials, molecular wires, photodynamic therapy, and so on.¹ Chemical functionalization of porphyrins has attracted increasing interest because it is not only helpful for understanding the intriguing properties of porphyrins but also of practical significance for potential applications. To date, many methods have been developed to modify porphyrin, and they are mainly focus on two aspects, the macrocycle and peripheral substituents.^{2–4} Among these studies, the introduction of fused π -conjugated segments to the macrocycle is both an important and interesting, which is due to only a small extension of the porphyrin π system maybe leading to largely altered properties.⁵

π -Extended porphyrins are well-known for their unusual properties such as strong absorption in the far-red region of the electromagnetic spectrum, which offers opportunities for technology and medicine that arise from their linear and nonlinear optical properties.^{6,7} In addition, the introduction of fused π -conjugated segments for porphyrins will give these new compounds a significant modification of their optical features, redox characteristics, and the HOMO–LUMO energy gap, which are expected to have applications in various types of functional materials.⁸ Until now, various methods have been utilized to synthesize π -extended porphyrins and a variety π -extended porphyrins have been synthesized by fusing benzene,⁹ corannulene,¹⁰ naphthalene,¹¹ anthracene,¹² pyrene,¹³ and azulene^{5a} through the meso- and β -positions of porphyrins. Thiophene, as an important heterocyclic compound, was also introduced to porphyrin and the 2,3-thieno-bridged porphyrin showed a larger antiaromatic contribution than did the 3,4-thieno-bridged porphyrin.¹⁴

In the present work, for the first time we report a high selectivity synthetic strategy to synthesis tetrahydrothiophene-fused porphyrin across the β -position of porphyrin by sulfa-Michael/aldol-type reaction between 2-NO₂-porphyrin and 1,4-dithiane-2,5-diol. And then, tetrahydrothiophene-fused porphyrin can transform to thiophene-fused porphyrin conveniently through a dehydration and aromatization reaction (Scheme 1).

1,4-Dithiane-2,5-diol,¹⁵ the mercaptoacetaldehyde dimer, is a convenient and efficient synthon which can react with



Scheme 1. Synthesis of tetrahydrothiophene-fused porphyrin and thiophene-fused porphyrin. Reaction conditions: a) 1,4-dithiane-2,5-diol (2 equiv), base, dichloromethane, rt; b) dimethyl sulfoxide (DMSO), 190 °C, 5 min; c) Zn(OAc)₂ (10 equiv), ethanol/chloroform, 50 °C, 3 h; d) Ni(OAc)₂ (10 equiv), ethanol/chloroform, 50 °C, 12 h.

Table 1. Optimization of the reaction conditions

Entry ^a	Base	Solvent	T/°C	t/h	Yield/%	
					2a	2b
1	Et ₃ N	toluene	rt	12	55	20
2	Et ₃ N	toluene	100	12	56	22
3	Et ₃ N	THF	rt	12	28	10
4	Et ₃ N	THF/CH ₃ OH ^b	rt	12	45	20
5	Et ₃ N	THF/CH ₃ OH ^b	70	12	46	24
6	Et ₃ N	DMF	rt	12	35	18
7	Et ₃ N	DCM	rt	12	60	25
8	K ₂ CO ₃	DCM	rt	12	32	16
9	Cs ₂ CO ₃	DCM	rt	12	48	12
10	DBU	DCM	rt	10 min	trace	40
11	Et ₃ N ^c	DCM	rt	2	70	trace

^aUnless otherwise specified, the reactions were carried out with **1** (0.015 mmol), 1,4-dithiane-2,5-diol (0.03 mmol), base (0.03 mmol), in the solvent (5 mL). ^bV_{THF}:V_{EtOH} = 5:1. ^cEt₃N (0.15 mmol) was used.

nitroalkenes and provide nitrotetrahydrothiophene derivatives. So we tested the sulfa-Michael/aldol cascade reaction of 1,4-dithiane-2,5-diol to 2-NO₂-porphyrin **1**. In an initial study, we investigated a series of organic solvents and bases for the sulfa-Michael/aldol cascade reaction between 2-NO₂-porphyrin **1** and 1,4-dithiane-2,5-diol (Table 1). First, we picked several solvents to test the influence of solvent in the sulfa-Michael/aldol cascade reaction. In each case the experiment was conducted for 12 h. The reaction was indicated by the change in the solution color from green to red-brown, and its progress was monitored

One-Pot Preparation of Multicolor Polymeric Nanoparticles with High Brightness by Single Wavelength Excitation

Jian Chen,^{1,2} Fuhua Huang,¹ Hong Wang,¹ Ya Li,¹ Shengli Liu,¹ Pinggui Yi¹

¹Key Laboratory of Theoretical Organic Chemistry and Functional Molecule of Ministry of Education, Hunan Province College Key Laboratory of QSAR/QSPR, School of Chemistry and Chemical Engineering, Hunan University of Science and Technology, Xiangtan 411201, People's Republic of China

²State Key Laboratory of Chemo/Biosensing and Chemometrics, Hunan University, Changsha 410082, People's Republic of China
 Correspondence to: J. Chen (E-mail: cj0066@gmail.com)

ABSTRACT: Fluorescent nanoparticles with multiplex distinct emission signatures and high brightness by a single wavelength excitation are substantially needed in multiplex bioassays and imaging. In this study, we synthesized fluorescent polymeric nanoparticles incorporated with three polymerizable organic dyes via a one-pot miniemulsion. By altering the doping ratio of three tandem dyes, the nanoparticles display abundant multiple fluorescence such as blue, cyan, green, orange, pink, red etc., together with distinguishable emission signatures under a single wavelength excitation, which were arising from the effective fluorescence resonance energy transfer (FRET) between the three energy-matched dyes. Meanwhile, a large Stokes shift (up to 250 nm) can be generated by taking place multiple FRET cascade mechanism between donor and acceptor fluorophores in nanoparticles, which also suggests broad applications in biological labeling and imaging. Moreover, these nanoparticles are uniform in size, highly bright, excellently photostable, and shown prominent longterm stability. Overall, the novel multicolor fluorescent polymeric nanoparticles augur well for their potential applications in multiplexed bioanalysis and emitting displays. © 2014 Wiley Periodicals, Inc. *J. Appl. Polym. Sci.* **2015**, *132*, 41492.

KEYWORDS: colloids; dyes/pigments; nanoparticles; nanowires and nanocrystals; optical properties

Received 27 June 2014; accepted 2 September 2014

DOI: 10.1002/app.41492

INTRODUCTION

Recently, elaboration of nanomaterials which emit multi distinguishable fluorescence signals under a single wavelength excitation have attracted considerable attention in many fields including multiplexed bioassay,¹ cell labelling,² detection of cancer cells,³ monitoring of bacteria,⁴ ratiometric sensor,⁵ and emitting displays⁶ etc. Generally, the known pathways toward fabrication of multicolor fluorescent system mainly concern quantum dots (QDs), which possess tunable emission wavelength and wide absorption bands.^{7,8} Ideally, by using QDs with six colours in 10 different intensities, a library of approximately one million optically encoded polymer microspheres were generated for parallel and high throughput analysis.¹ Moreover, QDs as multiplexed imaging probes have also revealed significant potential for *in vivo* applications. For example, QDs were evaluated for *in vivo* multiplex imaging of mouse embryonic stem cells and lymphatic basins,^{9,10} However, application of QDs as probes is often hindered by their sporadic blink, unsure long-term cytotoxicity and tedious surface functionalization.^{11,12}

Nowadays, other fascinating routes involve multicolor fluorescent nanoparticles (MFNs) assembled from materials like polymer, gold, silica and other inorganic materials have also been investigated.^{3–6,13–35} Most of these nanoparticles were designed with the encapsulation of three or more tandem organic/inorganic fluorophores, to construct a cascade fluorescence resonance energy transfer (FRET) system upon excitation.^{3–6,13–26} By varying the choice, the amount and the ratio of incorporated dyes, the MFN could reveal desired multicolor as well as fine-tuned emission spectra under a single wavelength excitation. For example, Tan et al.¹³ synthesized novel FRET-mediated multicolor silica nanoparticles, which exhibit tunable multi emissions by combination of three tandem fluorescent dyes, and further used them for simultaneous multiplexed monitoring of cancer cells and bacterial pathogens with the desired degree of sensitivity and selectivity.^{3,4} Law et al.¹⁴ prepared a series of biocompatible fluorescent polymer nanoparticles with multi distinct emission signatures by doping with combinations of four carbocyanine-based fluorophores, and used them for multiplexed imaging. Liu et al.¹⁷ reported the fabrication of

Additional Supporting Information may be found in the online version of this article.

© 2014 Wiley Periodicals, Inc.

Synthesis of novel spiro[cyclopropane-pyrrolizin] derivatives via Mg-mediated conjugate addition of bromoform

Bin Liu · Xiao Fang Li · Jie Zhang ·
Meng Ting Wang · Rong Jin Zeng

Received: 7 May 2013 / Accepted: 23 July 2013 / Published online: 9 August 2013
© Springer Science+Business Media Dordrecht 2013

Abstract The conjugate addition of bromoform with 2-arylene-2,3-dihydro-1*H*-pyrrolizin-1-ones in the presence of magnesium afforded novel 2,2-dibromo-3-arylspiro[cyclopropane-1,2'-pyrrolizin]-1'(3'*H*)-ones in moderate yield. The structures of all the products were characterized thoroughly by ¹H NMR, ¹³C NMR, infrared spectroscopy, and mass spectrum.

Keywords Spiroheterocycle · Conjugate addition · Cyclopropane · Pyrrolizin

Introduction

Pyrrolizinone is an important example of the heterocyclic compounds which contain a nitrogen atom [1, 2]. At the same time, pyrrolizinone is also a key building block of some natural pharmacologically relevant alkaloids [3]. Some compounds which have the structure of pyrrolizinone have aroused great interest because of their broad spectrum of biological activities, such as anti-inflammatory [4], analgesic [5], antidiabetic [6], psychostimulant [7], antitubulin [8], photosensitizing [9], and neurokinin-1 (NK1) antagonists [10].

On the other hand, the cyclopropane ring also has a significant part in a wide variety of natural products and drug molecules (Fig. 1) [11–13]. In the past years, a lot of chemists have examined methods of how to synthesis and separate them.

B. Liu · X. F. Li (✉) · J. Zhang · M. T. Wang · R. J. Zeng (✉)
Key Laboratory of Theoretical Chemistry and Molecular Simulation of Ministry of Education,
Hunan Province College Key Laboratory of QSAR/QSPR, School of Chemistry and Chemical
Engineering, Hunan University of Science and Technology, Xiangtan 411201, Hunan, China
e-mail: lixiaofang@iccas.ac.cn

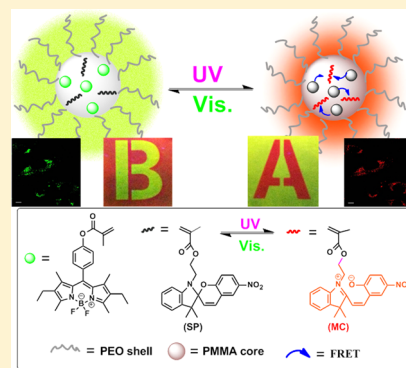
R. J. Zeng
e-mail: rjzeng@hnust.cn

Amphiphilic BODIPY-Based Photoswitchable Fluorescent Polymeric Nanoparticles for Rewritable Patterning and Dual-Color Cell Imaging

Jian Chen,^{*,†,‡} Weibang Zhong,[†] Ying Tang,[‡] Zhan Wu,[‡] Ya Li,[†] Pinggui Yi,^{*,†} and Jianhui Jiang^{*,‡}[†]Key Laboratory of Theoretical Organic Chemistry and Functional Molecule of Ministry of Education, Hunan University of Science and Technology, Xiangtan 411201, P. R. China[‡]State Key Laboratory of Chemo/Biosensing and Chemometrics, Hunan University, Changsha 410082, P. R. China

Supporting Information

ABSTRACT: Photoswitchable fluorescent polymeric nanoparticles (PFPNs) with controllable molecular weight, high contrast, biocompatibility, and prominent photostability are highly desirable but still scarce for rewritable printing, super-resolution bioimaging, and rewritable data storage. In this study, novel amphiphilic BODIPY-based PFPNs with considerable merits are first synthesized by a facile one-pot RAFT-mediated miniemulsion polymerization method. The polymerization is performed by adopting polymerizable BODIPY and spiropyran derivatives, together with MMA as monomer, and mediated by utilizing biocompatible PEO macro-RAFT agent as both control agent and reactive stabilizer. The amphiphilic BODIPY-based PFPNs not only exhibit reversibly photoswitchable fluorescence properties under the alternative UV and visible light illumination through induced intraparticle fluorescence resonance energy transfer (FRET) but also display controllable molecular weight with narrow polydispersity index (PDI), high contrast of fluorescence, tunable energy transfer efficiency, good biocompatibility, excellent photostability, favorable photo-reversibility, etc. The as-prepared PFPNs are successfully demonstrated for rewritable fluorescence patterning and high-contrast dual-color fluorescence imaging of living cells, implying its potential for rewritable data storage and broad biological applications in cell biology and diagnostics.



INTRODUCTION

The successful preparation of photoswitchable fluorescent nanoparticles (PFNs) has been extensively studied for their potential applications as chemical sensing, rewritable data storage, and ultrahigh-resolution biological imaging.¹ In general, PFNs often utilize photochromic compounds, such as spiropyrans,² diarylethenes,³ and spirooxazines,⁴ to bring photoswitchable fluorescence property. In a popular fluorescence resonance energy transfer (FRET) strategy, these photochromes, like spiropyrans,² usually act as switchable energy acceptors under the irradiation of UV or visible light to quench or recover the fluorescence of another nearby energy-matched fluorophores (energy donor). Obviously, these are the desired features which help to overcome the autofluorescence interference of cells in bioimaging or surpass the limitation of spatial resolution of ~250 nm for routine fluorescence microscopy.^{1a,5}

To date, various strategies such as surface modification,⁶ self-assembly method,⁷ and microemulsion^{2a,b} or miniemulsion polymerization,⁸ etc., have been employed to prepare various PFNs. However, it is noteworthy that the surface modification of fluorescent nanoparticles like quantum dots has potential defects such as blinking and cytotoxicity,⁹ and the self-assembly strategy often involves a complicated synthesis,⁷ while the adoption of microemulsion polymerization is hard to modulate the amount of embedded dyes,^{2a,b} which is ascribed to the

different diffusion coefficients between the selected dyes with monomer or matrix in water (or another media). In addition, many reported PFNs often introduced fluorescent dyes via doping or physical adsorption, which implies potential dye leakage and aggregation, significantly limiting their advanced biological applications.^{2d,8c} Notably, although traditional miniemulsion polymerization has displayed some advantages for preparing PFNs, such as facile and versatile preparation route, improved photostability, and tunable amount of incorporated dyes,⁸ there are still some problems like surfactant migration or desorption need to be resolved, when adopting general ionic surfactant like sodium dodecyl sulfate (SDS).¹⁰ In addition, the radical polymerization process in conventional miniemulsion strategy also cannot control the polymerization rate and the polydispersity index (PDI) of formed polymer, which will bring undesirable effects on the architecture of prepared polymers or the morphology of particles.¹⁰ To overcome these drawbacks, a facile and elegant way is to adopt reversible addition–fragmentation chain transfer (RAFT)-mediated miniemulsion polymerization strategy and use amphiphilic macromolecular (macro-) RAFT agents as both stabilizer and control agent.¹¹ These macro-RAFT agents

Received: March 30, 2015

Revised: May 4, 2015

Published: May 21, 2015



Short Communication

Facile hydrothermal-carbonization approach to carbon-modified BiVO₄ composites with enhanced photocatalytic activity



Jianting Tang^{a,*}, Beibei Song^a, Qian Deng^a, Hongchuan Xin^b

^a Key Laboratory of Theoretical Organic Chemistry and Function Molecule of Ministry of Education, Hunan Province College Key Laboratory of QSAR/QSPR, School of Chemistry and Chemical Engineering, Hunan University of Science and Technology, Xiangtan 411201, China

^b Key Laboratory of Biofuels, Qingdao Institute of Bioenergy and Bioprocess Technology, Chinese Academy of Sciences, Qingdao 266101, China

ARTICLE INFO

Available online 20 March 2015

Keywords:

Photocatalysis
Carbon-materials
Semiconductor
Composite materials

ABSTRACT

In this study, a series of carbon-modified BiVO₄ composites were prepared by hydrothermal-carbonization method using glucose as carbonaceous resource. The composites were characterized by X-ray diffraction (XRD), ultraviolet–visible diffuse reflectance spectrum (UV–vis DRS), scanning electron microscopy (SEM), transmission electron microscopy (TEM) and photoluminescence (PL) techniques. The photocatalytic activity of the composites was evaluated in degradation of methylene blue (MB) dye under irradiation of visible light. It was found that the carbon content of the composites plays an important role in the photocatalytic degradation, and the photocatalytic activity of carbon-modified BiVO₄ composites is higher than that of pure BiVO₄. The higher photocatalytic activity of the composites can be attributed to their higher adsorption capacity and higher separation efficiency of photo-generated carriers.

© 2015 Elsevier Ltd. All rights reserved.

1. Introduction

Recently, semiconductor photocatalysts are increasingly important due to their application in treatment of environmental pollution with sustainable solar energy [1–5]. The key issue to utilize solar energy in photocatalysis is the use of visible-light-responsive photocatalysts. Therefore, many efforts have been made to design novel materials as visible-light-responsive photocatalysts to deal with the environmental problems [6–9]. Bismuth vanadate (BiVO₄), with a band gap of 2.4 eV that allows direct photo-activation under visible light, has been widely used in photocatalytic evolution of O₂ and degradation of organic pollutants [10–12]. As a photocatalyst, BiVO₄ is attractive because of its low toxicity, low cost and high stability [10–12]. However, it

suffers from serious issue of low activity due to the rapid recombination of photogenerated electrons and holes in photocatalytic process [13,14], which is the main hindrance to its practical application in photocatalysis. Therefore, the BiVO₄ materials doped with other components have received increasing attention due to their improved photocatalytic activity as a result of the increased separation efficiency of photogenerated electron–hole pairs as well as the extended photo-responsive range, etc. [15–18].

The preparation of functional materials starting from cheap natural precursors through environmentally friendly processes is a highly interesting subject in material science today [19–21]. Much attention has been focused on hydrothermal-carbonization process with the use of plant biomass to produce functional carbonaceous materials because the process is facile and well-controlled. Various cheap and sustainable carbonaceous materials with desirable nanostructure were prepared by this method under mild conditions for a wide range of applications [19–21]. Recently,

* Corresponding author. Tel./fax: +86 73158290045.
E-mail address: jttang1103@126.com (J. Tang).

Comparison of the ^{13}C (C=N) chemical shifts of substituted *N*-(phenyl-ethylene)-anilines and substituted *N*-(benzylidene)-anilines

Zhongzhong Cao^{a,b}, Chaotun Cao^{a,b} and Chenzhong Cao^{a,b*}

Comparison of ^{13}C NMR of C=N bond chemical shifts $\delta_{\text{C}}(\text{C}=\text{N})$ in substituted *N*-(phenyl-ethylene)-anilines $\text{XArC}(\text{Me})=\text{NArY}$ (XPEAYs) with that in substituted *N*-(benzylidene)-anilines $\text{XArCH}=\text{NArY}$ (XBAYs) was carried out. The $\delta_{\text{C}}(\text{C}=\text{N})$ of 61 samples of XPEAYs were measured, and the substituent effect on their $\delta_{\text{C}}(\text{C}=\text{N})$ were investigated. The results show the factors affecting the $\delta_{\text{C}}(\text{C}=\text{N})$ of XPEAYs are quite different from that of XBAYs. A penta-parameter correlation equation was obtained for the 61 compounds, which has correlation coefficient 0.9922 and standard error 0.12 ppm. The result indicates that, in XPEAYs, the inductive effects of substituents X and Y are major factors affecting the $\delta_{\text{C}}(\text{C}=\text{N})$, while the conjugative effect of them have very little effect on the $\delta_{\text{C}}(\text{C}=\text{N})$ and can be ignored. The substituent-specific cross-interaction effects between X and Y and between Me of C=N bond and substituent Y are important factors affecting the $\delta_{\text{C}}(\text{C}=\text{N})$. Also, the excited-state substituent parameter of substitute Y has certain contribution to the $\delta_{\text{C}}(\text{C}=\text{N})$. Copyright © 2015 John Wiley & Sons, Ltd.

Keywords: ^{13}C NMR chemical shifts; excited-state substituent parameter; inductive effect of substituent; *N*-(phenyl-ethylene)-anilines; substituent specific cross-interaction effect

INTRODUCTION

The substituted anilines $\text{XArCR}=\text{NArY}$ have been attracted widespread attention because of its special nonlinear optical properties.^[1–10] Their molecules have a π -electron conjugate system carrying a group at one end and another group at the opposite end, so their optical and electrical properties are more susceptible to subtle changes of the molecular structures. Therefore, it is a meaningful work to probe the substituent effect on its regularity of molecular internal charge distribution for understanding and predicting the physicochemical property of this kind of compounds.^[10–17] The NMR spectra are often used for investigating^[5–7] the substituent effect on its regularity of molecular internal charge distribution by measuring the chemical shifts of the atom in molecular specific position.

Neuvonen^[3–12] has investigated the substituent effects on the electronic characteristic of the C=N bridging group in substituted *N*-(benzylidene)-anilines $\text{XArCH}=\text{NArY}$ (abbreviated XBAYs) with the ^{13}C NMR chemical shifts $\delta_{\text{C}}(\text{C}=\text{N})$ of C=N bond and obtained the valuable results: (1) for the X-substituents: electron-withdrawing group (EWG) cause shielding, while electron-donating group (EDG) behave oppositely; (2) in contrast, for the Y-substituents: EWG cause deshielding, while EDG cause shielding of the C=N bond. Neuvonen^[9,10] pointed out: 'the presence of the specific cross-interaction between X and Y could be verified', but this specific cross-interaction effect was not be quantified at that time. Recently, Cao^[18–20] *et al.* developed Neuvonen's research by exploring the other properties of XBAYs and proposed the parameter $\Delta\sigma^2$ to measure the substituent-specific cross-interaction effect between substituents X and Y. Here, $\Delta\sigma^2 = [\sigma_{\text{X}} - \sigma_{\text{Y}}]^2 = \{[\sigma_{\text{F}}(\text{X}) + \sigma_{\text{R}}(\text{X})] - [\sigma_{\text{F}}(\text{Y}) + \sigma_{\text{R}}(\text{Y})]\}^2$. They combined the electronic effects of substituents X and Y with the substituent specific cross-interaction between X

and Y to quantify the $\delta_{\text{C}}(\text{C}=\text{N})$. The obtained equation has good predictability. Basing on the previous research, we come up with another series of compounds, substituted *N*-(phenyl-ethylene)-anilines $\text{XArC}(\text{Me})=\text{NArY}$ (abbreviated XPEAYs), whose molecular structure is similar to the XBAYs. In XPEAYs, a group Me replaces the atom H in $\text{CH}=\text{N}$ of XBAYs, and results in more complicated cross-interactions of the substituted groups. For the compounds XBAYs, there are four situations^[18] of interactions among the substituents X and Y, while in the XPEAYs, Me is an EDG and will act with X and Y through the conjugate chain, respectively. It is a very attractive topic whether the change regularity of the $\delta_{\text{C}}(\text{C}=\text{N})$ in XPEAYs is as the same as that in XBAYs or not. Therefore, we investigated the aforementioned topic and obtained meaningful results in this work.

EXPERIMENTAL SECTIONS

Materials prepared

The target compounds were synthesized by heating reflux method.^[21–24] The substituted acetophenone (10 mmol) and the substituted aniline (11 mmol) were mixed in a 50 ml round-bottom flask with 5 ml toluene

* Correspondence to: C. Cao, School of Chemistry and Chemical Engineering, Hunan University of Science and Technology, Xiangtan, 411201, China. E-mail: czcao@hnust.edu.cn

a Z. Cao, C. Cao, C. Cao
School of Chemistry and Chemical Engineering, Hunan University of Science and Technology, Xiangtan, 411201, China

b Z. Cao, C. Cao, C. Cao
Key Laboratory of Theoretical Organic Chemistry and Function Molecule, Ministry of Education, Hunan University of Science and Technology, Xiangtan, 411201, China

Group effect on ionization potential for mono-substituted aliphatic compounds

Guanfan Chen^{a,b,c,*}, Mengzhuo Tang^a, Rongjin Zeng^{a,b,c}, Wanqiang Liu^{a,b,c} and Chenzhong Cao^{a,b,c,*}

ABSTRACT: The group effect on ionization potential for *mono*-substituted aliphatic compounds RX was investigated, and it was found that there is a good relationship between the ionization potential (*IP*) and the parameters, group electronegativity $\chi_{\text{eq},X}$, the group polarizability ΣPEI_{Xr} , and the disperse contribution of single non-bond electron E_{dc} for titled compounds, and these parameters earlier were easily calculated from the molecular structure. Moreover, the B3LYP density functional method was also employed to estimate *IP* values of the same *mono*-substituted aliphatic compounds. The results showed that it was difficult to get reliable ionization data using DFT method, and the regression equation with descriptors $\chi_{\text{eq},X}$, ΣPEI_{Xr} and E_{dc} was more effective than DFT method in predicting *IP* values for titled compounds. The results are helpful to understand the role of group effect on molecular properties. Copyright © 2015 John Wiley & Sons, Ltd.

Keywords: DFT method; group effect; ionization potential; *mono*-substituted aliphatic compound

INTRODUCTION

The ionization potential (*IP*) is an important molecular property that describes the process of removal of an electron from the molecule and the production of a mole-ion, and knowledge of its value is necessary to understand a wide range of processes in chemistry and biology.^[1–5] Although there are many kinds of measurements, such as photoelectron spectroscopy, photoionization mass spectrometry, electron impact techniques, and so on, used to measured *IP* values, there are *IP* values of many compounds untouched because of enormous experimental difficulties. Hence, there is still considerable interest in finding relations between the molecular structures and *IP* values of compounds and predicting the untouched *IP* values of compounds.

For a *mono*-substituted compound YX, it can be divided into a substituent/functional segment (collectively called group) X and parent Y, and thus there are two major threads of research. On the one hand, McGlynn *et al.* investigated the effect of variable alkyl R on the ionization potentials of alkylated molecules RX with the restricted Hartree–Fock Self-Consistent Field approach.^[6] Cauwelaert's work showed that there is a relationship between the ionization potential and the Taft factor when molecules belong to a homogeneous series of compounds.^[7] Cherkasov and Jonsson investigated ionization potentials for 48 C-centered radicals with operational atomic parameters, and obtained a good result.^[8] With the Polarizability Effect Index (*PEI*), Cao *et al.* discussed the polarization effect of variable R on the *IP* values for ROH, RSH, RNH₂, RI, RBr, RCHO, and so on.^[9,10] On the other hand, for *IP* data of some *mono*-substituted and *di*-substituted benzenes, Crable and Kearns^[11] found that there is a linear correlation between the *IP* values of *mono*-substituted benzenes or toluenes and σ^+ substituent constants. Benoit also observed that the *IP* values of *mono*-substituted and *di*-substituted benzenes are related to the sum of Brown's σ_p^+ of the substituents for both the *meta*-isomer and *para*-isomer.^[12] To our surprise, there are few researches of the functional segment/substituent effect (collectively called group effect) on

ionization potentials for aliphatic compounds. Recently, for aliphatic compounds, Yuan and Cao^[13] proposed a novel concept system, organic homo-rank compound, and studied the ionization potentials of three sets of homo-rank compounds with $IP_{(j)} = a + bIP_{(1)} + bPEI_{(R)}$, where $IP_{(1)}$ is the ionization potentials of MeX and $PEI_{(R)}$ is the polarization index of alkyl R.

Now, for aliphatic compounds RX in which alkyl R is fixed and group X is varied, what we particularly want to know is the group effect on their *IP* values. In the paper, we aim to extract the descriptors from molecular structures and develop a heuristic formula to quantify the group effect on *IP* values for aliphatic compounds.

RESULTS AND DISCUSSIONS

As we know, the ionization potential of a molecule is given by^[14]

$$IP = E_{\text{total}}^{\text{ion}} - E_{\text{total}}^{\text{molecule}}$$

Generally speaking, the ionization potential of organic compound depends on energy of two states: (1) energy of the initial state (molecular state) and (2) energy of the final state (ionic

* Correspondence to: Guanfan Chen and Chenzhong Cao, School of Chemistry and Chemical Engineering, Hunan University of Science and Technology, Xiangtan 411201, Hunan Province, China.
E-mail: chenguanfan@gmail.com; czcao@hnust.cn

a G. Chen, M. Tang, R. Zeng, W. Liu, C. Cao
School of Chemistry and Chemical Engineering, Hunan University of Science and Technology, Xiangtan 411201, Hunan Province, China

b G. Chen, R. Zeng, W. Liu, C. Cao
Key Laboratory of Theoretical Organic Chemistry and Function Molecule of Ministry of Education, Hunan University of Science and Technology, Xiangtan 411201, Hunan Province, China

c G. Chen, R. Zeng, W. Liu, C. Cao
Hunan Provincial University Key Laboratory of QSAR/QSPR, Xiangtan 411201, Hunan Province, China



One-pot synthesis of a Ni–Mn₃O₄ nanocomposite for supercapacitors



Guo-rong Xu^{*}, Jin-jin Shi, Wen-hao Dong, Ya Wen, Xiang-ping Min, An-ping Tang

School of Chemistry and Chemical Engineering, Hunan University of Science and Technology, Xiangtan 411201, PR China

ARTICLE INFO

Article history:

Received 1 August 2014

Received in revised form 10 January 2015

Accepted 13 January 2015

Available online 19 January 2015

Keywords:

Supercapacitor

Mn₃O₄

Nanocomposite

Chemical precipitation

Electrochemical properties

ABSTRACT

Ni–Mn₃O₄ nanocomposite has been prepared successfully by chemical oxidation in an alkaline solution of Mn²⁺ on the surface of Ni nanoparticles with OH functional groups using one-pot method. The obtained Ni–Mn₃O₄ nanocomposite was characterized using a scanning electron microscope (SEM), a transmission electron microscope (TEM), X-ray diffraction (XRD) analysis and various electrochemical techniques, such as cyclic voltammetry (CV), galvanostatic charge/discharge (GC/D) and electrochemical impedance spectroscopy (EIS). The average crystal sizes of Mn₃O₄ were found to decrease linearly with increasing Ni content in the Ni–Mn₃O₄ composite. The Ni–Mn₃O₄ nanocomposite could be easily conditioned and inverted to birnessite-type MnO₂. A specific capacitance of 230 F g^{−1} (based on pure Mn₃O₄) was obtained for the Ni (17.3%)–Mn₃O₄ nanocomposite at a current rate of 0.25 A g^{−1}, and 94% of the initial capacitance was retained after 1000 GC/D cycles at a current rate of 1 A g^{−1}. It is concluded that the Ni–Mn₃O₄ nanocomposite is a promising electrode materials for supercapacitors.

© 2015 Elsevier B.V. All rights reserved.

1. Introduction

In recent decades, supercapacitors, also known as electrochemical capacitors (ECs), have attracted extensive attention due to their higher power density, longer cycle life than batteries, and higher energy density than conventional dielectric capacitors [1,2]. The range of potential practical applications extends from personal electronics to hybrid electric vehicles. Depending on the charge storage mechanism, supercapacitors are generally divided into two types [3]. The first type is based on the formation of electrical double layers (EDLs) at the interface between surface of a conductive electrode and an electrolyte. The second type is based on a Faraday-type reaction occurring on the electrode material surface, which is called pseudocapacitance because it exhibits a capacitive behavior rather than a distinctly peaked redox behavior normally associated with intercalation. The transition metal oxides/hydroxides with variable valence have been used as electrode materials in pseudocapacitors [4–10]. Among the various candidate transition metal oxides, manganese oxides have been extensively investigated as supercapacitor electrode materials due to their low cost, non-toxicity and abundant raw materials [5,11,12].

Mn₃O₄ is one of the most stable manganese oxides and is considered as a mixed oxidation state of MnO·Mn₂O₃. Recently, a few reports have indicated that Mn₃O₄ can be electrochemically oxidized (conditioned) to birnessite-type MnO₂ after successive

potential cycles [13–18]. For example, Guo et al. reported the synthesis of Mn₃O₄ microspheres and obtained a specific capacitance of 219 F g^{−1} in 1 mol L^{−1} Na₂SO₄ aqueous solution after 400 potential cycles [17]. Komaba et al. studied the condition of the ball-milled Mn₃O₄ in detail and obtained a specific capacitance of 190 F g^{−1} in 1 mol L^{−1} Na₂SO₄ aqueous solution after 250 potential cycles [18]. However, the extremely low electrical conductivity (approximately 10^{−7}–10^{−8} S cm^{−1}) and long conditioning time of Mn₃O₄ largely hinders its practical application in the supercapacitors.

In order to improve the capacitive performance of Mn₃O₄, a promising approach is to fabricate a composite electrode with Mn₃O₄ decorated onto highly conductive materials. Previous work has focused mainly on carbon-based Mn₃O₄ composites [19–23]. For example, Cui et al. synthesized Mn₃O₄/CNTA (carbon nanotube array) composites using the dip-coating method; a specific capacitance of 292 F g^{−1} (based on Mn₃O₄) was obtained in 0.5 M Na₂SO₄ aqueous solution [19]. Li et al. prepared a Mn₃O₄/rGO (reduced graphene oxide) composite via microwave hydrothermal technique; a capacitance as high as 315 F g^{−1} (based on Mn₃O₄) was achieved in 1 M Na₂SO₄ aqueous solution [20]. More recently, Gao et al. developed a by-product free strategy to synthesize graphene/Mn₃O₄ composites with a maximum specific capacitance of 260 F g^{−1} in saturated K₂SO₄ aqueous solution [21]. Although the desired capacitive enhancements have been achieved to some degree, these fabrication techniques are often costly, experimentally intricate, and difficult to produce in large-scale. Despite inten-

^{*} Corresponding author. Tel.: +86 731 58290045.

E-mail address: grxu@hnust.edu.cn (G.-r. Xu).



Contents lists available at ScienceDirect

Bioorganic & Medicinal Chemistry Letters

journal homepage: www.elsevier.com/locate/bmcl

Synthesis and fungicidal activity of novel 2-aryl-3-(1,3,4-thiadiazolyl)-6(8)-methyl-1,3-benzoxazines

Zi-long Tang^{a,b,*}, Zan-wen Xia^a, Shu-hong Chang^a, Zhao-xu Wang^{a,b}^a School of Chemistry and Chemical Engineering, Hunan University of Science and Technology, Xiangtan 411201, China^b Key Laboratory of Theoretical Organic Chemistry and Function Molecule of Ministry of Education, Hunan University of Science and Technology, Xiangtan 411201, China

ARTICLE INFO

Article history:

Received 9 November 2014

Revised 21 April 2015

Accepted 6 May 2015

Available online 15 May 2015

Keywords:

(1,3,4-Thiadiazolyl)-1,3-benzoxazines

Synthesis

TMSCI

Fungicidal activity

ABSTRACT

A class of novel 2-aryl-3-(1,3,4-thiadiazolyl)-6(8)-methyl-1,3-benzoxazines was prepared by reactions of 2-methyl-6-((1,3,4-thiadiazolylamino)methyl)phenols or 4-methyl-2-((1,3,4-thiadiazolylamino)methyl)phenols and 2- or 4-nitrobenzaldehyde in the presence of TMSCI in refluxing toluene. The electron-donating methyl group on the benzene ring played an essential role on the reactivity of the substituted phenols, which was proved by DFT calculation. The fungicidal activity of the resultant products were also preliminarily evaluated, most of which displayed moderate to good fungicidal activity. Especially, compound **6f** showed 98.0% activity against *Sclerotonia sclerotiorum* and *Botrytis cinerea* at concentration of 25 µg/mL.

© 2015 Elsevier Ltd. All rights reserved.

The importance of 1,3-benzoxazine derivatives in biological systems has received much attention because of their broad biological activities, such as analgesic,¹ anticancer,^{2–4} antitumour,⁵ antiplatelet,⁶ antibacterial and fungicidal,^{7–9} antituberculosis,¹⁰ antihypertensive,¹¹ and antithrombotic activities.¹² Particularly, some 1,3-benzoxazines are potential and orally bioavailable CCR2 and CCR5 dual antagonist,¹³ epidermal growth factor receptor (EGFR) tyrosine kinase inhibitors,⁴ anticancer agents¹⁴ and HCV NS5a inhibitor.¹⁵ In addition, 2-unsubstituted 1,3-benzoxazine derivatives are important materials to prepare phenol-formaldehyde resins.^{16–18} Consequently, the synthesis of new 1,3-benzoxazine derivatives with special character attracts great interests from organic chemists. Therefore, many reports have been disclosed to access these chemicals in the past few decades.^{19–26} Previously, we reported the synthesis of substituted 1,3-benzoxazines by reactions of 2-aminomethylphenols and aromatic aldehydes with SnCl₄, (CH₃)₃SiCl (TMSCI) as catalysts,^{8,27–29} and most of which showed good fungicidal activity. As a part of our continuous project aimed at searching for new effective fungicides, we planned to prepare a series of new 2-aryl-3-(1,3,4-thiadiazolyl)-1,3-benzoxazines. However, under the same conditions, the reactions of 2-(1,3,4-thiadiazolylaminomethyl)phenols **4a** or **4b** and aromatic aldehydes to prepare the target compounds failed. Presumably, the reactivity of 2-((1,3,4-thiadiazolylamino)methyl)phenol might be so low because of the electron-withdrawing effect of

1,3,4-thiadiazolyl group. Alternatively, we prepared a new class of 3-(1,3,4-thiadiazolyl)-1,3-benzoxazines by phase transfer catalyzed reactions of 2-((1,3,4-thiadiazolylamino)methyl)phenols and CH₂Cl₂.³⁰ Interestingly, we found that 2-methyl-6-((1,3,4-thiadiazolylamino)methyl)phenol formed by introducing a methyl group on the benzene ring can smoothly react with aromatic aldehydes under the aforementioned conditions, affording the desired 2-aryl-3-(1,3,4-thiadiazolyl)-6(8)-methyl-1,3-benzoxazines (**Scheme 1**). Thus, we present herein the results on the synthesis and fungicidal activity investigation of these compounds.

According to the synthetic route as shown in **Scheme 1**, reactions of 2-amino-5-alkyl/aryl-1,3,4-thiadiazoles **2** with salicylaldehyde or substituted salicylaldehydes with TsOH as catalyst in refluxing anhydrous ethanol smoothly gave out the corresponding Schiff bases **3**, which was reduced by NaBH₄ to 2-((1,3,4-thiadiazolylamino)methyl)phenols **4a–4i**.^{30,31} We then tried the reaction of **4a** (R¹ = H, R² = Me) with 4-nitrobenzaldehyde **5a** in toluene or THF or chloroform/cyclohexane (v:v = 1:4) with SnCl₄ as catalyst,²⁷ the reaction did not occur at all (No. 1–3, **Table 1**), neither did the reaction with TMSCI as catalyst in toluene (No. 4).^{28,29} It was also observed that the reaction of **4b** (R¹ = H, R² = Et) with **5a** in the presence of TMSCI or (CH₃)₃SiI (TMSI) in toluene or chloroform/cyclohexane (v:v = 1:4) failed to yield the desired product (No. 5–7). Likewise, the reaction of **4a** with formaldehyde using TMSCI as catalyst in toluene did not generate the desired product (No. 8). The main reason for these failure is possibly the low reactivity of compound **4a** and **4b** caused by the electron-withdrawing nature of 1,3,4-thiadiazolyl group. Of course,

* Corresponding author. Tel./fax: +86 731 58291379.
E-mail address: zltang67@aliyun.com (Z.-l. Tang).

Polyurethane Membrane with Temperature- and pH-Controllable Permeability for Amino-Acids

Hu Zhou*, Ruiping Xun, Kejian Wu, Zhihua Zhou*, Bin Yu, Youxin Tang, and Ning Li

Key Laboratory of Theoretical Organic Chemistry and Function Molecule, Ministry of Education, Hunan Province College Key Laboratory of QSAR/QSPR, School of Chemistry and Chemical Engineering, Hunan University of Science and Technology, Xiangtan 411201, P. R. China

Received July 31, 2014; Revised September 15, 2014; Accepted September 19, 2014

Abstract: This work was focused on the investigation of the temperature- and pH-responsive polyurethane (PU) membranes and their permeability to amino-acids in response to environmental stimuli. The PU membrane was prepared from a wet phase inversion method and a two-step solution polymerization from polycaprolactone diols (PCL), 4,4'-diphenylmethane diisocyanate (MDI), dimethylol propionic acid (DMPA), *etc.* The chemical structure, phase state, morphology and surface wettability of the membrane were characterized with Fourier transform infrared (FTIR) spectrometer, differential scanning calorimetry (DSC), scanning electron microscopy (SEM) and contact angle tester, respectively. The temperature and pH responses of the membrane were investigated by means of an amino-acid permeate experiment. The L-phenylalanine (L-Phe) was chosen as model amino-acids. The permeation of the L-Phe was measured using a dead-end flow filtration at varied temperatures and pH, and characterized by the permeate flux (J) and rejection coefficient (R). J of the L-Phe across the PU membrane increased with increasing temperature and showed a sharp increase when temperature was raised to the crystalline melting temperature (T_m) of the soft segment of PU, while decreased with increasing pH and having a sharp decrease when pH reached the dissociation constant (pK_a) of DMPA contained in PU macromolecules. While, the R behavior of L-Phe was just opposite from the results of J , which decreased with increasing temperature and increased with increasing pH, also showing the temperature and pH responses. Hopefully, the PU membrane with temperature- and pH-controllable permeability has promising prospects in water treatment, membrane separation, drug delivery system, *etc.*

Keywords: polyurethane, membrane, temperature response, pH response, L-phenylalanine, permeate flux, rejection coefficient.

Introduction

Stimuli-sensitive or -responsive membranes, also called smart membranes, have continuously been studied over several years.¹⁻³ These membranes can reversibly change their pore size, permeability, surface wettability, *etc.* on receiving external stimuli, such as temperature, pH value, ionic strength, chemical cues, light or magnetic fields in environmental conditions.³⁻⁶ Thus, the mass transfer and separation properties of these membranes can be easily regulated by adjusting external stimuli. In particular, the membranes that can respond to dual or even multiple external stimuli are of particular interest, and have been widely studied in recent years. Of all dual stimuli-responsive ones, temperature- and pH-responsive membranes have drawn much attention,⁷⁻⁹ because most physiological environments manifest themselves by a change in tempera-

ture and/or pH.

Thermal sensitive polyurethane (TSPU) is one of the most popular and prominent temperature-responsive polymeric materials.¹⁰⁻¹³ TSPU has a typical block or segmented structure consisting of thermally reversible phases (soft segments) and fixed phases (hard segments).^{10,11} In many cases, the soft segment shows a phase transition temperature (crystalline melting transition or glass transition temperature), which can be used as a switch temperature (T_s). Soft segment softens or hardens when temperature is raised above or reduced below the T_s with sharp changes in physical properties of polymers, especially the changes of free volume hole size or pore size, and micro-Brownian motion of macromolecules.^{10,13} In recent years, many researchers including our team members have focused on utilizing the phase transitions of TSPU to design smart membranes with controllable permeability and applied them in many fields, such as gas purification, food packaging, membrane separation, *etc.*^{10,12-14} Here is an idea: is there a method to fabricate a new kind of PU mem-

*Corresponding Authors. E-mails: hnustchem@163.com or zhouzhihuawu@163.com



Electrochemical preparation, characterization and application of electrodes modified with nickel–cobalt hexacyanoferrate/graphene oxide–carbon nanotubes



Keqin Deng^{a,*}, Chunxiang Li^a, Xiyang Qiu^a, Jianhong Zhou^b, Zhaohui Hou^{c,*}

^a Key Laboratory of Theoretical Organic Chemistry and Function Molecule, Ministry of Education, School of Chemistry and Chemical Engineering, Hunan University of Science and Technology, Xiangtan 411201, PR China

^b School of Life Science, Hunan University of Science and Technology, Xiangtan 411201, PR China

^c School of Chemistry and Chemical Engineering, Hunan Institute of Science and Technology, Yueyang 414006, PR China

ARTICLE INFO

Article history:

Received 24 May 2015

Received in revised form 10 July 2015

Accepted 2 August 2015

Available online 5 August 2015

Keywords:

Graphene oxide

Multi-walled carbon nanotubes

Nickel–cobalt hybrid hexacyanoferrate

Hydroxylamine

ABSTRACT

A nanohybrid of graphene oxide and multiwalled carbon nanotubes (GO–CNTs) was synthesized through π – π interaction. The nickel–cobalt hybrid hexacyanoferrate decorated GO–CNTs (NiCoHCF/GO–CNTs) was prepared by electrodeposition of NiCoHCF in different ratios of Co^{2+} to Ni^{2+} solution on GO–CNTs. The characterization was performed by UV–vis, FT–IR, Raman spectroscopy, and SEM. The electrochemistry behavior of NiCoHCF/GO–CNTs was studied by cyclic voltammetry. The NiCoHCF/GO–CNT modified GCE (NiCoHCF/GO–CNT/GCE) exhibited greatly improved electrocatalytic activity towards electrooxidation of hydroxylamine. The modified electrode exhibited a wide linear range from 0.2 μM to 150 μM and a low detection limit (LOD) of 0.08 μM .

© 2015 Published by Elsevier B.V.

1. Introduction

Graphene oxide (GO) possesses many unique advantages, such as good hydrophilicity, low toxicity, high surface area, and excellent biocompatibility [1]. But, its poor electrical conductivity limits its direct application as electrically active materials. Nanohybrid or nanocomposites can combine the advantages of each component and exhibit improved properties [2–4]. Carbon nanotubes (CNTs) are also very attractive in electroanalysis [5], so combining one-dimensional CNTs with two-dimensional GO and using the hierarchical carbon nanohybrid in the electrochemical determination is worthwhile. Not only can the combination of CNTs and graphene increase the conductivity of GO, but the synergy between CNTs and GO can enhance the electrocatalysis properties of nanohybrid over CNTs or GO alone [6–8].

Metal-hexacyanoferrates (MHCs) belong to a class of polynuclear inorganic compounds. The hybrid hexacyanoferrates, such as nickel–cobalt hexacyanoferrate [9], copper–cobalt hexacyanoferrate [10,11], nickel–palladium hexacyanoferrate [12], cobalt–iron hexacyanoferrate [13,14], and nickel–iron hexacyanoferrate [15] have been studied. These hybrid MHCs possess unique electrochemical property to mediate electrochemical reactions such as electro-catalyzed oxidation of hydrazine [10], cysteine [11], isoniazid [13], and H_2O_2 [14]. They can improve the stability and have a different electrochemical behavior

compared to single component [16]. Recently, the combination of graphene and MHCs for construction of electrochemical sensor has been proposed [17–19]. Due to the synergic electrocatalytic action between graphene and MHCs, the nanocomposites of graphene and MHCs were proved to expand their applications in electroanalytical field [18,19].

In this study, the nanohybrid of GO nanosheets and carboxylated CNTs (GO–CNTs) was prepared through π – π interaction. The nickel–cobalt hybrid hexacyanoferrate (NiCoHCF) was used to decorate the GO–CNTs by electrodeposition process for the first time. The morphology and the electrochemical behavior of the NiCoHCF decorated the GO–CNT nanohybrid (NiCoHCF/GO–CNTs) were characterized. The nanohybrid was used for the electrochemical detection of hydroxylamine with low detection, wide linear rang and good selectivity.

2. Experimental

2.1. Reagents and materials

Graphene oxide was purchased from Nanjing XFNANO Materials Tech Co., Ltd (China). Multi-wall carbon nanotubes (CNTs >95% purity, diameter 10–20 nm, length 5–10 μm) were bought from Aladdin Industrial Inc. Nickel chloride hexahydrate ($\text{NiCl}_2 \cdot 6\text{H}_2\text{O}$), cobalt chloride hexahydrate ($\text{CoCl}_2 \cdot 6\text{H}_2\text{O}$), hydroxylamine, and potassium ferrocyanide ($\text{K}_4\text{Fe}(\text{CN})_6$) were obtained from Shanghai Chemical Reagent Co. (China). All other materials and solvents were of analytical grade and

* Corresponding authors.

E-mail addresses: keqindeng@hnust.edu.cn (K. Deng), zhqh96@163.com (Z. Hou).

CrossMark
click for updatesCite this: *Anal. Methods*, 2015, 7, 266

Trace copper ion detection by the suppressed decolorization of chromotrope 2R complex†

Lili Fu, Yuan Xiong, Shu Chen and Yunfei Long*

Chromotrope 2R (CR) is a monoazo dye, which can be easily degraded under ultraviolet C (UVC) light irradiation. However, the degradation extent of CR is suppressed after it is chelated with Cu^{2+} ions to form a coordination complex (Cu^{2+} -CR). This phenomenon was developed as a novel method for the quantitative detection of Cu^{2+} ions, which is based on determining the change in absorbance (ΔA , the absorbance of Cu^{2+} -CR complex subtracted by that of CR after UVC light irradiation) by UV-visible absorption spectrum. Under the optimal detection conditions, ΔA at 509 nm highly depends on the concentration of Cu^{2+} ions in the range from 5.0×10^{-9} to 1.0×10^{-6} M as expressed by the following equation: $\Delta A = 0.3066 + 0.03605 \lg c$ with the correlation coefficient of $r = 0.9912$. The limit of detection (ld) is 3.4 nM as calculated by the formula $3\sigma = 0.3066 + 0.03605 \lg ld$. This method provides affordable and selective detection of Cu^{2+} ions and was used to detect Cu^{2+} ions in a human hair sample.

Received 10th October 2014
Accepted 30th October 2014

DOI: 10.1039/c4ay02414a

www.rsc.org/methods

1. Introduction

Copper ion (Cu^{2+}) is one of the essential transition metal ions in the human body, and its deficiency or excess may cause health problems.¹ The deficiency of Cu^{2+} may lead to hematological manifestations² and diverse neurological problems.³ Moreover, excess amount of Cu^{2+} may cause gastrointestinal disturbance and neurotoxicity, which is commonly known as Parkinson's disease and Alzheimer's disease, through the deposition of Cu^{2+} in the lenticular nucleus of the brain and liver.^{4,5} Therefore, the analysis and detection of Cu^{2+} in environmental and/or biological samples is of great importance. Various sensors and techniques have been developed for the determination of Cu^{2+} ,⁶⁻⁹ such as organic fluorophores¹⁰ or chromogenic sensors,¹¹ a DNazyme-based method,¹² the colorimetric detection,¹³ absorbance spectrophotometry,¹⁴ atomic absorption spectroscopy (AAS),¹⁵ and inductively coupled plasma mass spectroscopy (ICP-MS).¹⁶ However, a sensitive and selective method for Cu^{2+} detection is still needed.

Chromotrope 2R (ref. 17) (abbreviated as CR, the structure is shown in Scheme 1) is a type of azo dye.^{18,19} CR and/or its homologs have been used to detect nitrate,²⁰ formaldehyde,²¹ methanol,²² titanium,²³ and unsymmetrical dimethylhydrazine.²⁴ Moreover, they were used as chelating agents for metal ions, particularly Cu^{2+} ions.²⁵⁻²⁷ For example, chromotropic acid-intercalated Zn-Al layered double hydroxides have been used to remove Cu^{2+} ions,²⁸ and polyurethane foam/2-(6'-ethyl-

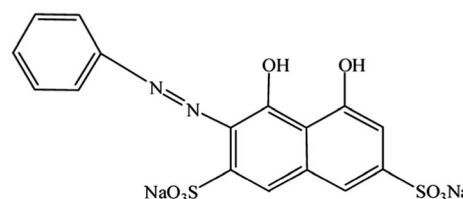
2'-benzothiazolylazo) chromotropic acid has been used to pre-concentrate Cu^{2+} ions in water samples.²⁹

Herein, we found that UVC light induced decolorization of CR could be suppressed after coordinating with Cu^{2+} ions. Furthermore, the decolorization extent of CR depends on the concentration of Cu^{2+} ions. Thus, a novel method for the detection of Cu^{2+} ions was established using UV-visible spectroscopy. The content of Cu^{2+} ions in a human hair sample was detected successfully, indicating its potential application in other environmental and biological samples.

2. Experiment

2.1 Instrumentation

UV-visible absorption spectra were recorded using a Lambda-35 UV-visible spectrophotometer (Perkin Elmer Instruments Inc., USA) and a quartz cell ($1 \times 1 \text{ cm}^2$). Mass spectroscopy (MS) were recorded using an ACQUITY UPLC/Xevo Q-TOF (Waters, USA) instrument. A UVC lamp of 110 W (wavelength range 200–275 nm, Shanghai Yanguang Electronic Technology Co. Ltd., China) was used as the UVC light source. A QL-901 Vortex (Qilinbeier Instrument Manufacturing Co. Ltd., Haimen, China) was used to mix the reaction solution.



Scheme 1 Chemical structure of CR.

Key Laboratory of Theoretical Organic Chemistry and Function Molecule, Ministry of Education, School of Chemistry and Chemical Engineering, Hunan University of Science and Technology, Xiangtan, 411201, PR China. E-mail: L_yunfei927@163.com

† Electronic supplementary information (ESI) available. See DOI: 10.1039/c4ay02414a

A QSPR correlation on the ^{13}C NMR chemical shifts of bridge carbons for different series of aromatic Schiff bases

Guanfan Chen,^{a,b,c,*} Xiangsi Wu,^{a,b,c} Chenzhong Cao,^{a,b,c,*} Fengping Liu,^{a,b,c} Rongjin Zeng^{a,b,c} and Wanqiang Liu^{a,b,c}

Introduction

Nuclear magnetic resonance (NMR) spectroscopy has attracted immense attention because of playing an important role in not only determining molecular structures but also explaining reaction mechanisms, molecular dynamics, chemical equilibrium, etc.^[1] With the advancement of NMR technology, there is more and more NMR experimental information obtained. Consequently, many efforts have been made to understand relationships between molecular structures and different kinds of NMR chemical shifts.^[2–14]

In investigations on ^{13}C NMR of specific carbons for aromatic systems with a changing substituent, the chemical shift (δ_{C}) values are usually calculated with the single substituent parameter treatment or the dual substituent parameter treatment,^[15] shown as Eqns (1) and (2), where σ , σ_{F} (or σ_{I}) and σ_{R} are the Hammett parameter, inductive parameter, and resonance parameter, respectively, and C is a constant.

$$\delta_{\text{C}} = \rho\sigma + C \quad (1)$$

$$\delta_{\text{C}} = \rho_{\text{I}}\sigma_{\text{I}}(\text{or}\rho_{\text{F}}\sigma_{\text{F}}) + \rho_{\text{R}}\sigma_{\text{R}} + C \quad (2)$$

When two substituents in aromatic systems change simultaneously, what will happen to the substituent effect on δ_{C} values of specific carbons? In Neuvonen's studies on δ_{C} values of bridge carbons for *para*-disubstituted benzylidene anilines^[7] (*p*-XBAY-*p*, shown in Scheme 1) and *para*-disubstituted phenyl benzoates,^[6] Eqn (3) was recommended to correlate with the corresponding experimental dataset. Cao's group synthesized successively a series of *para*-disubstituted cinnamyl anilines (*p*-XCAY-*p*)^[16] and a series of *para*-disubstituted benzylidene *N*-(4-substituted styryl)anilines (*p*-XBSAY-*p*)^[17] whose structures are shown in Scheme 1, and research results indicated that δ_{C} values of specific bridge carbons can be correlated well with Eqn (3).

$$\delta_{\text{C}} = \rho\sigma_{\text{F}}(\text{X}) + \rho\sigma_{\text{R}}(\text{X}) + \rho\sigma_{\text{F}}(\text{Y}) + \rho\sigma_{\text{R}}(\text{Y}) + C \quad (3)$$

On this basis, Cao *et al.* studied further the alteration of substituent effects on δ_{C} of different bridge carbons for *p*-XCAY-*p*^[18] and on δ_{C} values of the same type of carbons for different series of aromatic Schiff bases.^[19] Now, what is interesting for us is the regularity of

substituent effects on the chemical shifts of the previously mentioned two types of specific carbons. That is to say, what is the regularity of substituent effects on δ_{C} values of specific bridge carbons for different aromatic Schiff bases? Although the alteration of substituent effects was confirmed to associate with the distance between the substituent and the corresponding carbon, the forms of substituent parameters in two papers were different. In this paper, the connection between the strength of the substituent effect and the distance is further investigated, and it is helpful to understand the regularity of the substituent effect on δ_{C} values of specific bridge carbons for aromatic compounds.

Results and discussions

The model establishment

In the conventional chemistry theory, the strength of substituent inductive effect has long been considered to gradually decrease with chemical bonds. Cherkasov^[20] ever recommended that the substituent inductive effect should change with the inverse square of the distance between the corresponding substituent and the reaction center, shown as Eqn (4), where σ_{A} is an overall empirical atomic value, and r is the distance between the corresponding atom of the substituent and the reaction center. However, for the strength of the substituent conjugative effect, it does not decrease by the length of the conjugated chain, but the charge signs of adjacent

* Correspondence to: Guanfan Chen, School of Chemistry and Chemical Engineering, Hunan University of Science and Technology, Xiangtan 411201, China. E-mail: gfchen@hnust.edu.cn

**Correspondence to: Chenzhong Cao, School of Chemistry and Chemical Engineering, Hunan University of Science and Technology, Xiangtan 411201, China. E-mail: czcao@hnust.cn

a School of Chemistry and Chemical Engineering, Hunan University of Science and Technology, Xiangtan 411201, China

b Key Laboratory of Theoretical Chemistry and Molecular Simulation of Ministry of Education, Hunan University of Science and Technology, Xiangtan, China

c Hunan Provincial University Key Laboratory of QSAR/QSPR, Hunan University of Science and Technology, Xiangtan, China



Construction of MnO₂/3-dimensional porous crack Ni for high-performance supercapacitors



Guo-rong Xu^{a,b,*}, Ya Wen^b, Xiang-ping Min^b, Wen-hao Dong^b, An-ping Tang^b, Hai-shen Song^{a,b}

^a Key Laboratory of Theoretical Chemistry and Molecular Simulation of Ministry of Education and Hunan Province, PR China

^b School of Chemistry and Chemical Engineering, Hunan University of Science and Technology, Xiangtan 411201, PR China

ARTICLE INFO

Article history:

Received 5 June 2015

Received in revised form 1 October 2015

Accepted 23 October 2015

Available online 30 October 2015

Keywords:

Supercapacitor

Porous crack nickel

Manganese dioxide

Electrochemical performance

ABSTRACT

MnO₂/3-dimensional porous crack nickel (MnO₂/3-DPCNi) electrode has been fabricated via an alloying/dealloying process and an electrochemical oxidation process. The construction of the 3-DPCNi was achieved by means of electrodeposition of Zn-Ni alloy on Ni foam substrate, followed by chemically dealloying process under free corrosion conditions. Scanning electronic microscopy (SEM) and X-ray diffraction (XRD) were used to characterize the morphology and structure of the 3-DPCNi. The electrochemical properties of the MnO₂/3-DPCNi electrode were investigated using cyclic voltammetry (CV), galvanostatic charge/discharge (GC/D) and electrochemical impedance spectroscopy (EIS) technique. It is shown that a layer Ni with a cracked network was well coated on the Ni foam substrate. Such porous crack structures of 3-DPCNi not only provided a conductive network to enhance the charge transport and mass transfer in the electrochemical process but also achieved a large MnO₂ mass loading capacity of 14.4 mg cm⁻², which resulted in a high areal capacitance of 3.18 F cm⁻² at a current rate of 0.25 A g⁻¹. A specific capacitance of 682.8 F g⁻¹ was obtained based on the MnO₂ mass loading density of 2.5 mg cm⁻² at a current rate of 0.25 A g⁻¹. Moreover, the MnO₂/3-DPCNi electrode also exhibited a low ions diffusion resistance and a good cycling performance along with 93.3% specific capacitance retained after 1000 cycles. These results demonstrated that the 3-DPCNi was a promising supporting material for energy conversion and storage devices.

© 2015 Elsevier Ltd. All rights reserved.

1. Introduction

During the past years, supercapacitors, which are also known as electrochemical capacitors or ultracapacitors, have attracted intensive attention owing to their high power density and super-high cycling life [1–2]. The range of potential practical applications extends from mobile electronic devices to hybrid electric vehicles. Depending on the charge storage mechanism, supercapacitors are generally classified into two types [3]. The first type is based on the formation of electrical double layers (EDLs) at the interface between surface of a conductive electrode and an electrolyte. The second type is based on a Faraday-type reaction occurring on electrode material surface, which is called pseudocapacitance because it exhibits a capacitive behavior rather than a distinctly peaked redox behavior normally associated with intercalation.

The transition metal oxides/hydroxides with variable valence have been used as electrode materials in pseudocapacitors [4–10]. Among the various candidate transition metal oxides, manganese oxides have been extensively investigated as pseudocapacitors electrode materials with respect to their low cost, high theoretical capacity, environment friendliness and abundant raw materials [5,11–12]. Unfortunately, the poor electrical conductivity and slow ions diffusion of manganese oxides limit the full utilization of their high pseudocapacitance. To improve on the above mentioned shortcomings for better performing supercapacitive electrodes, porous supports with high electrical conductivities and high surface area to host manganese oxides have been extensively investigated, including various carbon-based materials [13–17], porous metal [18], and conductive oxide [19]. Specific capacitances (SC) of 400–1200 F g⁻¹ have been achieved for manganese oxides in the above investigations. For example, Li et al. reported that the SC for flowery α-MnO_x nanostructure on hierarchically porous graphene-carbon nanotube structure was 1200 F g⁻¹, which is close the theoretical capacitance value [15]; Xiao et al. [18] deposited a MnO₂ film on porous Ni scaffold substrate, and

* Corresponding author. Tel.: +86 731 58290045.
E-mail address: grxu@hnust.edu.cn (G.-r. Xu).



Synthesis of Cobalt hexacyanoferrate decorated graphene oxide/carbon nanotubes-COOH hybrid and their application for sensitive detection of hydrazine



Keqin Deng^{a,*}, Chunxiang Li^a, Xiyang Qiu^a, Jianhong Zhou^b, Zhaohui Hou^{c,*}

^a Key Laboratory of Theoretical Organic Chemistry and Function Molecule, Ministry of Education, School of Chemistry and Chemical Engineering, Hunan University of Science and Technology, Xiangtan 411201, PR China

^b School of Life Science, Hunan University of Science and Technology, Xiangtan 411201, PR China

^c School of Chemistry and Chemical Engineering, Hunan Institute of Science and Technology, Yueyang 414006, PR China

ARTICLE INFO

Article history:

Received 20 May 2015

Accepted 20 June 2015

Available online 27 June 2015

Keywords:

Nanohybrid

Graphene oxide

Multi-walled carbon nanotubes-COOH

Cobalt hexacyanoferrate

Hydrazine

ABSTRACT

A three-dimensional graphene oxide/carbon nanotubes-COOH hybrid (GO/CNTs-COOH) consisted of two-dimensional graphene oxide (GO) and one-dimensional carbon nanotubes-COOH (CNTs-COOH) was synthesized. The GO/CNTs-COOH hybrid exhibited excellent water-solubility owing to the high hydrophilicity of GO components and the carboxylation of carbon nanotubes. The cobalt hexacyanoferrate decorated GO/CNTs-COOH (CoHCF/GO/CNTs-COOH) has been prepared using electrostatic adsorption of Co^{2+} on GO/CNTs-COOH and $\text{K}_4[\text{Fe}(\text{CN})_6]$ as an in-situ chemical precipitant. FT-IR, Raman spectroscopy, TEM, SEM, and cyclic voltammetry were utilized to characterize the nanohybrid. The electrochemistry behavior of hydrazine on different modified electrodes was also studied. The CoHCF/GO/CNTs-COOH modified GCE (CoHCF/GO/CNTs-COOH/GCE) exhibited greatly enhanced electrocatalytic performance towards electro-oxidation of hydrazine. The oxidation peak currents showed good linear relationships with concentration of hydrazine. It can be applied to detect hydrazine in samples sensitively.

© 2015 Elsevier Ltd. All rights reserved.

1. Introduction

Graphene oxide (GO) possesses much advantage, including facile synthesis, high surface area, substantial solubility, low toxicity, good hydrophilicity, and excellent biocompatibility [1]. Its various oxygen-containing functional groups may protect carbon sheets from restacking and agglomeration, make it disperse in water and some other solvents readily [2,3], and also serve as the combining sites for graphene-based nanocomposites. But, its poor electrical conductivity limits its direct application as electrically active materials. Thus, to decorate GO with electroactive species noncovalently via π - π stacking, cation- π , van der Waals interactions, or hydrogen bonding emerged [4–6]. Carbon nanotubes (CNTs), as a one-dimensional carbon material, are recommendable to hybridize with GO. The hybridization of CNTs not only enhances the conductivity of GO, but there exists a great synergy between CNTs and GO, which helps the nanocomposites to obtain

the excellent electrocatalysis properties over CNTs or GO alone [7–9].

Transition-metal hexacyanoferrates (TMHCFs) have been used as electrocatalytic reaction mediators for their excellent electron-transfer properties [10]. A variety of TMHCFs and the associated composites have been developed [11–15]. Among them, cobalt hexacyanoferrate (CoHCF) has been well applied for its unique electrochemical property [15–19]. Li et al. have applied the CoHCF modified MWCNTs/graphite composite electrode for amperometric detection of hydrazine on microfluidic chip [15]. Oiyé proposed CoHCF modified platinum disk electrode for detection of cocaine [16]. The hybrid cobalt-iron hexacyanoferrate nanoparticles modified electrode was fabricated by electrochemical methods using MWCNT as a template [19]. Recently, increasing attention has been paid to the combination of graphene and TMHCFs for construction of electrochemical sensor [11–13,18]. Due to the synergic electrocatalytic action between graphene and TMHCFs, the scheme has been proved to expand electroanalytical applications [12–13].

As mentioned above, seeing that GO, CNT, and CoHCF has their own advantages, we planed to use two-dimensional GO nanosheets and one-dimensional carboxylated CNTs (CNTs-COOH) to

* Corresponding authors. Tel.: +86 0731 58290045.

E-mail addresses: keqindeng@hnust.edu.cn (K. Deng), zhqh96@163.com (Z. Hou).

Group effect on ionization potential for mono-substituted aliphatic compounds

Guanfan Chen^{a,b,c,*}, Mengzhuo Tang^a, Rongjin Zeng^{a,b,c}, Wanqiang Liu^{a,b,c} and Chenzhong Cao^{a,b,c,*}

ABSTRACT: The group effect on ionization potential for *mono*-substituted aliphatic compounds RX was investigated, and it was found that there is a good relationship between the ionization potential (*IP*) and the parameters, group electronegativity $\chi_{\text{eq},X}$, the group polarizability $\Sigma PEI_{X,r}$, and the disperse contribution of single non-bond electron E_{dc} for titled compounds, and these parameters earlier were easily calculated from the molecular structure. Moreover, the B3LYP density functional method was also employed to estimate *IP* values of the same *mono*-substituted aliphatic compounds. The results showed that it was difficult to get reliable ionization data using DFT method, and the regression equation with descriptors $\chi_{\text{eq},X}$, $\Sigma PEI_{X,r}$ and E_{dc} was more effective than DFT method in predicting *IP* values for titled compounds. The results are helpful to understand the role of group effect on molecular properties. Copyright © 2015 John Wiley & Sons, Ltd.

Keywords: DFT method; group effect; ionization potential; *mono*-substituted aliphatic compound

INTRODUCTION

The ionization potential (*IP*) is an important molecular property that describes the process of removal of an electron from the molecule and the production of a mole-ion, and knowledge of its value is necessary to understand a wide range of processes in chemistry and biology.^[1–5] Although there are many kinds of measurements, such as photoelectron spectroscopy, photoionization mass spectrometry, electron impact techniques, and so on, used to measured *IP* values, there are *IP* values of many compounds untouched because of enormous experimental difficulties. Hence, there is still considerable interest in finding relations between the molecular structures and *IP* values of compounds and predicting the untouched *IP* values of compounds.

For a *mono*-substituted compound YX, it can be divided into a substituent/functional segment (collectively called group) X and parent Y, and thus there are two major threads of research. On the one hand, McGlynn *et al.* investigated the effect of variable alkyl R on the ionization potentials of alkylated molecules RX with the restricted Hartree–Fock Self-Consistent Field approach.^[6] Cauwelaert's work showed that there is a relationship between the ionization potential and the Taft factor when molecules belong to a homogeneous series of compounds.^[7] Cherkasov and Jonsson investigated ionization potentials for 48 C-centered radicals with operational atomic parameters, and obtained a good result.^[8] With the Polarizability Effect Index (*PEI*), Cao *et al.* discussed the polarization effect of variable R on the *IP* values for ROH, RSH, RNH₂, RI, RBr, RCHO, and so on.^[9,10] On the other hand, for *IP* data of some *mono*-substituted and *di*-substituted benzenes, Crable and Kearns^[11] found that there is a linear correlation between the *IP* values of *mono*-substituted benzenes or toluenes and σ^+ substituent constants. Benoit also observed that the *IP* values of *mono*-substituted and *di*-substituted benzenes are related to the sum of Brown's σ_p^+ of the substituents for both the *meta*-isomer and *para*-isomer.^[12] To our surprise, there are few researches of the functional segment/substituent effect (collectively called group effect) on

ionization potentials for aliphatic compounds. Recently, for aliphatic compounds, Yuan and Cao^[13] proposed a novel concept system, organic homo-rank compound, and studied the ionization potentials of three sets of homo-rank compounds with $IP_{(j)} = a + bIP_{(1)} + bPEI_{(R)}$, where $IP_{(1)}$ is the ionization potentials of MeX and $PEI_{(R)}$ is the polarization index of alkyl R.

Now, for aliphatic compounds RX in which alkyl R is fixed and group X is varied, what we particularly want to know is the group effect on their *IP* values. In the paper, we aim to extract the descriptors from molecular structures and develop a heuristic formula to quantify the group effect on *IP* values for aliphatic compounds.

RESULTS AND DISCUSSIONS

As we know, the ionization potential of a molecule is given by^[14]

$$IP = E_{\text{total}}^{\text{ion}} - E_{\text{total}}^{\text{molecule}}$$

Generally speaking, the ionization potential of organic compound depends on energy of two states: (1) energy of the initial state (molecular state) and (2) energy of the final state (ionic

* Correspondence to: Guanfan Chen and Chenzhong Cao, School of Chemistry and Chemical Engineering, Hunan University of Science and Technology, Xiangtan 411201, Hunan Province, China.
E-mail: chenguanfan@gmail.com; czcao@hnust.cn

a G. Chen, M. Tang, R. Zeng, W. Liu, C. Cao
School of Chemistry and Chemical Engineering, Hunan University of Science and Technology, Xiangtan 411201, Hunan Province, China

b G. Chen, R. Zeng, W. Liu, C. Cao
Key Laboratory of Theoretical Organic Chemistry and Function Molecule of Ministry of Education, Hunan University of Science and Technology, Xiangtan 411201, Hunan Province, China

c G. Chen, R. Zeng, W. Liu, C. Cao
Hunan Provincial University Key Laboratory of QSAR/QSPR, Xiangtan 411201, Hunan Province, China

CrossMark
click for updatesCite this: *Anal. Methods*, 2015, 7, 296

Detection of Fe(III) and bio-copper in human serum based on fluorescent AuAg nanoclusters†

Qian Zhao, Shenna Chen, Lingyang Zhang and Haowen Huang*

In this study, a fluorescence assay for the successive determination of Fe³⁺ and Cu²⁺ ions based on the quenching fluorescence of composite AuAg nanoclusters (AuAg NCs) was developed. Using this binary fluorescence sensor, the Fe(III) level in a human serum sample can be directly detected without pretreatment. After the nitrification of human serum, the bio-copper level in human serum may be measured with a quick response. Human serum samples were analyzed, and the average concentration of Fe(III) and bio-copper were found to be 2.33×10^{-5} and 2.91×10^{-5} M, respectively. This assay was not only sensitively responsive to blood iron(III) but also to serum copper, suggesting significant potential applications for successively monitoring the Fe(III) and bio-copper levels, and their changes during the progression of a biological process.

Received 28th September 2014
Accepted 4th November 2014

DOI: 10.1039/c4ay02297a

www.rsc.org/methods

1. Introduction

Noble metal clusters are an emerging class of fluorescent nanomaterials, such as Au nanoclusters (NCs) and Ag NCs,^{1,2} circumventing most of the drawbacks of common fluorescent compounds, which have drawn wide attention in single-molecule optoelectronic nanodevices, biological labeling, optical sensing, novel catalysis, and surface-enhanced Raman spectroscopy (SERS).^{3–8} Recognition and quantification of metal ions are considerably significant due to the fact that these ions play important roles in various biological and environmental processes.^{9,10} In the past few years, there have been numerous reports on the design of fluorescent sensors for the detection of various metal ions, such as Hg²⁺,¹¹ Fe³⁺,¹² Cu²⁺ and Cd²⁺,^{13,14} and Pb²⁺,¹⁵ because of their high sensitivity, specificity, and real-time monitoring with fast response time.

Previous studies have demonstrated that copper and iron deficiency may lead to a wide variety of neurological problems,^{16,17} cardiovascular disease and kidney damage.¹⁸ The development of specific sensors, determining these metal ions in aqueous media, constantly attract attention. Current approaches for detecting Fe³⁺ and Cu²⁺ ions include inductively coupled plasma mass spectrometry (ICP-MS),^{19,20} atomic absorption spectrometry^{21,22} and electrochemical methods.^{23,24} Although these methods offer excellent sensitivity, they are rather costly, time-consuming and complex. Most of the developed approaches to detect copper and iron ions are concentrated

on the design of selective sensors, only for one kind of metal ion. In contrast, the investigation of sensors on successive or simultaneously detecting two kinds of these ions is rare. Thus, it is important to develop a binary sensor to determine iron and copper in practical samples, especially in the biological samples.

In this study, a type of composite metal nanoclusters, AuAg NCs, with strong fluorescence have been prepared. A fluorescent probe for the successive determination of Fe³⁺ and Cu²⁺ ions, based on the quenching fluorescence of AuAg NCs, has been developed. Using this binary fluorescence sensor, a practical application of a human serum sample was performed to determine Fe(III) and bio-copper levels. This assay shows a quick response not only to the blood iron level but also to serum copper, suggesting significant potential applications for successively monitoring Fe(III) and bio-copper concentrations, and their changes during the progression of a biological process.

2. Experimental

2.1 Chemicals

HAuCl₄·3H₂O, silver nitrate (AgNO₃), glutathione (GSH), disodium ethylenediamine tetraacetate (EDTA), NH₄F, ferric chloride (FeCl₃), and cupric chloride (CuCl₂) were purchased from Sinopharm Chemical Reagent Co., Ltd (Shanghai, China). A series of different concentrations of solutions were obtained by dilution. The aqueous solutions were prepared with doubly distilled water. The K⁺, Ca²⁺, Na⁺, Mg²⁺, Zn²⁺, Mn²⁺, Cd²⁺, Ni²⁺, Br⁻, I⁻, F⁻, bovine serum albumin (BSA), cysteine, pepsin, Co²⁺, Fe³⁺, Cu²⁺, Pb²⁺ and Al³⁺ metal ion solutions and molecules were prepared to examine the metal ion induced emission enhancement or quenching. The concentration of all prepared metal ion solutions was 1×10^{-2} M. All reagents were of analytical reagent grade and used as received.

Laboratory of Theoretical Chemistry and Molecular Simulation of Ministry of Education, Hunan Provincial University Key Laboratory of QSAR/QSPR, School of Chemistry and Chemical Engineering, Hunan University of Science and Technology, Xiangtan, China. E-mail: hhw09@163.com; Tel: +86-731-58290045

† Electronic supplementary information (ESI) available. See DOI: 10.1039/c4ay02297a

See discussions, stats, and author profiles for this publication at: <https://www.researchgate.net/publication/270769684>

Fractional Transfer of a Free Unpaired Electron to Overcome Energy Barriers in the Formation of Fe₄⁺ from Fe₃⁺ during Core...

Article in *Organic & Biomolecular Chemistry* · January 2015

DOI: 10.1039/C4OB02429J

CITATIONS

5

READS

29

5 authors, including:



Qihua Liu

Hunan University of Science and Technology

19 PUBLICATIONS 120 CITATIONS

SEE PROFILE



Zaichun Zhou

Hunan University of Science and Technology

26 PUBLICATIONS 141 CITATIONS

SEE PROFILE

Some of the authors of this publication are also working on these related projects:



new members of porphyrin family [View project](#)



Contents lists available at ScienceDirect

Spectrochimica Acta Part A: Molecular and Biomolecular Spectroscopy

journal homepage: www.elsevier.com/locate/saa

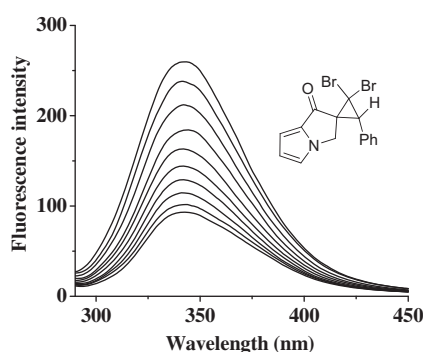
Spectroscopic analyses on interaction of bovine serum albumin with novel spiro[cyclopropane-pyrrolizin]

Xianyong Yu^{a,b,c,*}, Zhixi Liao^a, Bingfei Jiang^a, Xiaolian Hu^a, Xiaofang Li^{a,*}^a Key Laboratory of Theoretical Organic Chemistry and Function Molecule, Ministry of Education, Hunan Province College Key Laboratory of QSAR/QSPR, School of Chemistry and Chemical Engineering, Hunan University of Science and Technology, Xiangtan 411201, China^b State Key Laboratory of Physical Chemistry of Solid Surfaces, Xiamen University, Xiamen 361005, China^c Key Laboratory of Computational Physical Sciences (Fudan University), Ministry of Education, Shanghai 200433, China

HIGHLIGHTS

- The interaction between novel spiro[cyclopropane-pyrrolizin] (NSCP) and bovine serum albumin (BSA) and was studied.
- The fluorescence quenching mechanism is static quenching.
- The binding constants and binding sites were calculated.
- Hydrogen binds and van der Waals interaction force played a major role in stabilizing the complex.
- NSCP can affect the conformation of BSA.

GRAPHICAL ABSTRACT



ARTICLE INFO

Article history:

Received 16 June 2014

Received in revised form 9 August 2014

Accepted 24 August 2014

Available online 3 September 2014

Keywords:

Interaction

Novel spiro[cyclopropane-pyrrolizin]

Bovine serum albumin

Fluorescence spectroscopy

Ultraviolet–visible spectroscopy

ABSTRACT

The interaction between novel spiro[cyclopropane-pyrrolizin] (NSCP) and bovine serum albumin (BSA) was analyzed by fluorescence and ultraviolet–visible (UV–Vis) spectroscopy at 298 K, 304 K and 310 K under simulative physiological conditions. The results showed that NSCP can effectively quench the intrinsic fluorescence of BSA via static quenching. The binding constants, binding sites of NSCP with BSA were calculated. Hydrogen binds and van der Waals force played a major role in stabilizing the complex and the binding reaction were spontaneous. According to the Förster non-radiation energy transfer theory, the average binding distances between NSCP and BSA were obtained. What is more, the synchronous fluorescence spectra indicated that the conformation of BSA has been changed.

© 2014 Elsevier B.V. All rights reserved.

Introduction

Serum albumin (SA) is an important protein in the circulatory system, which has been extensively studied among all proteins and plays a significant role in the transport, distribution and metabolic pathway of many exogenous ligands, such as fatty acids, amino acids, drugs and pharmaceuticals [1–3]. Bovine serum albumin (BSA) has an inherent fluorescing property attributed to the presence of aromatic amino acids [4–6]. In our study, the BSA is

* Corresponding authors. Address: Key Laboratory of Theoretical Organic Chemistry and Function Molecule, Ministry of Education, Hunan Province College Key Laboratory of QSAR/QSPR, School of Chemistry and Chemical Engineering, Hunan University of Science and Technology, Xiangtan 411201, China (X. Yu). Tel.: +86 731 58290187; fax: +86 731 58290509.

E-mail addresses: yu_xianyong@163.com (X. Yu), lixiaofang@iccas.ac.cn (X. Li).

CrossMark
click for updates

Cite this: DOI: 10.1039/c4ay02722a

Successive detection of glucose and bio-copper in human serum based on a multiplex biosensor of gold nanorods†

Shenna Chen, Qian Zhao, Lingyang Zhang, Xiaodong Xia and Haowen Huang*

In this paper, a promising combined assay for the successive detection of blood glucose and sera copper levels based on etching of gold nanorods (GNRs) was developed. A hydroxyl radical-enhanced GNR oxidation under ultraviolet irradiation facilitates the establishment of a plasmonic biosensor that may quickly detect blood glucose. A linear relationship between the change of the plasmonic wavelength and the glucose concentration was found ($\Delta\lambda = 4.2284 + 132.0c$) in the range of 0.23 to 0.928 mM and the LOD was 0.45 μM . The determination of blood glucose using this proposed method was satisfactory and closely comparable to the results given by the local hospital. On the other hand, a blue-shift of the longitudinal plasmon wavelength induced by various forms of copper in the presence of $\text{Na}_2\text{S}_2\text{O}_3$ provides a sensitive approach to detect the total copper level in a biological sample. The copper levels of human sera were measured and corroborated by flame atomic absorption spectrometry, which confirms that this approach might be applicable for bio-copper analysis with high accuracy. A combined assay for the successive detection of the blood glucose level and serum copper was subsequently developed. Compared to other related biosensors requiring a modified design, bio-molecular modification or/and sophisticated instruments, the dual glucose and copper sensor is very simple, cost-effective and easy to use for detection, suggesting great potential applications for successively monitoring blood glucose and copper concentrations and their changes during the progression of diabetes.

Received 15th November 2014
Accepted 29th November 2014

DOI: 10.1039/c4ay02722a

www.rsc.org/methods

Introduction

Gold nanorods (GNRs) have attracted much attention in the past decade due to their physical and chemical properties.^{1–4} Their unique properties make them suitable for photothermal therapy,^{5,6} imaging,^{7,8} gene delivery⁹ and data storage.¹⁰ Numerous biosensors for the detection of biological targets, such as antibodies (or antigens) and DNA, were developed due to GNRs being sensitive to the dielectric constant of the surrounding medium.^{11–16} As for their use as a chemical sensor, the determination of dissociated metal ions in an aqueous solution could be achieved by modulating the plasmonic properties of the GNRs.^{17,18} This work greatly expanded the biosensing application of GNRs, which provoked further efforts to develop their bio-analytical applications.

Diabetes mellitus is one of the leading causes of death and disability, which is a worldwide public health problem. The main feature of diabetes is chronic hyperglycemia, which leads

to the disturbance of carbohydrate, fat and protein metabolism.^{19,20} Moreover, various secondary complications may occur such as renal dysfunction and failure,²¹ cardiac abnormalities,²² diabetic retinopathy,²³ neuropathy²⁴ and atherosclerosis.²⁵ The blood glucose level is used as a clinical indicator of diabetes mellitus. Therefore, efforts to explore biosensors for fast and reliable glucose monitoring in the diagnosis of diabetes have received continuous interest. Meanwhile, there is accumulating evidence that the metabolism of several trace elements such as copper and zinc are altered in diabetes mellitus and that these nutrients might have specific roles in the pathogenesis and progression of this disease.^{26–28} Plasma copper levels have been found to be elevated in type-1 diabetes mellitus patients and the urinary excretion of copper has been found to be affected by diabetes mellitus.²⁹ Recently, novel approaches for the detection of copper have attracted increasing attention.^{30–32} Specific glucose and copper detection for the diagnosis of diabetes mellitus using simple and low-cost assays is important in clinical diagnostics. Most current methods for the quantification of blood glucose levels and serum copper require costly and sophisticated instruments which are time-consuming, labor intensive and expensive with complicated procedures. Therefore, it is necessary to develop a quick and successive assay for the combined detection of glucose and serum copper in order to

Key Laboratory of Theoretical Organic Chemistry and Function Molecule, Ministry of Education, Hunan Provincial University Key Laboratory of QSAR/QSPR, School of Chemistry and Chemical Engineering, Hunan University of Science and Technology, Xiangtan, China. E-mail: hhwn09@163.com; Tel: +86-731-58290045

† Electronic supplementary information (ESI) available. See DOI: 10.1039/c4ay02722a



Short communication

Facile hydrothermal-carbonization preparation of carbon-modified Sb₂S₃ composites for photocatalytic degradation of methyl orange dyes



Jianting Tang*, Jiayin Li, Yang Cheng, Peng Huang, Qian Deng

Key Laboratory of Theoretical Organic Chemistry and Functional Molecule for Ministry of Education, Hunan Province College Key Laboratory of QSAR/QSPR, School of Chemistry and Chemical Engineering, Hunan University of Science and Technology, Xiangtan 411201, China

ARTICLE INFO

Article history:

Received 7 April 2015

Received in revised form

2 May 2015

Accepted 1 June 2015

Available online 11 June 2015

Keywords:

Photocatalytic degradation

Carbon

Antimony sulfide

Composite materials

ABSTRACT

A series of carbon-modified antimony sulfide (Sb₂S₃) composites were prepared by facile hydrothermal-carbonization method using glucose as carbonaceous resource. The composites were characterized by X-ray diffraction (XRD), ultraviolet–visible diffuse reflectance spectrum (UV–vis DRS), scanning electron microscopy (SEM), transmission electron microscopy (TEM) and photoluminescence (PL) techniques. The photocatalytic activity of the composites was tested in degradation of methyl orange (MO) dye under irradiation of visible light. The carbon content of the composites plays an important role in the photocatalytic degradation. The photocatalytic activity of carbon-modified Sb₂S₃ composites is higher than that of pure Sb₂S₃. The higher photocatalytic activity of the carbon-modified Sb₂S₃ photocatalysts can be attributed to their higher adsorption capacity and higher separation efficiency of photogenerated carriers.

© 2015 Elsevier Ltd. All rights reserved.

Recently, semiconductor photocatalysts received increasing attention because they can be applied in treatment of environmental pollution with sustainable solar energy [1–3]. The key issue to utilize solar energy in photocatalysis is the use of visible-light-responsive photocatalysts. Therefore, many efforts have been dedicated to develop new visible-light-responsive photocatalysts to deal with the environmental problems [4–8]. Antimony sulfide (Sb₂S₃), a photocatalyst that can be activated under visible light, has been widely used in photocatalytic degradation of organic pollutants [9]. However, activity of photocatalysts is limited due to rapid recombination of photogenerated electrons and holes in photocatalytic process [10]. Doping Sb₂S₃ with other components may alter its physicochemical property, increase separation efficiency of photogenerated carriers and hence improve its photocatalytic activity [11–13]. Therefore, the doped Sb₂S₃ photocatalysts have become a hot research topic in recent years [11–13].

Preparing functional materials from cheap natural precursors through environmentally friendly processes is a highly interesting subject in material science [14]. Hydrothermal-carbonization is a facile and well-controlled process with the use of plant biomass to

produce functional carbonaceous materials [14]. Recently, the hydrothermal-carbonization method appeared promising for fabricating carbon-modified photocatalysts with high photocatalytic performance. By this method, carbon-coated CdS photocatalysts with uniform morphology were prepared, which showed excellent photostability and enhanced photocatalytic activity in degradation of MO and rhodamine B dyes [15]. Also by the hydrothermal-carbonization method, carbon-doped ZnO or BiVO₄ composites were successfully obtained to achieve higher photocatalytic activity than pure ZnO or BiVO₄ photocatalyst, respectively [16,17].

To the best of our knowledge, the carbon-modified Sb₂S₃ photocatalysts prepared by the hydrothermal-carbonization method were not reported yet. We envisioned if Sb₂S₃ can be carbonized through the facile process, its physicochemical properties and hence photocatalytic performance should be improved similarly. In this work, we attempted the preparation of carbon-modified Sb₂S₃ composites through the hydrothermal-carbonization process using widely available glucose as carbonaceous resource. The carbon-modified Sb₂S₃ composites exhibited improved photocatalytic performance in degradation of MO dyes under illumination of visible light. The photocatalytic mechanism of the carbon-modified Sb₂S₃ photocatalysts was also proposed.

* Corresponding author. Tel./fax: +86 731 58290045.
E-mail address: jttang1103@126.com (J. Tang).



Contents lists available at ScienceDirect

Spectrochimica Acta Part A: Molecular and Biomolecular Spectroscopy

journal homepage: www.elsevier.com/locate/saa

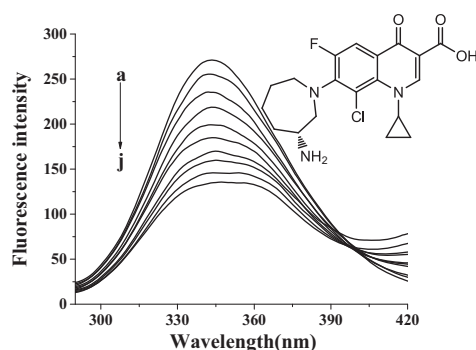
Study on the interaction between Besifloxacin and bovine serum albumin by spectroscopic techniques

Xianyong Yu^{a,b,*}, Bingfei Jiang^a, Zhixi Liao^a, Yue Jiao^c, Pinggui Yi^{a,*}^aKey Laboratory of Theoretical Organic Chemistry and Function Molecule, Ministry of Education, Hunan Province College Key Laboratory of QSAR/QSPR, School of Chemistry and Chemical Engineering, Hunan University of Science and Technology, Xiangtan 411201, China^bKey Laboratory of Computational Physical Sciences, Fudan University, Ministry of Education, Shanghai, China^cNanjing Chemipioneer Pharma&Tech Co., Ltd, Nanjing 210032, China

HIGHLIGHTS

- We explored the interaction of BSA and BFLX by spectroscopic techniques.
- The fluorescence quenching mechanism is static quenching.
- The binding constants and binding sites were calculated.
- Electrostatic forces were the main force in stabilizing the complex.
- The conformation of BSA was changed affected by BFLX.

GRAPHICAL ABSTRACT



ARTICLE INFO

Article history:

Received 27 September 2014

Received in revised form 17 March 2015

Accepted 14 April 2015

Available online 20 April 2015

Keywords:

Interaction
Besifloxacin
Bovine serum albumin
Spectroscopic techniques
Circular dichroism spectrum

ABSTRACT

The interaction between Besifloxacin (BFLX) and bovine serum albumin (BSA) was investigated by spectroscopic (fluorescence, UV–Vis absorption and circular dichroism) techniques under imitated physiological conditions. The experiments were conducted at different temperatures (298, 304 and 310 K) and the results showed that the BFLX caused the fluorescence quenching of BSA through a static quenching procedure. The binding constant (K_b), binding sites (n) were obtained. The corresponding thermodynamic parameters (ΔH , ΔS and ΔG) of the interaction system were calculated at different temperatures. The results revealed that the binding process was spontaneous and the acting force between BFLX and BSA were mainly electrostatic forces. According to Förster non-radiation energy transfer theory, the binding distance between BFLX and BSA was calculated to be 4.96 nm. What is more, both synchronous fluorescence and circular dichroism spectra confirmed conformational changes of BSA.

© 2015 Elsevier B.V. All rights reserved.

Introduction

Drug–protein interactions have greatly influence the absorption, distribution, metabolism and excretion properties of drugs [1]. Serum albumins are one of the most abundant proteins in blood plasma, which are the major soluble protein and constituents of the circulatory system [2–4]. In this work, bovine serum albumin (BSA) is selected as our protein model due to its

* Corresponding authors at: Key Laboratory of Theoretical Organic Chemistry and Function Molecule, Ministry of Education, Hunan Province College Key Laboratory of QSAR/QSPR, School of Chemistry and Chemical Engineering, Hunan University of Science and Technology, Xiangtan 411201, China (X. Yu). Tel.: +86 731 58290187; fax: +86 731 58290509.

E-mail addresses: yu_xianyong@163.com (X. Yu), pgyi@hnust.cn (P. Yi).



CrossMark
click for updates

Cite this: *RSC Adv.*, 2015, 5, 8933

Received 21st October 2014
Accepted 2nd January 2015

DOI: 10.1039/c4ra12834f

www.rsc.org/advances

Novel ferrocene-based nanoporous organic polymers for clean energy application†

Qingquan Liu,^{*a} Zhe Tang,^a Minda Wu,^a Bo Liao,^a Hu Zhou,^a Baoli Ou,^a Guipeng Yu,^b Zhihua Zhou^{*a} and Xiaojuan Li^a

A novel ferrocene-based nanoporous organic polymer (FNOPs-1) for clean energy application has been prepared by coupling 1,1'-ferrocene-dicarboxaldehyde with melamine. The BET surface area and the total pore volume of FNOPs-1 are 752.4 m² g⁻¹ and 1.32 cm³ g⁻¹, respectively. FNOPs-1 exhibits excellent gas storage capacities such as 16.61 wt% of carbon dioxide, 3.48 wt% of methane, and 1.27 wt% of hydrogen at 273 K/1.0 bar.

The dramatic increases in the amounts of greenhouse gases such as CO₂ and CH₄ in the atmosphere are believed to be responsible for global warming, sea level rise, and climate change. Hydrogen is recognized as the cleanest energy source nowadays since combustion of hydrogen has high caloric value and environmentally compatible byproducts. In addition, methane is the main component of natural gas and at present, there is a great interest in expanding its application for fueling automobiles because of its wide availability and its lower CO₂ emission in comparison with petroleum. However, a current challenge for the development of hydrogen-based and methane-based technology is the available materials, which can store and deliver large amount of hydrogen or methane near room temperature and at low pressures.¹ In the past two decades, various porous polymers such as covalent organic frameworks (COFs),^{2,3} conjugated microporous polymers (CMPs),^{4,5} polymer with intrinsic microporosity (PIMs),⁶ hypercrosslinked polymers (HCPs),^{7,8} and nanoporous organic polymers (NOPs)^{9–11} were developed as adsorbents for gas storage and gas selective separation. As an emerging solid adsorbent, NOPs has attracted

extensive interests and hold the greatest potential for commercial use due to a series of advantages like high porosity, low density, and excellent stability.^{12–14} Recently, NOPs with functional building units was intensively investigated to obtain high gas storage capacity.¹⁵

Ferrocene and its derivatives are a kind of special organic metal complexes and have extensive applications in the field of electric catalytic and biological sensors.¹⁶ To date, there are very few reports about the preparation and the application of ferrocene-based nanoporous frameworks.^{17,18} Weber and Kistan¹⁷ prepared microporous ferrocenyl Schiff base network with a BET surface area of 430 m² g⁻¹ by the coupling of 1,1'-diacetyl ferrocene with melamine. Recently, ferrocene-based statistical copolymers of poly(ferrocenyl)-*co*-divinylbenzene produced by Kleitz *et al.*¹⁸ showed porous properties with BET surface areas ranging from 385 to 899 m² g⁻¹ and hydrogen uptake of 0.4–0.67 wt%. Ferrocene possesses a double-deck sandwich structure, which can be used as a rigid building unit to expanded porosity of NOPs. Therefore, it would be valuable to use ferrocene derivatives as a building unit for NOPs and endow NOPs with new properties and application prospects.

Inspired by the above works, the strategy of ferrocene being a building unit of NOPs was demonstrated. We synthesized a novel ferrocenyl nanoporous organic polymer (FNOPs-1) by the coupling of 1,1'-ferrocenedicarboxaldehyde and melamine in the medium of dimethyl sulfoxide (DMSO) at 180 °C, and investigated its gas uptake capacity. Scheme 1 shows the synthesis route of FNOP-1.

The synthesized FNOPs-1 was insoluble in any common organic solvent such as DMSO, *N,N'*-dimethylformamide (DMF), and tetrahydrofuran (THF), as well as in diluted HCl solution (~10 wt%). There was no weight loss can be found after soaked in diluted acid for 48 h, moreover, the BET surface area value of acid soaked FNOPs-1 was very close to that of the original FNOPs-1. These facts suggested that FNOPs-1 has a hypercrosslinked and physicochemical stable property. The thermal stability of FNOPs-1 was investigated by

^aSchool of Chemistry and Chemical Engineering, Key Laboratory of Theoretical Chemistry and Molecular Simulation of Ministry of Education, Hunan University of Science and Technology, Xiangtan 411201, China. E-mail: qqliu@hmust.edu.cn; zhou7381@126.com

^bKey Laboratory of Resources Chemistry of Nonferrous Metals Ministry of Education, College of Chemistry and Chemical Engineering, Central South University, Changsha 410083, China

† Electronic supplementary information (ESI) available. See DOI: 10.1039/c4ra12834f

Fullerenes

Synthesis and Photophysical Properties of a $\text{Sc}_3\text{N@C}_{80}$ -Corrole Electron Donor–Acceptor ConjugateBin Liu,^[a] Hongyun Fang,^[b] Xiaofang Li,^{*[a]} Wenting Cai,^[b] Lipiao Bao,^[b] Marc Rudolf,^[c] Fabian Plass,^[c] Louzhen Fan,^[d] Xing Lu,^{*[b]} and Dirk M. Guldi^{*[c]}

Abstract: Embedding endohedral metallofullerenes (EMFs) into electron donor–acceptor systems is still a challenging task owing to their limited quantities and their still largely unexplored chemical properties. In this study, we have performed a 1,3-dipolar cycloaddition reaction of a corrole-based precursor with $\text{Sc}_3\text{N@C}_{80}$ to regioselectively form a [5,6]-adduct (**1**). The successful attachment of the corrole moiety was confirmed by mass spectrometry. In the electronic ground state, absorption spectra suggest sizeable electronic communications between the electron acceptor

and the electron donor. Moreover, the addition pattern occurring at a [5,6]-bond junction is firmly proven by NMR spectroscopy and electrochemical investigations performed with **1**. In the electronically excited state, which is probed in photophysical assays with **1**, a fast electron-transfer yields the radical ion pair state consisting of the one-electron-reduced $\text{Sc}_3\text{N@C}_{80}$ and of the one-electron-oxidized corrole upon its exclusive photoexcitation. As such, our results shed new light on the practical work utilizing EMFs as building blocks in photovoltaics.

Introduction

As a focal point of research, studies on artificial electron donor–acceptor conjugates and hybrids mimicking the primary events of natural photosynthesis lying at the heart of photosynthetic solar energy conversion have drawn great attention and the related works have yielded exciting results.^[1–4]

In principle, an electron donor–acceptor system contains two main constituents, that is, an electron acceptor and an electron donor. As for the electron donor, corroles, as porphy-

rin isomers bearing a direct pyrrole–pyrrole link, have attracted considerable attention in recent years due to their unique structural, spectroscopic, and photophysical properties, which are not seen in porphyrins or any other metal-ligating molecules.^[5] Even though Johnson and Kay^[6] synthesized corrole for the first time as part of their works on synthetic models of Vitamin B12 as early as in 1964, the research of corrole had been very slow until facile synthetic methods appeared.^[7] The corrole macrocycles exhibit interesting properties, such as high Stokes shift, low oxidation potentials, high fluorescence quantum yields, and intense absorption in the red region of the solar spectrum, especially when compared with analogous porphyrins.^[8] Accordingly, assemblies of appropriately functionalized corroles with other redox-active and photoactive constituents for applications in various fields have been of intensive interest.^[9] In general, corroles are less stable than porphyrins, but once they are incorporated into an electron donor–acceptor conjugate they tend to be rather stable, which prompts to their great potential in the area of photovoltaics.^[10] Accordingly, the research on the synthesis and properties of corrole-based electron donor–acceptor conjugates has attracted great attention.

As far as electron acceptors are concerned, empty fullerenes such as C_{60} and C_{70} have been demonstrated as superior electron acceptors due to their remarkable reduction properties and their low reorganization energies in electron-transfer reactions.^[11] These features render them unique and have resulted in noteworthy advances in the areas of light-induced electron-transfer chemistry and solar-energy conversion. For example, some electron donor–acceptor conjugates, for which the generation of charge-separated states with lifetimes comparable to those observed in natural photosynthetic systems have

[a] B. Liu,[†] Prof. X. Li

Key Laboratory of Theoretical Chemistry
Molecular Simulation of Ministry of Education
Hunan Province College Key Laboratory of QSAR/QSPR
School of Chemistry and Chemical Engineering
Hunan University of Science and Technology
Xiangtan, Hunan 411201 (China)
E-mail: lixiaofang@ccas.ac.cn

[b] H. Fang,[†] W. Cai, L. Bao, Prof. X. Lu

State Key Laboratory of Materials Processing, Die & Mold Technology
School of Materials Science and Engineering
Huazhong University of Science and Technology, Wuhan 430074 (China)
E-mail: lux@hust.edu.cn

[c] M. Rudolf, F. Plass, Prof. D. M. Guldi

Department of Chemistry and Pharmacy
Interdisciplinary Center for Molecular Materials
Friedrich-Alexander-Universität Erlangen-Nürnberg
Erlangen 91058 (Germany)
E-mail: dirk.guldi@fau.de

[d] Prof. L. Fan

Department of Chemistry, Beijing Normal University
Beijing 100875 (China)

[†] These authors contributed equally to this work.

Supporting information for this article is available on the WWW under <http://dx.doi.org/10.1002/chem.201405572>.



Contents lists available at ScienceDirect

Spectrochimica Acta Part A: Molecular and Biomolecular Spectroscopy

journal homepage: www.elsevier.com/locate/saa

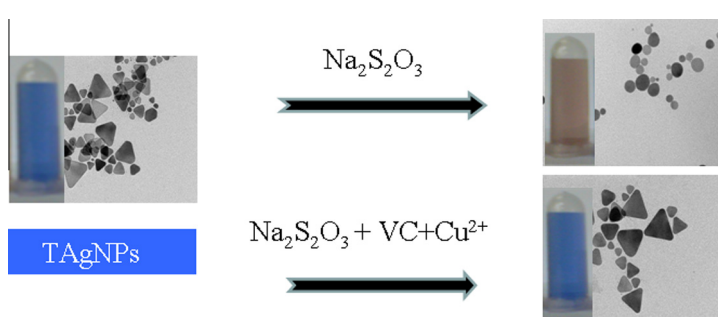
Visual detection of trace copper ions based on copper-catalyzed reaction of ascorbic acid with oxygen

Xin Yan Hou^a, Shu Chen^a, Lian Ju Shun^a, Yi Ni Zhao^a, Zhi Wu Zhang^a, Yun Fei Long^{a,*}, Li Zhu^{b,*}^a Key Laboratory of Theoretical Organic Chemistry and Function Molecule, Ministry of Education, School of Chemistry and Chemical Engineering, Hunan University of Science and Technology, Xiangtan 411201, PR China^b School of Chemistry and Chemical Engineering, Beijing Union University, Beijing 100101, PR China

HIGHLIGHTS

- A new colorimetric method for copper ion detection is established.
- Copper ion could be detected by naked eye in the range of 0.075–0.50 μM .
- High selectivity and sensitivity allow the Cu^{2+} detection in human hair sample.

GRAPHICAL ABSTRACT



ARTICLE INFO

Article history:

Received 26 February 2015
 Received in revised form 13 April 2015
 Accepted 16 April 2015
 Available online 22 April 2015

Keywords:

Triangular silver nanoplates
 Copper(II) ions
 Sodium thiosulfate
 Visual detection

ABSTRACT

A visual detection method for trace Cu^{2+} in aqueous solutions using triangular silver nanoplates (abbreviated as TAgNPs) as the probe was developed. The method is based on that TAgNPs could be corroded in sodium thiosulfate ($\text{Na}_2\text{S}_2\text{O}_3$) solutions. The absorption spectrum of TAgNPs solution changed when it is corroded by $\text{Na}_2\text{S}_2\text{O}_3$. The reaction of oxygen with ascorbic acid (Vc) in the presence of a low concentration of Cu^{2+} generates hydrogen peroxide that reacts with $\text{Na}_2\text{S}_2\text{O}_3$, which leads the concentration of $\text{Na}_2\text{S}_2\text{O}_3$ in the solution to be decreased. Therefore, the reaction between TAgNPs and the reacted mixture of $\text{Na}_2\text{S}_2\text{O}_3/\text{Vc}/\text{Cu}^{2+}$ was prevented efficiently. When the $\text{Na}_2\text{S}_2\text{O}_3$ concentration and reaction time are constant, the decrease in the concentration of $\text{Na}_2\text{S}_2\text{O}_3$ is directly proportional to the Cu^{2+} concentration. Thus, morphology, color, and maximum absorption wavelength of TAgNPs changed with the change of Cu^{2+} concentration. The changed maximum absorption wavelength of TAgNPs ($\Delta\lambda$) is proportional to Cu^{2+} concentration in the range from 7.5×10^{-9} to 5.0×10^{-7} M with a correlation coefficient of $r = 0.9956$. Moreover, color change of TAgNP solution was observed clearly over a Cu^{2+} concentration range from 7.5×10^{-8} to 5.0×10^{-7} M. This method has been used to detect the Cu^{2+} content of a human hair sample, and the result is in agreement with that obtained by the atomic absorption spectroscopy (AAS) method.

© 2015 Elsevier B.V. All rights reserved.

Introduction

Metallic nanostructures are able to application in many fields such as sensing, biological labeling, and other biological and

chemical fields [1–4]. However, the optical, physical, and chemical properties of metallic nanostructures depend on their size and shape, particularly for silver nanostructures [5,6]. In this study, triangular silver nanoplates (TAgNPs) were synthesized using the method of Zhang et al., [7] and it was used to detect trace Cu^{2+} . Studies have shown that the interaction between TAgNPs and other corrosion substances is easy at the three corners of the

* Corresponding authors. Tel.: +86 731 58388503 (Y.F. Long).

E-mail addresses: L_yunfei927@163.com (Y.F. Long), x694200@163.com (L. Zhu).

Comparison of the substituent effects on the ^{13}C NMR with the ^1H NMR chemical shifts of $\text{CH}=\text{N}$ in substituted benzylideneanilines

Linyan Wang,^{a,b} Chaotun Cao^b and Chenzhong Cao^{a,b,*}

Fifty-two samples of substituted benzylideneanilines $\text{XPhCH}=\text{NPhYs}$ (XBAYs) were synthesized, and their NMR spectra were determined in this paper. Together with the NMR data of other 77 samples of XBAYs quoted from literatures, the ^1H NMR chemical shifts ($\delta_{\text{H}}(\text{CH}=\text{N})$) and ^{13}C NMR chemical shifts ($\delta_{\text{C}}(\text{CH}=\text{N})$) of the $\text{CH}=\text{N}$ bridging group were investigated for total of 129 samples of XBAYs. The result shows that the $\delta_{\text{H}}(\text{CH}=\text{N})$ and $\delta_{\text{C}}(\text{CH}=\text{N})$ have no distinctive linear relationship, which is contrary to the theoretical thought that declared the $\delta_{\text{H}}(\text{CH}=\text{N})$ values would increase as the $\delta_{\text{C}}(\text{CH}=\text{N})$ values increase. With the in-depth analysis, we found that the effects of σ_{F} and σ_{R} of X/Y group on the $\delta_{\text{H}}(\text{CH}=\text{N})$ and the $\delta_{\text{C}}(\text{CH}=\text{N})$ are opposite; the effects of the substituent specific cross-interaction effect between X and Y ($\Delta\sigma^2$) on the $\delta_{\text{H}}(\text{CH}=\text{N})$ and the $\delta_{\text{C}}(\text{CH}=\text{N})$ are different; the contributions of parameters in the regression equations of the $\delta_{\text{H}}(\text{CH}=\text{N})$ and the $\delta_{\text{C}}(\text{CH}=\text{N})$ [Eqns (4 and 7), respectively] also have an obvious difference. Copyright © 2015 John Wiley & Sons, Ltd.

Keywords: benzylideneanilines; substituent effects; ^1H NMR chemical shifts; ^{13}C NMR chemical shifts; substituent specific cross-interaction

Introduction

The benzylideneanilines $\text{XPhCH}=\text{NPhYs}$ (abbreviated XBAYs) are a kind of typical compounds with π conjugate system and have been applied extensively in the fields of liquid crystal and nonlinear optical material.^[1–3] In the molecule of XBAY, $\text{CH}=\text{N}$ is a bridge linking two aromatic rings, in which one ring carries substituent X and another ring carries substituent Y. The substituents X and Y can act as electron donors and/or electron acceptors. Changes of X and Y in XBAY can affect its molecular overall electron distribution and the properties of optoelectronic materials containing the molecule of XBAY. Therefore, the substituent effects on the performance of the $\text{CH}=\text{N}$ bridging group attained great interest in recent years.^[4–11]

As we know, the NMR shielding is affected by the electron density, and the field of resonance increases with the increasing electron density of the protons and carbon nucleus in the molecule.^[12,13] So the NMR chemical shifts of $\text{CH}=\text{N}$ ($\delta_{\text{H}}(\text{CH}=\text{N})$ and $\delta_{\text{C}}(\text{CH}=\text{N})$) were always applied by many researchers to study the substituent effects on the molecules in the past years.^[4–6,8,14,15]

Echevarria *et al.*^[14] have made sketchy studies about the ^1H NMR and ^{13}C NMR of $\text{CH}=\text{N}$ by employing 24 samples of substituted benzylideneanilines and discussed the linear relationship between the $\delta_{\text{H}}(\text{CH}=\text{N})$ values or $\delta_{\text{C}}(\text{CH}=\text{N})$ values and the Hammett substituent constant σ_{p} . They obtained results: the $\delta_{\text{H}}(\text{CH}=\text{N})$ presented linear relation with σ_{p} of the benzaldehyde ring substituents but did not present linear relation with the σ_{p} of the aniline ring substituents; in addition, the effects of the aniline ring substituents on the $\delta_{\text{C}}(\text{CH}=\text{N})$ were larger than that of the benzaldehyde ring substituents. Afterwards, the substituent effects on the $\delta_{\text{C}}(\text{CH}=\text{N})$ of some title compounds were analyzed by employing several different single and dual substituent parameter approaches, and the relatively best equation [Eqn (1)] was attained by Neuvonen *et al.*^[7,16] In their research, they pointed out that the presence of the substituent

specific cross-interaction between X and Y could be verified. Although they did not quantify the cross-interaction, their works strongly promotes the research of the substituent effects on the $\delta_{\text{C}}(\text{CH}=\text{N})$ of title compounds. In our recent work,^[17] the substituent specific cross-interaction effects was quantified with the item $\Delta\sigma^2$ ($\Delta\sigma^2 = (\sigma_{\text{X}} - \sigma_{\text{Y}})^2$) and a more effective five-parameter equation [Eqn (2)] was proposed to quantify the $\delta_{\text{C}}(\text{CH}=\text{N})$ of substituted benzylideneanilines by adding $\Delta\sigma^2$ item to Eqn (1). σ_{F} is the inductive effect; σ_{R} is the conjugative effect; $\Delta\sigma^2$ is the substituent specific cross-interaction effect; ρ is the coefficient of corresponding parameter.

$$\delta_{\text{C}}(\text{CH}=\text{N}) = \text{constant} + \rho_{\text{F}}(\text{X})\sigma_{\text{F}}(\text{X}) + \rho_{\text{F}}(\text{Y})\sigma_{\text{F}}(\text{Y}) + \rho_{\text{R}}(\text{X})\sigma_{\text{R}}(\text{X}) + \rho_{\text{R}}(\text{Y})\sigma_{\text{R}}(\text{Y}) \quad (1)$$

$$\delta_{\text{C}}(\text{CH}=\text{N}) = \text{constant} + \rho_{\text{F}}(\text{X})\sigma_{\text{F}}(\text{X}) + \rho_{\text{F}}(\text{Y})\sigma_{\text{F}}(\text{Y}) + \rho_{\text{R}}(\text{X})\sigma_{\text{R}}(\text{X}) + \rho_{\text{R}}(\text{Y})\sigma_{\text{R}}(\text{Y}) + \rho_{(\Delta\sigma^2)}\Delta\sigma^2 \quad (2)$$

* Correspondence to: Chenzhong Cao, School of Chemistry and Chemical Engineering, Hunan University of Science and Technology, Key Laboratory of Theoretical Organic Chemistry and Function Molecule (Hunan University of Science and Technology), Ministry of Education, Hunan Provincial University Key Laboratory of QSAR/QSPR, Xiangtan 411201, China. E-mail: czcao@hnust.edu.cn

a School of Chemistry and Chemical Engineering, Central South University, Changsha 410083, China

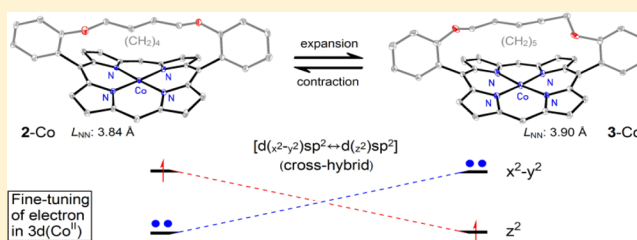
b School of Chemistry and Chemical Engineering, Hunan University of Science and Technology, Key Laboratory of Theoretical Organic Chemistry and Function Molecule (Hunan University of Science and Technology), Ministry of Education, Hunan Provincial University Key Laboratory of QSAR/QSPR, Xiangtan 411201, China

Fine-Tuning of Electronic Structure of Cobalt(II) Ion in Nonplanar Porphyrins and Tracking of a Cross-Hybrid Stage: Implications for the Distortion of Natural Tetrapyrrole Macrocycles

Qiuhua Liu,^{†,‡} Xi Zhang,[‡] Wennan Zeng,[‡] Jianxiu Wang,^{*,†} and Zaichun Zhou^{*,‡}[†]College of Chemistry and Chemical Engineering, Central South University, Changsha 410083, China[‡]Key Laboratory of Theoretical Organic Chemistry and Functional Molecule of the Ministry of Education; School of Chemistry and Chemical Engineering, Hunan University of Science and Technology, Xiangtan 411201, China

S Supporting Information

ABSTRACT: The core size of the porphyrin macrocycles was closely related to their stability of the different electron structure in the central metal ion. Cobalt(II) ions can undergo a conversion in electron configurations upon N_4 core contraction of 0.05 Å in nonplanar porphyrins, and these ions still maintain low spin forms after and before conversion. The structural fine-tuning can induce the appearance of a cross-hybrid stage $[d(x^2-y^2)sp^2 \leftrightarrow d(z^2)sp^2]$ based on quadrilateral coordination of the planar core. The results indicate that the configuration conversion plays a key role in electron transfer in redox catalysis involving cobalt complexes. The electronic properties of six monostrapped cobalt(II) porphyrins were investigated by spectral, paramagnetic, and electrochemical methods. The macrocyclic deformations and size parameters of Co-containing model compounds were directly obtained from their crystal structures.



1. INTRODUCTION

Metalloporphyrins are extensively used as catalysts for various organic transformations that are difficult to achieve using regular metal complexes, and this is possible because of their unique structure.¹ Cobalt atom complexes have easily accessible oxidation states of Co(I), Co(II), Co(III),² and even Co(IV) and Co(V) under electrochemical conditions.³ The Co(III)/Co(II) interconversion in porphyrins is readily achieved upon aerobic oxidation^{4–6} or mild reduction⁷ in high yield. Modified Co(II) porphyrins are efficient and versatile catalysts for the selective olefination of carbonyl compounds⁸ and olefin cyclopropanation⁹ with suitable diazo compounds. These reactions depend on “cobalt(III)–carbene radicals” for olefin cyclopropanation¹⁰ and “cobalt(III)–nitrene intermediates” for C–H amination.¹¹

The macrocycle in coenzyme B₁₂, however, is a confused tetrapyrrole-substituted or reduced, corrole,¹² rather than the classic macrocycle, such as modified porphyrin in heme¹³ or chlorophyll.¹⁴ The smaller core size of free corrole compared with that in porphyrin may be crucial for these functions, including the high reactivity and the stability of high valence Co in coenzyme B₁₂ and in corrole.¹⁵ The coenzyme B₁₂ was observed very early to bring about distortion of the corrole ring system in performing its latent catalysis.^{16–18} Recent theoretical studies have suggested that conformational changes in the macrocycle of many enzymes, e.g., heme¹⁹ and cytochrome P450,²⁰ may play a very important role in their functions. Macrocyclic distortion and the resulting core contraction can

result in changes in the electronic^{21–23} and magnetic properties^{24–26} of the central iron ion²⁷ and in the nonbonding interaction of the *meso*-aryl.²⁸ These results imply that the reason “why nature does not use the porphyrin ligand in vitamin B₁₂” is a possible size mismatching of core to Co³⁺ ions rather than sterical inflexibility of the macrocycle.²⁹

In a recent report, we clarified the role of macrocyclic deformation modes and of the degree of distortion in heme for a series of ruffle-type porphyrins and a dome-type porphyrin.^{30,31} We found a conversion of electronic configuration and the formation of cross-hybrid states in the central iron and zinc ions under core contraction for different nonplanar metalloporphyrins.^{32–34} These findings provided experimental support to the assertion that distorted heme can generate and stabilize a high valent iron(V)-oxo complex³⁵ by a change in its macrocyclic deformations and its related core size.

The core size is smaller in the corrole macrocycle with one less porphyrin *meso*-carbon³⁶ (Figure 1). For Co(II) porphyrin, the 3.90 Å core diameter (Figure 1, right) is much smaller than the free cavity ($L_{NN} \sim 4.10$ Å) of free base porphyrin, which implies an imperfect size-matching between the diameter of the metallic ion and the macrocyclic core size. A smaller cavity ($L_{NN} < 3.90$ Å) is required to adjust the metal's electronic configuration when complexed with a small ion, such as

Received: August 29, 2015

Revised: October 13, 2015

Published: October 13, 2015

CrossMark
click for updatesCite this: *Anal. Methods*, 2015, 7, 2542

Visual detection of trace copper(II) based on its catalytic action in the dissociation of thiosulfate†

Xin Yan Hou,^a Shu Chen,^a Jian Tang,^a Yun Fei Long^{*a} and Li Zhu^{*b}

In this study, we report a new method for the detection of Cu^{2+} based on triangular silver nanoplates (TAg-NPs), which could be corroded by sodium thiosulfate ($\text{Na}_2\text{S}_2\text{O}_3$). TAg-NPs with blue color can be changed to yellow color in the presence of a certain concentration of $\text{Na}_2\text{S}_2\text{O}_3$, however, its color change is unclear when $\text{Na}_2\text{S}_2\text{O}_3$ was heated in the presence of Cu^{2+} . The reason may be that $\text{Na}_2\text{S}_2\text{O}_3$ dissociates on heating in the presence of Cu^{2+} , which leads the concentration of $\text{Na}_2\text{S}_2\text{O}_3$ to be decreased. Furthermore, when the heating time is fixed, the decrease in the concentration of $\text{Na}_2\text{S}_2\text{O}_3$ is proportional to the concentration of Cu^{2+} . As a result, the color of the mixture solution of TAg-NP/ Cu^{2+} / $\text{Na}_2\text{S}_2\text{O}_3$ and the absorbance at the position of the maximum absorption peak of TAg-NPs changed with the change in the concentration of Cu^{2+} . The changes in the values of absorbance (ΔA , the absorbance of TAg-NP/ Cu^{2+} / $\text{Na}_2\text{S}_2\text{O}_3$ subtracted from that of TAg-NP/ $\text{Na}_2\text{S}_2\text{O}_3$ at the position of the maximum absorption peak) were proportional to the concentrations of Cu^{2+} . Thus, a new method was established by studying the UV-vis absorption spectrum or the naked eye observation, which is simple, fast and of low cost for copper ion detection. Using this method, the concentration of Cu^{2+} could be detected accurately in the range of 2.5×10^{-9} to 7.5×10^{-7} mol L⁻¹ with the correlation coefficient of $r = 0.9983$. Moreover, the color change of TAg-NPs could be observed in the Cu^{2+} concentration of 2.5×10^{-8} to 7.5×10^{-7} mol L⁻¹.

Received 27th January 2015
Accepted 1st February 2015

DOI: 10.1039/c5ay00227c

www.rsc.org/methods

1. Introduction

In recent years, metal nanomaterials have attracted great attention due to their special properties¹⁻³ and potential applications in many fields.⁴⁻⁶ Furthermore, many of them have low toxicity,⁷ complex optical features in the region spanning the visible and near infrared spectra,⁸ and exhibit facile surface functionalization chemistry.⁹ These physical and chemical properties of metal nanomaterials depended on their shape and size^{10,11} especially for silver nanostructures. So, shape-controlled synthesis of silver nanostructures has attracted the attention of scientists, and a large number of methods have been devoted to the synthesis of silver nanostructures with different shapes.¹²⁻¹⁵ On the other hand, applications of silver nanostructures mainly depend on their shapes because higher atomic fractions are located at the corners, edges and defects of the silver nanostructures.^{16,17} Recently, triangular silver nanoplates (TAg-NPs) have been widely used as chromogenic

components in colorimetric sensing systems owing to their special optical properties.^{18,19}

Copper ion is one of the most abundant transition metal ions, and is commonly found as Cu^{2+} in natural water. However, the deficient or excessive amount of Cu^{2+} also brings about serious environmental pollution and potential toxicity to living organisms. As microorganisms are affected by even sub-micromolar concentrations of Cu^{2+} ,²⁰ its deficiency or excess can cause anemia, pancytopenia,²¹ gastrointestinal disturbance and/or damage to the liver and kidneys.^{22,23} Various methods have been developed for the determination of Cu^{2+} at trace quantity levels in many kinds of samples, such as infrared absorption spectroscopy,²⁴ anodic stripping voltammetry,²⁵ atomic absorption spectroscopy (AAS),^{26,27} and inductively coupled plasma spectroscopy (ICP).^{28,29} Moreover, many visual methods have been discovered for the detection of Cu^{2+} .³⁰⁻³⁴ These visual detection methods are simple, because they could be achieved with the naked eye. However, it needs a special reagent, and the sensitivity is still not very high. Therefore, developing a visual method with high sensitivity for Cu^{2+} detection is still needed.

Herein, we report a novel optical and visual method for detecting Cu^{2+} by UV-visible spectroscopy or naked eye observation. The higher atomic fractions with higher activity atoms at the three corners of the TAg-NPs could react with $\text{Na}_2\text{S}_2\text{O}_3$ easily.¹⁷ As a result, the UV-visible spectra and the color of the solution changed clearly. $\text{Na}_2\text{S}_2\text{O}_3$ could be dissociated when it

^aKey Laboratory of Theoretical Organic Chemistry and Function Molecule, Ministry of Education, School of Chemistry and Chemical Engineering, Hunan University of Science and Technology, Xiangtan, 411201, PR China. E-mail: L_yunfei927@163.com; Fax: +86 731 58372324; Tel: +86 731 58388503

^bSchool of Chemistry and Chemical Engineering, Beijing Union University, Beijing, 100101, PR China. E-mail: x694200@163.com

† Electronic supplementary information (ESI) available. See DOI: 10.1039/c5ay00227c



Letter

Fe₄I₃O₂₄H₁₅: A novel semiconductor with high performance in photodegradation of rhodamine B dyes under visible light irradiation



Datang Li*, Jianting Tang*, Jing Li

Key Laboratory of Theoretical Organic Chemistry and Function Molecule of Ministry of Education, School of Chemistry and Chemical Engineering, Hunan University of Science and Technology, Xiangtan 411201, China

ARTICLE INFO

Article history:

Received 2 October 2014

Received in revised form 24 November 2014

Accepted 3 January 2015

Available online 30 January 2015

Keywords:

Semiconductor

Photodegradation

Photosensitization

ABSTRACT

In this study, a new semiconductor, Fe₄I₃O₂₄H₁₅, was successfully developed. The results of UV–vis diffuse reflectance spectra indicated that Fe₄I₃O₂₄H₁₅ is visible-light-responsive, its absorption band edge is around the wavelength of 540 nm and its band gap is about 2.30 eV. The Fe₄I₃O₂₄H₁₅ semiconductor showed high activity and high stability in photodegradation of rhodamine B dyes under irradiation of visible light. Its activity is close to that of the highly efficient photocatalyst, Ag₃PO₄. The Fe₄I₃O₂₄H₁₅ semiconductor can be reused for at least 5 times without obvious loss of its activity in the photodegradation experiment.

© 2015 Elsevier B.V. All rights reserved.

1. Introduction

Semiconductors are of great importance because of their applications in environmental pollution treatment, water splitting for hydrogen energy production, etc., with sustainable solar energy through the processes of photosensitization [1–5] or photocatalysis [6–10]. The key issue to utilize solar energy through photosensitization or photocatalysis is the utilization of visible light during these processes. Therefore, many efforts have been dedicated to develop suitable semiconductor materials for visible light utilization to deal with the problems of environmental pollution and energy crisis [1–10]. As a case in point, Ag₃PO₄ semiconductor photocatalyst showed much higher photocatalytic activity than the widely used ones including BiVO₄, N-doped TiO₂, etc., in water oxidation and photodegradation of organic pollutants under visible light irradiation [11].

However, the developed semiconductors usually suffer from the inherent limitations of poor stability, high cost or high toxicity. For example, photocorrosion is easy to occur in the mostly used CdS semiconductor because its photogenerated holes are strong enough to oxidize the surface S²⁻ ions [12–14]. Silver-containing semiconductor photocatalysts like Ag₃AsO₄ [15], AgIO₄ [16], Ag₃PO₄ [17,18], Ag₂CO₃ [19–22], Ag₂CrO₄ [23,24], although highly active, are silver-containing and thus high-cost. Also, the silver-containing semiconductors are unstable because it is energetically possible for their surface ions to undergo photocorrosion reduction

or oxidation through their photogenerated carriers. Therefore, it is highly desirable to obtain stable, low-cost, and low-toxic semiconductors for efficient utilization of solar energy through the processes of photosensitization or photocatalysis.

The Fe₄I₃O₂₄H₁₅ compound was successfully prepared and its chemical composition was determined early in 1962 [25,26], but hitherto there is little data available on its structure and property, including XRD pattern, light-responsive range and photochemical activity, etc. In this work, we successfully prepared the Fe₄I₃O₂₄H₁₅ compound and further characterized its light-absorption property. Interestingly, we found that it, as a novel semiconductor with a band gap of 2.30 eV, is highly efficient in photodegradation of RhB dyes under visible light irradiation. The Fe₄I₃O₂₄H₁₅ semiconductor is attractive firstly in that it is noble-metal-free and does not contain highly toxic element. Also importantly, the Fe₄I₃O₂₄H₁₅ semiconductor showed high activity and high stability in photodegradation of RhB dyes.

2. Experimental

2.1. Preparation

The Fe₄I₃O₂₄H₁₅ and Ag₃PO₄ semiconductors were prepared according to the previously reported procedure [17,25,26].

2.2. Characterization

Scanning electron microscopy (SEM) experiment was undertaken on a FEI Quanta-200 microscope at an accelerating voltage of 20 kV. Transmission electron microscopy (TEM) experiment was performed using a FEI Tecnai G² Spirit instrument at an acceleration voltage of 120 kV. Ultraviolet–visible diffuse reflectance

* Corresponding authors. Tel./fax: +86 731 58290045.

E-mail addresses: dtlhx@163.com, jttang1103@126.com (J. Tang).

纳米腔限制环境下 2-(2-羟苯基) 苯并噻唑的质子转移

向俊峰, 易平贵, 于贤勇, 陈建, 郝艳雷, 任志勇

(湖南科技大学化学化工学院, 理论有机化学与功能分子教育部重点实验室, 分子构效关系湖南省普通高校重点实验室, 湘潭 411201)

摘要 采用稳态和瞬态荧光法对 2-(2-羟苯基) 苯并噻唑 (HBT) 与七元瓜环 (CB7) 的超分子作用及 CB7 分子纳米腔限制作用对 HBT 激发态质子转移 (ESIPT) 过程进行了研究, 并采用 Benesi-Hildebrand 方程对荧光数据进行处理, 以确定超分子复合物的组成比。结果表明, 在 *N,N*-二甲基甲酰胺 (DMF) 和二氯甲烷溶液中, CB7 与 HBT 的作用均形成化学计量比为 1:1 的主客体复合物, HBT 的质子转移对溶剂很敏感, CB7 的加入, 使 HBT 的荧光寿命降低, 量子产率增大。在 DMF 溶液中, CB7 的加入促进了酚氧负离子的形成, 而在二氯甲烷溶液中, CB7 的加入限制了 HBT 的激发态质子转移。结构优化计算表明, CB7 与 HBT 能形成化学计量比为 1:1 的复合物。

关键词 2-(2-羟苯基) 苯并噻唑; 质子转移; 七元瓜环; 纳米腔; 荧光光谱; 量子化学计算

中图分类号 O621.1; O621.3

文献标志码 A

质子转移是一类重要的反应, 广泛存在于化学和生物过程中。Weller^[1] 利用紫外光谱和荧光光谱研究 2-羟基苯甲酸与 2-氨基苯甲酸时发现两者的 Stoke 位移差别很大, 进一步的研究表明激发态分子内质子转移 (ESIPT) 是其主要原因。近年来, 有关质子转移的基础研究、应用研究、实验研究和理论研究被广泛开展^[2~7], 其中环糊精及瓜环^[8~11] (Cucurbit[*n*]uril) 等具有纳米级空腔的大环化合物被广泛应用于主客体化合物的研究, 其大环分子所具有的纳米级空腔结构对质子转移体所产生的相互作用备受关注^[12~15]。

2-(2-羟苯基) 苯并噻唑^[16] (HBT) 具有可发生激发态质子转移的性质^[17,18], 其光物理性质和光化学性质已经得到深入研究, 但其与瓜环的相互作用研究尚未见报道。

本文以七元瓜环 (CB7, 空腔高度 0.91 nm, 端口直径 0.54 nm, 口腔直径 0.73 nm, 结构见图 1) 为主体化合物, 与客体分子 HBT 相互作用, 研究大环分子 CB7 对 HBT 质子转移 (图 1) 性质的影响。

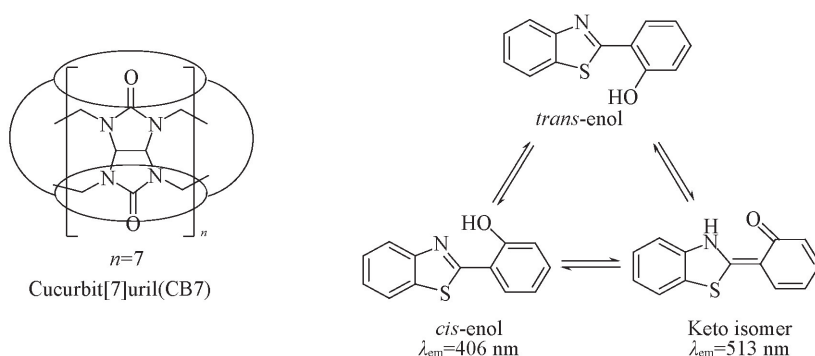


Fig. 1 Structure of CB7 and proton transfer process of HBT

收稿日期: 2014-12-05. 网络出版日期: 2015-03-18.

基金项目: 国家自然科学基金 (批准号: 21172066, 20971041) 和湖南省高校科技创新团队项目 (批准号: 湘教通[2012]318) 资助。

联系人简介: 易平贵, 男, 博士, 教授, 博士生导师, 主要从事分子构效关系与理论计算化学研究. E-mail: yipinggui@sohu.com



Contents lists available at ScienceDirect

Spectrochimica Acta Part A: Molecular and Biomolecular Spectroscopy

journal homepage: www.elsevier.com/locate/saa

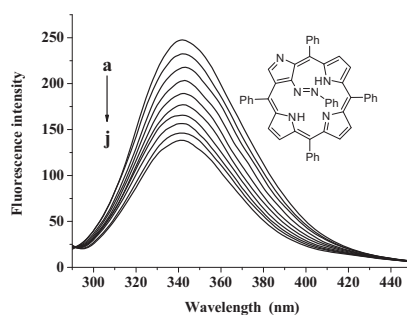
Study on the interaction between 21-(Ph-N=N)-NCTPP and bovine serum albumin by spectroscopic techniques

Xianyong Yu^{a,b,*}, Bingfei Jiang^a, Zhixi Liao^a, Xiaofang Li^{a,*}^aKey Laboratory of Theoretical Organic Chemistry and Function Molecule, Ministry of Education, Hunan Province College Key Laboratory of QSAR/QSPR, School of Chemistry and Chemical Engineering, Hunan University of Science and Technology, Xiangtan 411201, China^bKey Laboratory of Computational Physical Sciences, Fudan University, Ministry of Education, Shanghai, China

HIGHLIGHTS

- The interaction between BSA and 21-(ph-N=N)-NCTPP was studied.
- The fluorescence quenching mechanism was explored.
- The binding constants and binding sites were calculated.
- Hydrophobic interaction played a major role in the binding process.
- High probability of the energy transfer from BSA to 21-(ph-N=N)-NCTPP occurred.

GRAPHICAL ABSTRACT



ARTICLE INFO

Article history:

Received 13 October 2014

Received in revised form 15 December 2014

Accepted 31 January 2015

Available online 9 February 2015

Keywords:

Interaction

21-(Ph-N=N)-NCTPP

Bovine serum albumin

Fluorescence spectroscopy

Ultraviolet–visible spectroscopy

ABSTRACT

The interaction between 21-(Ph-N=N)-NCTPP and bovine serum albumin (BSA) was investigated by fluorescence and ultraviolet–visible (UV–Vis) spectroscopy under imitated physiological conditions. The results showed that the intrinsic fluorescence of BSA was quenched strongly by 21-(Ph-N=N)-NCTPP. The binding constants (K_b) and the binding sites (n) were obtained at three different temperatures (298, 304, and 310 K). The thermodynamic parameters (ΔH , ΔS and ΔG) of the interaction system were calculated, the results indicated that the binding process was spontaneous and the hydrophobic interaction played a major role in [21-(Ph-N=N)-NCTPP]–BSA binding process. Based on the Förster non-radiation energy transfer theory, the binding distance from 21-(Ph-N=N)-NCTPP to BSA was estimated to be about 3.51 nm. What's more, the synchronous fluorescence spectra indicated that the conformation of BSA has not been changed.

© 2015 Elsevier B.V. All rights reserved.

Introduction

Serum albumin (SA) is the most abundant protein constituent of blood plasma. The most outstanding function of SA is that it can

depot and transport various endogenous and exogenous ligands, such as fatty acid, amino acid, drugs and pharmaceuticals to particular biotargets [1–3]. The serum protein used in this study is bovine serum albumin (BSA), whose structure is similar to human serum albumin (HSA) in 76%. BSA is considered as an in vitro model for studying drug-chain 582 amino acid globular nonglycoprotein cross-linked with 17 cystine residues [4,5]. Studies on the binding of drug with protein is not only to have a considerable impact on metabolism and transporting process of drug, but also to help explaining the relationship between the structure and the function of the protein [6].

* Corresponding authors at: Key Laboratory of Theoretical Organic Chemistry and Function Molecule, Ministry of Education, Hunan Province College Key Laboratory of QSAR/QSPR, School of Chemistry and Chemical Engineering, Hunan University of Science and Technology, Xiangtan 411201, China (X. Yu). Tel.: +86 731 58290187; fax: +86 731 58290509.

E-mail addresses: yu_xianyong@163.com (X. Yu), lixiaofang@iccas.ac.cn (X. Li).



A novel membrane-less direct alcohol fuel cell



Qingfeng Yi*, Qinghua Chen, Zheng Yang

School of Chemistry and Chemical Engineering, Hunan University of Science and Technology, Xiangtan 411201, China

HIGHLIGHTS

- A membrane-less direct alcohol fuel cell was constructed.
- Anode catalyst was PdSnNi/MWCNT and cathode catalyst was Fe/C-PANI.
- Methanol, ethanol, propanol and butanol were used as the fuels.
- The cells with ethanol and n-propanol as fuels show the highest power density.

ARTICLE INFO

Article history:

Received 30 May 2015

Received in revised form

11 August 2015

Accepted 13 August 2015

Available online 24 August 2015

Keywords:

Alcohol
Fuel cell
Palladium

ABSTRACT

Membrane-less fuel cell possesses such advantages as simplified design and lower cost. In this paper, a membrane-less direct alcohol fuel cell is constructed by using multi-walled carbon nanotubes (MWCNT) supported Pd and ternary PdSnNi composites as the anode catalysts and Fe/C-PANI composite, produced by direct pyrolysis of Fe-doped polyaniline precursor, as the oxygen reduction reaction (ORR) catalyst. The alcohols investigated in the present study are methanol, ethanol, n-propanol, iso-propanol, n-butanol, iso-butanol and sec-butanol. The cathode catalyst Fe/C-PANI is electrochemically inactive to oxidation of the alcohols. The performance of the cell with various alcohols in 1 mol L⁻¹ NaOH solution on either Pd/MWCNT or PdSnNi/MWCNT catalyst has been evaluated. In any case, the performance of the cell using the anode catalyst PdSnNi/MWCNT is considerably better than Pd/MWCNT. For the PdSnNi/MWCNT, the maximum power densities of the cell using methanol (0.5 mol L⁻¹), ethanol (0.5 mol L⁻¹), n-propanol (0.5 mol L⁻¹), iso-propanol (0.5 mol L⁻¹), n-butanol (0.2 mol L⁻¹), iso-butanol (0.2 mol L⁻¹) and sec-butanol (0.2 mol L⁻¹) are 0.34, 1.03, 1.07, 0.44, 0.50, 0.31 and 0.15 mW cm⁻², respectively.

© 2015 Elsevier B.V. All rights reserved.

1. Introduction

A direct alcohol fuel cell (DAFC) uses alcohols including methanol, ethanol, propanol and butanol as the fuels to convert chemical energy into electricity. It possesses such characteristics as high efficiency of energy transformation, non-toxic emission and high specific energy density, and it is especially suitable to be used as mobile and portable power. A DAFC is generally composed of anode, cathode and ion exchange membrane. Pt and PtRu catalysts are usually applied to fabricate the anode and cathode due to their high electroactivity for alcohol oxidation (AO) and oxygen reduction reaction (ORR). Yet, their practical application is greatly limited by their high cost and easy poisoning caused by the intermediates formed during AO. In addition, alcohol molecules can cross over the

membrane to the cathode, leading to the rapid decline of the cathodic catalyst activity for ORR. Therefore, preparation of the anodic catalysts with lower Pt loadings and higher electroactivity for AO has been paid much attention. These catalysts include PtRu [1,2], PtNi [3,4], PtSn [5–7], PtIrRu [8,9], and PtAu [10]. These Pt-based catalysts, however, still suffer from the high cost because of the high Pt mass percentage in these Pt-based composites. Thus, it is worthwhile to utilize non-Pt metals to replace these Pt-based catalysts. Although palladium (Pd) is still a precious metal among the non-Pt metals, it is cheaper and much more abundant on earth than Pt. In addition, Pd and Pd-based catalysts present excellent electrocatalytic activity for AO in alkaline media [11–14]. Therefore, Pd is considered to be the best alternative to Pt for AO in alkaline media. Recently, we reported the preparation of Pd-based catalysts like nanoporous Pd nanoparticles [14], binary Pd–Ru catalysts [15] and Pd–Ni nanoparticles loaded on multi-walled carbon nanotubes (MWCNTs) modified with β -cyclodextrin [16], and MWCNT-supported PdSn and PSnNi nanoparticles [17], and they show

* Corresponding author.

E-mail address: yqfy2001@hnust.edu.cn (Q. Yi).



In situ preparation and high electrocatalytic activity of binary Pd-Ni nanocatalysts with low Pd-loadings



Qingfeng Yi*, Qinghua Chen

School of chemistry and Chemical Engineering, Hunan University of Science and Technology, Xiangtan 411201, Hunan, China

ARTICLE INFO

Article history:

Received 19 July 2015

Received in revised form 5 September 2015

Accepted 9 September 2015

Available online 11 September 2015

Keywords:

Pd

Ni

Ethanol oxidation

Fuel cell

ABSTRACT

Palladium nanoparticles supported on multi-walled carbon nanotube (MWCNT), with ultra-low Pd loadings (wt%) of 1.1%–1.9%, have been prepared through an in situ reduction of Pd²⁺ by Ni nanoparticles immobilized on MWCNT. That is, Ni nanoparticles are firstly loaded on MWCNT by chemical reduction method to fabricate the catalyst nanoNi/MWCNT. Then, aqueous PdCl₂ solution with various concentrations is added to the nanoNi/MWCNT catalyst stepwise, leading to the formation of Pd nanoparticles and subsequent in situ deposition on the nanoNi/MWCNT. The as-synthesized nanocatalysts (Pd_{4.1}Ni₁/MWCNT, Pd_{3.7}Ni₁/MWCNT and Pd_{1.3}Ni₁/MWCNT) have been characterized by SEM, XRD and XPS. Their electrocatalytic activity for ethanol oxidation in alkaline media has been investigated. Compared to the Pd/MWCNT catalyst prepared by the conventional NaBH₄ reduction method, the as-prepared Pd-Ni/MWCNT catalysts present low Pd-loading and significantly high electroactivity for ethanol oxidation. According to the cyclic voltammetric data, the forward-scan anodic peak current density *j*(Pd) on the Pd_{3.7}Ni₁/MWCNT catalyst is 130.9 mA cm⁻² μg⁻¹, which is over 11 times higher than on the Pd/MWCNT.

© 2015 Elsevier Ltd. All rights reserved.

1. Introduction

Direct liquid fuel cells (DLFCs) use liquid fuels to feed fuel cells and they possess more advantages than H₂/O₂ fuel cell [1]. Among the DLFCs, direct alcohol fuel cells (DAFCs) use liquid alcohols like methanol and ethanol, as fuels to keep the anodic reactions of the DAFCs. Further, compared to methanol, ethanol is considered to exhibit obvious superiority such as non-toxicity, natural availability and renewability. In addition, a direct ethanol fuel cell (DEFC) possesses the advantages of higher power density and zero greenhouse contribution to the atmosphere. In order to guarantee the normal operation of the DEFC, electro-oxidation of ethanol should be catalyzed on efficient catalysts. Pt and Pt-based materials have been considered to be efficient electro-catalysts for ethanol oxidation both in acidic and in alkaline media [2–4]. However, owing to the reasons known to all like high cost and scarce resources of Pt, and the poisoning effect of Pt by some intermediates formed during electro-oxidation of ethanol, practical application of Pt catalysts to fuel cells is severely limited [5,6]. Development of other catalysts with high electroactivity for ethanol oxidation, therefore, is of very significance. Among them,

Pd and Pd-based catalysts are alternatives to Pt catalysts for ethanol oxidation in alkaline media [7–13]. Ethanol electro-oxidation in an alkaline medium on a Pd catalyst takes place via the mechanism of the removal of the adsorbed ethoxy by the adsorbed hydroxyl on the Pd electrode [8], which is different from the mechanism on a Pt catalyst [6]. Various Pd catalysts have been prepared to investigate their electroactivity for ethanol oxidation in alkaline media. Dispersing Pd into nano-scale sizes particles and alloying of Pd with other metals like Ni [12–16], Ru [11], and Sn [3–5] et al., are common methods used to enhance the electro-activity of the Pd catalysts for ethanol oxidation.

Although Pd is relatively low-cost compared with Pt, it still belongs to a noble metal. The large scale practical application of Pd catalysts will be limited due to the higher cost of Pd. Thus, it is significant to reduce the Pd loading on catalysts but also to maintain or improve their electroactivity for ethanol oxidation. Marchionni et al. reported a Pd-based composite catalyst Pd-(Ni-Zn)/C with Pd-loading of 6.4% (wt%), which was prepared through the chemical deposition of Pd nanoparticles on (Ni-Zn)/C solid that was fabricated with the reaction of Zn powder with Ni²⁺ [17]. This catalyst exhibited excellent electroactivity for electro-oxidation of ethylene glycol (EG) and glycerol (G) in alkaline media.

Multi-walled carbon nanotubes (MWCNTs) possess high specific surface areas and are extensively used as excellent supports of catalyst particles. In this work, we firstly synthesized

* Corresponding author.

E-mail address: yqfyy2001@hnust.edu.cn (Q. Yi).

聚氨酯基合成纸的制备及性能

周 虎¹, 吴科建¹, 余 斌¹, 李 宁¹, 周智华¹, 孙汉洲²

(1. 湖南科技大学化学化工学院 理论有机化学与功能分子教育部重点实验室, 湖南 湘潭 411201;

2. 中南林业科技大学 理学院, 湖南 长沙 410004)

摘要:以聚氨酯(PU)和碳酸钙(CaCO_3)为主要原料,通过湿法转相技术和无机矿物质填充改性技术,成功制备了一种聚氨酯基合成纸。利用扫描电镜对合成纸的微观结构和形貌进行了研究,并对合成纸的力学性能、阻燃性、吸水率和吸墨性等性能进行了分析。SEM 观察表明,合成纸的截面孔洞内分散着 CaCO_3 颗粒,且 CaCO_3 分散较均匀,未出现明显的团聚现象。随着 CaCO_3 含量逐渐增加,合成纸的拉伸强度和断裂伸长率降低;但阻燃性却呈现一定的增大趋势,吸水率和吸墨性也明显提升。综合研究表明,当 CaCO_3 含量为 60.0% 时,合成纸综合性能最好,且具有良好的印刷性和书写性。

关键词:聚氨酯;碳酸钙;吸水率;吸墨性;接触角

中图分类号:TQ323.8

文献标识码:A

文章编号:1000-7555(2015)11-0176-05

合成纸又称塑料纸或薄膜纸,是以高分子树脂和无机填料为主要原料,并添加多种助剂,利用高分子界面化学原理和无机矿物质填充改性技术,经特殊加工工艺制备而成的具有塑料和纸张特征的多功能用纸。合成纸是一种塑料新型产品,具有与植物纤维纸同样的书写性和印刷性效果,并且拥有比重轻、强度大、抗撕裂、耐候性、耐折和经久耐用等特点^[1]。此外,合成纸生产过程中污染少、能耗低,是现代纸生产的一次重大改革。目前合成纸所使用的高分子材料主要为聚烯烃类,如聚乙烯、聚丙烯、聚氯乙烯等。这些聚烯烃类材料极性小、表面张力低,润湿性差、附着性差,而且其生物降解性差,易造成白色污染^[2]。因此,目前合成纸产品需进行技术改进。

聚氨酯(PU)是一种由多异氰酸酯和聚酯或聚醚多元醇反应而成的高聚物,其伸长率大、硬度范围广,具有优良的耐磨、抗撕裂、抗曲挠等性能,广泛应用于皮革、橡胶、塑料、胶粘剂及涂料等方面。同时,聚氨酯中含有亲水性官能团,具有良好的生物相容性和生物可降解性。另外,无机矿物质填充改性技术已成为近年来研究的热点。利用无机矿物粒子对高分子材料进行填充改性,不仅能使聚合物综合物理性能提高,还能使其尺寸稳定性得到相应改善。可见,聚氨酯材料以及无机矿物质填充改性技术的发展,为聚氨酯基合成

纸的研制奠定了良好的基础。

本文以 PU 和碳酸钙(CaCO_3)为主要原材料,利用湿法转相技术和无机矿物质填充改性技术,成功制备出一种新型聚氨酯基合成纸,并系统研究了不同 CaCO_3 含量对合成纸力学性能、阻燃性、吸水率和吸墨性的影响。旨在开拓聚氨酯材料的应用范围,为有机/无机复合材料的发展提供借鉴。

1 实验部分

1.1 原料

聚氨酯颗粒:聚酯型, $\bar{M}_w = 10$ 万,邵氏硬度 90A,由四川大学轻纺与食品学院提供; CaCO_3 : 500 mesh,益阳市桃矿石化工厂; N, N-二甲基甲酰胺(DMF): 分析纯,广东光华科技股份有限公司。

1.2 聚氨酯基合成纸的制备

采用湿法转相技术制备聚氨酯基合成纸,具体制备方案见 Tab 1。首先,用适量的溶剂 DMF 将聚氨酯颗粒溶解,得到透明的聚氨酯溶液;然后将不同含量的 CaCO_3 粉末加入到聚氨酯溶液中,并搅拌均匀,即得到合成纸胶液;再将合成纸胶液倾倒在成膜板上、推平成膜(控制厚度为 0.20 mm),迅速将其浸渍到去离子水中浸泡(0.5 h),待成膜后用蒸馏水冲洗 3 次,并放入真空干燥箱中于 50~60 °C 干燥 12 h,烘干后从成

收稿日期: 2014-11-28

基金项目: 国家科技部林业公益性行业科研专项(201304603); 国家自然科学基金资助项目(51443002, 51273062); 湖南省自然科学基金资助项目(14JJ5013); 湖南省教育厅青年项目(14B064)

通讯联系人: 周虎,主要从事聚氨酯材料研究, E-mail: hnustchem@163.com

新型 *N*-(1,3,4-噻二唑基)噻唑甲酰胺的合成及其杀菌活性

唐子龙^{*1}, 王恋¹, 马红伟¹, 王宏清²

(1. 湖南科技大学 化学化工学院 理论有机化学与功能分子教育部重点实验室 湖南 湘潭 411201;

2. 南华大学 化学化工学院 湖南 衡阳 421001)

摘要:以 5-羟基-2-氨基-1,3,4-噻二唑和 2-甲基-4-三氟甲基噻唑-5-甲酰氯为原料,在三乙胺的作用下合成了新型结构的标题化合物,并且发现化合物中与 1,3,4-噻二唑基相连的苯环上有吸电子取代基的产率比苯环上无取代基的产率低。产物的结构用 IR、¹HNMR、¹³CNMR 和元素分析进行了表征。测试了目标化合物的杀菌活性,其对所测菌种均表现出一定的杀菌活性,而且 1,3,4-噻二唑环上连有烷基的活性明显高于连有芳基的活性。

关键词:噻唑甲酰胺; 1,3,4-噻二唑; 合成; 杀菌活性

中图分类号: O622.6 文献标识码: A 文章编号: 0258-3283(2015)04-0298-03

Synthesis and Fungicidal Activity of Novel *N*-(1,3,4-Thiadiazolyl) thiazolyl Carboxamides TANG Zi-long^{*1}, WANG Lian¹, MA Hong-wei¹, WANG Hong-qing² (1. Key Laboratory of Theoretical Organic Chemistry and Function Molecules of Ministry of Education, School of Chemistry and Chemical Engineering, Hunan University of Science and Technology, Xiangtan 411201, China; 2. School of Chemistry and Chemical Engineering, University of South China, Hengyang 421001, China) *Huaxue Shiji* 2015 **37** (4) 298 ~ 300; 338

Abstract: Three new *N*-(1,3,4-thiadiazolyl) thiazole carboxamides were synthesized in moderate yields by reaction of 5-alkyl(aryl)-2-amino-1,3,4-thiadiazoles with 2-methyl-4-trifluoromethylthiazol-5-carboxychloride in the presence of triethyl amine. The compound with electron-withdrawing group on the phenyl ring connected with 1,3,4-thiadiazolyl was formed in higher yield than those with unsubstituted phenyl group. The structures of the compounds were confirmed by IR, ¹HNMR, ¹³CNMR and elemental analysis. The fungicidal activity of the compounds was also evaluated and moderate activity against the tested fungi was obtained. The compounds with alkyl group on the 1,3,4-thiadiazolyl ring exhibited higher activity than those with aryl group.

Key words: thiazole carboxamide; 1,3,4-thiadiazole; synthesis; fungicidal activity

酰胺类化合物是一类重要的化合物,具有广泛的生物活性,作为杀菌剂已有 40 多年历史^[1],在世界农药市场中占有相当重要的地位。近年来,关于噻唑甲酰胺类化合物杀菌活性的研究日益受到广泛关注^[2],其中开发为杀菌剂的有噻氟菌胺(Trifluzanide)^[3]和噻唑菌胺(Ethaboxam)^[4]。此外,具有良好杀菌活性的噻唑酰胺类化合物时有报道,日本农药化学株式会社报道含吡唑基的噻唑酰胺在 200 mg/L 剂量下,对苹果黑星病和大麦白粉病的防效达 70% 以上^[5]。拜耳农作物科学公司开发的噻唑酰环己基胺类化合物在 100 g/hm² 下对黑星病的防效为 100%^[6]。巴斯夫公司研制的三氟甲基噻唑甲酰胺苯胺类化合物在 63 mg/L 剂量下,对豆类植物锈病防效大于 74%^[7];该公司研制的另一个三氟甲基噻唑甲酰胺联苯胺类化合物在 4 mg/L 剂量下,对小麦叶锈病防效达 93%^[8]。2009 年,罗斐贤等^[9]报道了一类 *N*-苯并噁嗪基取代的噻唑酰胺类化合物在 500 mg/L

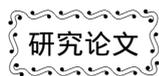
剂量下,对小麦白粉病菌抑制率为 95% 以上。

另一方面,1,3,4-噻二唑类化合物通常具有杀虫、杀菌、消炎、调节植物生长和除草等广泛的生物活性^[10,11],成为新农药创制研究的热点之一。但文献对既含噻唑甲酰基又含 1,3,4-噻二唑基的酰胺类化合物鲜见报道。因此,为了寻找新型高杀菌活性的噻唑甲酰胺类化合物,根据拼合原理,将 1,3,4-噻二唑基引入噻唑甲酰胺设计成新型结构的 *N*-(1,3,4-噻二唑基)噻唑甲酰胺类化合物(3a~3c),并研究其合成和杀菌活性。其合成路线如下所示。

收稿日期: 2014-07-15

基金项目: 国家自然科学基金资助项目(21372070); 湖南省高校创新平台开放基金资助项目(13K089); 理论有机化学与功能分子教育部重点实验室开放基金项目(LKF1302)。

作者简介: 唐子龙(1967-),男,湖南洞口人,博士,教授,主要从事有机合成、农药化学和药物化学研究, E-mail: zltang67@aliyun.com。



2,3-二芳基-1,3-苯并噁嗪的合成及杀菌活性

唐子龙^{a, b*} 夏赞稳^b 王宏清^c 王恋^b 焦银春^{a, b} 陈金文^b

(^a 湖南科技大学 理论有机化学与功能分子教育部重点实验室 湖南 湘潭 411201;

^b 湖南科技大学 化学化工学院 湖南 湘潭 411201; ^c 南华大学化学化工学院 湖南 衡阳 421001)

摘要 在三甲基氯硅烷(TMSCl)的催化作用下,取代苯甲醛与邻(芳胺甲基)苯酚经N杂缩醛化反应生成了一系列2,3-二芳基-1,3-苯并噁嗪类化合物。目标化合物的结构用IR、¹H NMR、¹³C NMR和元素分析等技术手段进行了表征。对所合成的化合物进行了初步杀菌活性测试,部分表现出良好的杀菌活性,化合物6e对菌株病菌的抑制活性为79.0%,化合物6a和6d均为74.8%,化合物6e对灰霉菌的抑制活性为77.9%。

关键词 二芳基-苯并噁嗪;合成;杀菌活性

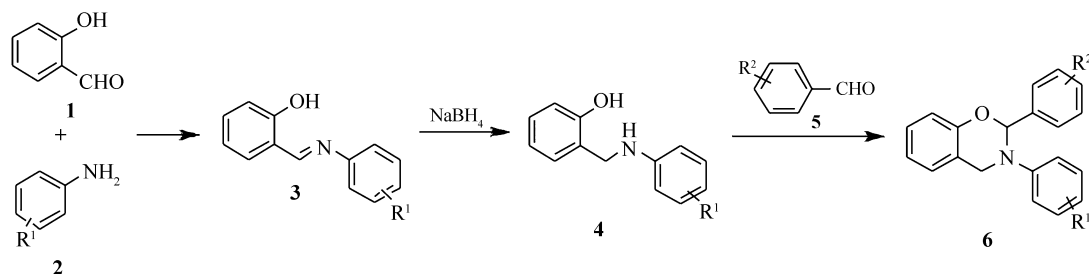
中图分类号:O626

文献标识码:A

文章编号:1000-0518(2015)02-0143-08

DOI: 10.11944/j.issn.1000-0518.2015.02.140191

1,3-苯并噁嗪类化合物具有广泛的生物活性,如抗癌^[1-3]、抗肿瘤^[4]、抗血小板凝聚^[5]、抑制细菌和真菌^[6-8]和抗结核^[9]等活性。特别是,有些1,3-苯并噁嗪类化合物可作为潜在的与自我免疫或炎症有关的CC(C代表半胱氨酸)趋化因子受体CCR2和CCR5的拮抗剂^[10]、潜在的表皮生长因子受体(EGFR)酪氨酸激酶抑制剂^[4]、潜在的抗癌药物^[11]和潜在治疗慢性乙型肝炎C病毒(HCV)靶标NS5a(非结构蛋白5a)的抑制剂^[12]。此外,2-位未取代的1,3-苯并噁嗪衍生物是制备苯酚甲醛树脂的重要材料^[13-15]。最近,有报道称1,3-苯并噁嗪衍生物具有非常有趣的光致变色活性^[16-18]。因此,1,3-苯并噁嗪类化合物的合成与应用研究受到广泛关注。许多文献报道了该类化合物的合成。一种常用而又简单的合成方法就是Mannich反应法:伯胺、甲醛和苯酚经两次Mannich反应可生成1,3-苯并噁嗪类化合物^[19-22]。然而,这种方法仅适用于合成2-位未取代的1,3-苯并噁嗪。伯胺和含氧的二卤代化合物经亲核取代反应也可以生成1,3-苯并噁嗪^[23],但是,反应原料含氧二卤代化合物不容易制备。邻氨基苯酚在催化剂如对甲苯磺酸的作用下与醛或酮反应缩合成环,为1,3-苯并噁嗪衍生物的合成提供了一条应用范围更广的途径^[24-27]。最近,文献[28]报道了一种通过仲胺 α -H的Redox-Neutral氧化并与水杨醛反应合成1,3-苯并噁嗪类化合物的新方法。我们以前报道了四氯化锡或三甲基氯硅烷(TMSCl)均是活性较好的催化剂,能够很好地促进邻氨基苯酚与芳醛的N杂缩醛化反应,制备了一系列多取代1,3-苯并噁嗪类化合物^[7, 29-31]。最近,我们报道了相转移催化法合成3-(1,3,4-噁二唑基)-1,3-苯并噁嗪类



Scheme 1 Synthesis of 1,3-benzoxazine derivatives(R: see the definition in tables vide infra)

2014-05-28 收稿 2014-07-21 修回 2014-09-19 接受

国家自然科学基金(No. 21372070)、国家科技支撑计划项目子课题(2011BAE06B01)、湖南省高校创新平台开放基金(13K089)、理论有机化学与功能分子教育部重点实验室开放基金(LKF1302)资助项目

通讯联系人:唐子龙,教授;Tel:0731-58291379; Fax:0731-58290509; E-mail: zltang67@aliyun.com; 研究方向:有机合成,农药化学,药物化学

含双键酰胺咪唑啉季铵盐缓蚀性能研究

黄康利^{1,2,3}, 石顺存^{1,2,3}, 胡 薇^{1,2,3}, 刘 蓓^{1,2,3}, 闫 东^{1,2,3}

- (1. 湖南科技大学化学化工学院, 湖南湘潭 411201;
2. 分子构效关系湖南省普通高等学校重点实验室, 湖南湘潭 411201;
3. 理论化学与分子模拟省部共建教育部重点实验室, 湖南湘潭 411201)

[摘要] 以高纯环烷酸等为原料, 合成了一种含双键酰胺咪唑啉季铵盐缓蚀剂(DAQS), 采用挂片失重法和电化学方法评价了其缓蚀性能。失重法结果表明: 该药剂对碳钢具有良好的缓蚀效果, 在强酸性溶液中, 控制适当的条件均可使缓蚀率达 90% 左右; 极化曲线表明, 该药剂是以阴极型为主的混合型缓蚀剂; 交流阻抗谱得出其缓蚀率随药剂浓度变化的顺序关系与碳钢挂片试验结果相一致。

[关键词] 环烷酸; 咪唑啉; 酰胺咪唑啉季铵盐; 缓蚀性能

[中图分类号] X703.1 [文献标识码] A [文章编号] 1005-829X(2015)09-0040-04

Study on corrosion inhibition capacity of amide imidazoline quaternary ammonium salt containing double bond inhibitor

Huang Kangli^{1,2,3}, Shi Shuncun^{1,2,3}, Hu Wei^{1,2,3}, Liu Bei^{1,2,3}, Yan Dong^{1,2,3}

- (1. China School of Chemistry and Chemical Engineering, Hunan University of Science and Technology, Xiangtan 411201, China;
2. Theoretical Chemistry and Molecular Simulation, Key Laboratory of Hunan Province General Institute of Higher Education of Structure-Activity Relationship, Xiangtan 411201, China;
3. Key Laboratory of the Province-Ministry Co-Constructed Section of Education Xiangtan 411201, China)

Abstract: Amide imidazoline quaternary ammonium salt containing double bond(DAQS) has been synthesized with naphthenic acid, etc. as raw materials, and its corrosion capacity evaluated by coupon weight loss method and electrochemical method. The results of weight loss method show that this chemical has good corrosion inhibition effect on carbon steel. In strong acidic solution, the corrosion inhibiting rate is about 90%, if the conditions are controlled properly. Polarization curves show that this chemical is a kind of mixed-type corrosion inhibitor, mainly cathode type. AC impedance spectroscopy displays that the result of the ordinal relationship of the corrosion inhibiting rate which changes with the change of reagent concentration and the result of carbon steel coupon experiments are consistent.

Key words: naphthenic acid; imidazoline; amide imidazoline quaternary ammonium salt; corrosion inhibition performance

咪唑啉类衍生物是一种环境友好型缓蚀剂^[1], 由于其原料具有易得、制备简单、低毒、高效等特点, 在国内外油气田、酸清洗、钢铁厂冷轧等领域广泛使用^[2]。目前使用较多的咪唑啉季铵盐类缓蚀剂是由有机酸与多胺经过脱水缩合得到油溶性的咪唑啉, 再经过烷基化后而得到。咪唑啉季铵盐是一种吸附膜型缓蚀剂, 缓蚀剂分子基团越大, 在金属表面的吸附就越完全, 缓蚀剂就越高效。为提高缓蚀率, 国内外学者对有机酸和烷基化试剂做了大量的选择, 但

随着缓蚀剂相对分子质量的增大, 势必会影响其水溶性, 因此如何在引入取代基增强缓蚀效果的同时又保证其水溶性, 仍是一个值得研究的课题。

咪唑啉季铵盐类缓蚀剂是带正电的季铵阳离子, 吸附在带负电的金属表面, 长的碳链作为疏水基远离金属, 从而形成一层致密的保护膜, 使得氢离子难以接近金属表面^[3]。由于—C=C—双键 π 电子易与金属原子空轨道发生作用^[4], 如果把双键引入缓蚀剂分子中, 有望进一步增强缓蚀剂分子在金属表

[基金项目] 湖南省教育厅资助项目(12k102)

两性高分子重金属螯合絮凝剂的合成 及其对 Cu(II) 的去除性能

刘立华 刘星 李艳红 杨刚刚 周智华 徐国荣

(湖南科技大学化学化工学院 理论有机化学与功能分子教育部重点实验室,
分子构效关系湖南省普通高等学校重点实验室 湘潭 411201)

摘要 合成了一种新型两性高分子重金属螯合絮凝剂聚(氯化二烯丙基甲基羟丙多胺基铵)基二硫代甲酸钠(PDAMHACDTC),采用元素分析、红外光谱、紫外光谱和核磁共振谱对其结构进行表征。考察了其对于含 Cu²⁺ 废水的处理效果,以及絮体的沉降速度;测定了微絮体的 ζ 电位,采用扫描电镜考察了絮体的形貌。结果表明,当 PDAMHACDTC 中 —CSS⁻ 与 Cu²⁺ 的物质的量之比接近 2:1 对 Cu²⁺ 的去除率大于 99.7% 残余 Cu²⁺ 浓度远低于国家污水综合排放一级标准 0.5 mg/L;在相同 —CSS⁻ 投加量时,形成的微絮体的 ζ 电位和絮体沉降速度分别比以聚(二甲基二烯丙基氯化铵-丙烯酰胺)为母体合成的两性高分子螯合絮凝剂(ACPF)形成絮体大,说明 PDAMHACDTC 比 ACPF 更利于中和絮体上过剩负电荷,促进絮体的形成和生长。

关键词 聚(氯化二烯丙基甲基羟丙多胺基铵)基二硫代甲酸钠 铜离子 螯合 絮凝 去除率

中图分类号 X703.5 文献标识码 A 文章编号 1673-9108(2015)03-1049-08

Synthesis of a heavy metal amphoteric chelating polymer flocculant and its removal performance towards Cu(II)

Liu Lihua Liu Xing Li Yanhong Yang Ganggang Zhou Zhihua Xu Guorong

(Key Laboratory of Theoretical Organic Chemistry and Function Molecule, Ministry of Education, Hunan Province College Key Laboratory of QSAR/QSPR, School of Chemistry and Chemical Engineering, Hunan University of Science and Technology, Xiangtan 411201, China)

Abstract A novel amphoteric chelating polymer flocculant poly(diallyl methyl hydroxypropoxy ammonium chloride)-based dithiocarbamate sodium (PDAMHACDTC) was synthesized and its structure was characterized by elemental analysis, FT-IR, ultraviolet spectroscopy and ¹H-NMR spectroscopy. The removal efficiency of Cu²⁺ by PDAMHACDTC and the sedimentation rate of flocs formed were investigated; the zeta potential changes of microflocs were determined, and the images of flocs were investigated by using scanning electron microscope. The results show that when the molar ratio of —CSS⁻ to Cu²⁺ is near 2:1, the removal rate of Cu²⁺ is above 99.7%, and the concentration of residual Cu²⁺ is far below 0.5 mg/L of the first grade criteria of China's Integrated Wastewater Discharge Standard. When the dosage of —CSS⁻ is the same, the zeta potential changes of microflocs and the sedimentation rate of flocs formed are higher than those formed by amphoteric chelating polymer flocculant (ACPF) based on poly(dimethyldiallylammonium chloride-acrylamide), respectively, indicating that PDAMHACDTC is more conducive to neutralizing the excess negative charge of flocs, thereby facilitating the formation and growth of flocs.

Key words poly(diallyl methyl hydroxypropoxy ammonium chloride)-based dithiocarbamate sodium (PDAMHACDTC); copper ion; chelation; flocculation; removal rate

Hg、Pb、Cd、Cr、As、Ni、Cu 等重金属不能被生物降解,即使微量也可产生显著毒性效应,并易在生物体内蓄积而引起中毒,因此,重金属废水是对环境污染最严重、对人类危害最大的废水之一^[1-2]。在已研发的重金属废水处理方法中^[3-5],螯合沉淀法因其工艺简单、高效而又经济,适于大规模重金属废水的处理,比其他方法更具推广应用价值^[6]。但其处

理效果取决于所使用的螯合絮凝剂的性能。单一功

基金项目:国家自然科学基金资助项目(51078141, 51378201);湖南省科技计划项目(2010FJ3030);湖南科技大学研究生创新基金项目(S100123)

收稿日期:2014-02-09; 修订日期:2014-02-28

作者简介:刘立华(1969—),男,博士,教授,硕士生导师,主要从事功能高分子和污染治理技术等领域的研究。

E-mail: llh213@163.com

光致抗蚀剂的制备及其性能研究

周虎 李宁 蒋敏

(湖南科技大学化学化工学院 理论有机化学与功能分子教育部重点实验室, 湖南 湘潭 411201)

罗小阳 唐甲林 秦先志

(深圳市柳鑫实业有限公司, 广东 深圳 518107)

摘要 以甲基丙烯酸甲酯(MMA)、丙烯酸丁酯(BA)、甲基丙烯酸(MAA)等为基本原料,以过氧化苯甲酰(BPO)为引发剂,分别选用无水乙醇、丁酮、乙酸乙酯为溶剂,采用溶液聚合法制备了成膜树脂;并以三羟甲基丙烷三丙烯酸酯(TMPTA)为交联剂,二苯甲酮(BP)为光引发剂,开发了光致抗蚀剂。研究表明,单体质量比MMA:BA:MAA为45:40:15时,反应生成了三元共聚物,在引发剂用量为单体用量的1%~2%、反应温度控制在(80~85)℃的条件下,以无水乙醇作溶剂制备的成膜树脂最稳定,耐水性优于丁酮和乙酸乙酯作溶剂时制备的树脂。经紫外固化测试发现,固化时间控制在2 min左右比较合适,光引发剂用量在6%左右最适宜。该研究为光致抗蚀剂进一步的研究提供了思路,具有一定的借鉴意义。

关键词 光刻胶; 电路板; 成膜树脂; 紫外固化; 甲基丙烯酸甲酯

中图分类号: TN41 文献标识码: A 文章编号: 1009-0096(2015)09-0010-04

Preparation and application properties of photoresist

ZHOU Hu LI Ning JIANG Min LUO Xiao-yang TANG Jia-lin QIN Xian-zhi

Abstract A solvent-based polyacrylate matrix resin was prepared from the methyl methacrylate(MMA), the butyl acrylate(BA), and methacrylic acid(MAA) with absolute ethanol, 2-methyl ethyl ketone(MEK), ethyl acetate(EAC) as solvent respectively, benzoyl peroxide(BPO) as initiator by a solution polymerization and it was prepared into photoresist with trimethylol propane triacrylate(TMPTA) as crosslinker and benzophenone(BP) as photoinitiators. The results indicated that the ternary copolymer was synthesized in the reaction with the monomer ratio MAA:MMA:BA of 45:40:15. The matrix resin had relatively better combination property with absolute ethanol acted as the solvent and its water resistance compared with the matrix resin prepared with 2-methyl ethyl ketone(MEK), ethyl acetate(EAC) as solvent respectively is better when the BPO concentration was 1%~2%, polymerization temperature was at 80℃~85℃. Curing time controlled at about 2 min is more appropriate and the amount of photoinitiator about 6% turns out to be the most appropriate after UV curing test. To some extent, this paper can offer a significant reference to the further researches of photoresist.

Key words Photoresist; PCB; Matrix Resin; UV Curing; MMA

光致抗蚀剂(photoresist)又称光刻胶,具有光化学敏感性的媒介,它在半导体及印制电路板生产加工中是不可缺少的^{[1][2]}。光刻胶经紫外光固化后,其硬度、溶解性等物理性质均发生变化,通过加入适当的溶剂处理,得到所需图像。经紫外光固化得

到的聚合物因具有抗蚀性,所以叫做抗蚀剂^[1]。

光刻胶常用于印制电路板生产加工中,通常由粘结树脂、交联剂、光引发剂、增塑剂、增粘剂、溶剂和色料等组成^[3]。成膜树脂是整个光刻胶的主要成分,又称粘结树脂。粘结树脂通常有聚苯丁树

文章编号: 1001-8719(2015)04-0912-08

酰胺咪唑啉季铵盐合成及其缓蚀性能

石顺存¹, 黄康利¹, 潘 蕾², 焦银春¹

(1. 湖南科技大学 化学化工学院 理论有机化学与功能分子教育部重点实验室 分子构效关系湖南省普通高校重点实验室, 湖南 湘潭 411201;
2. 北京大学 第四临床医学院 北京积水潭医院病案统计室, 北京 100035)

摘要: 以高纯环烷酸为原料合成了系列酰胺咪唑啉季铵盐水溶性缓蚀剂, 探讨了其咪唑啉环 N₍₁₎ 原子上取代基与缓蚀性能之间的关系。采用取代基电子效应法和碳钢挂片失重法, 从理论与实验两方面探讨了酰胺咪唑啉季铵盐对碳钢的缓蚀性能。利用数理统计方法得出, 其缓蚀效率(η)与基团极化效应参数(PEI_r)和—C=C—键效应指示变量 D 之间符合定量线性关系 $\eta = a + b \text{PEI}_r + c D$ (a, b, c 为常数), 相关系数 $R \geq 0.996$ 。该研究成果, 能为离子型缓蚀剂分子设计提供一种简便易行的新方法, 为找到具有更佳缓蚀性能的新型咪唑啉缓蚀剂提供参考。

关键词: 咪唑啉; 酰胺咪唑啉季铵盐; 缓蚀剂; 电子效应; 环烷酸

中图分类号: O622.6 文献标识码: A doi: 10.3969/j.issn.1001-8719.2015.04.012

Synthesis and Corrosion Inhibition Performance of Amidogen Imidazoliny Quaternary Ammonium Salts

SHI Shuncun¹, HUANG Kangli¹, PAN Lei², JIAO Yinchun¹

(1. School of Chemistry and Chemical Engineering, Hunan University of Science and Technology, Key Laboratory of Theoretical Organic Chemistry and Function Molecule, Ministry of Education, Hunan Provincial University Key Laboratory of QSAR/QSPR, Xiangtan 411201, China; 2. Department of Medical Record and Statistics of Beijing Jishuitan Hospital, the 4th Medical College of Peking University, Beijing 100035, China)

Abstract: A series of water-soluble amidogen imidazoliny quaternary ammonium salt corrosion inhibitors were synthesized from highly pure naphthenic acids. The relationship between the alkyl group connecting N₍₁₎ of the imidazoline ring and corrosion inhibition performance was investigated. Both the electronic effect method of substituent and the mass loss method for carbon steel samples were used to investigate their corrosion inhibition performance in both theoretical and experimental aspects. With the method of mathematical statistics, it was derived that the linear relationship between the corrosion inhibition efficiency η and group polarizability effect parameter PEI_r and variable indicator D for —C=C— bond was in the form of $\eta = a + b \text{PEI}_r + c D$, in which a, b and c were constants, with the correlation coefficient $R \geq 0.996$. Such research results may provide a new and simple method for the molecular design of ionic inhibitor, as well as a reference to find new imidazoline inhibitors with better corrosion inhibition performance.

Key words: imidazoline; amidogen imidazoliny quaternary ammonium salt; corrosion inhibitor; electronic effect; naphthenic acid

收稿日期: 2014-04-09

基金项目: 湖南省教育厅项目(12k102) 和湖南省高校科技创新团队支持计划资助

通讯联系人: 石顺存, 男, 教授, 硕士, 从事水处理缓蚀剂研究开发; E-mail: shishuncun@163.com

锂离子电池正极材料 LiMBO_3 研究进展

唐安平¹, 钟倩雯¹, 胡拥军², 刘立华¹, 徐国荣¹

(1. 湖南科技大学 化学化工学院 理论有机化学与功能分子教育部重点实验室 湖南 湘潭 411201;

2. 湖南城市学院 化学系 湖南 益阳 413000)

摘要 LiMBO_3 (M=Mn, Fe, Co) 硼酸盐作为新一代锂离子电池正极材料具有摩尔质量小、资源丰富、环境友好、理论比容量高等优点。对 LiFeBO_3 、 LiMnBO_3 、 LiCoBO_3 等硼酸盐正极材料的结构、制备方法、电化学性能的研究现状进行了综述, 并对存在的主要问题提出了改进方法。

关键词 锂离子电池; 正极材料; 硼酸盐; LiFeBO_3 ; LiMnBO_3

中图分类号: TM 912.9

文献标识码: A

文章编号: 1002-087 X(2015)07-1533-03

Research progress in LiMBO_3 (M=Mn, Fe, Co) cathode materials for Li ion batteries

TANG An-ping¹, ZHONG Qian-wen¹, HU Yong-jun², LIU Li-hua¹, XU Guo-rong¹

(1. Key Laboratory of Theoretical Organic Chemistry and Function Molecule, Ministry of Education, School of Chemistry and Chemical Engineering, Hunan University of Science and Technology, Xiangtan Hunan 411201, China; 2. Department of Chemistry, Hunan City

University, Yiyang Hunan 413000, China)

Abstract: LiMnBO_3 (M = Mn, Fe, Co) borate cathodes for lithium ion batteries offer several appealing features, such as relatively light molar mass, abundant resources, environmental friendliness and relatively high theoretical specific capacities. Borate cathode materials such as LiFeBO_3 , LiMnBO_3 and LiCoBO_3 were reviewed. The recent research progress on their structures, preparation methods and electrochemical performances were described. In addition, the defects were improved.

Key words: lithium ion batteries; cathode material; borate; LiFeBO_3 ; LiMBO_3

自 1997 年 Goodenough 小组^[1]报道了 LiFePO_4 的可逆脱嵌锂特性以来, 以橄榄石型 LiFePO_4 为代表的聚阴离子型锂离子电池正极材料的研究引起了人们的广泛关注。到目前为止, 大部分研究聚焦在由 SO_4^{2-} 、 PO_4^{3-} 或 SiO_4^{4-} 等聚阴离子组成的正极材料的电化学性能。最近, LiMBO_3 (M=Mn, Fe, Co) 硼酸盐作为锂离子电池正极材料也吸引了一定的注意力^[2-3]。

与 SO_4^{2-} 、 PO_4^{3-} 或 SiO_4^{4-} 等聚阴离子相比, BO_3^{3-} 的优点是摩尔质量小 (58.8 g/mol)。因此, LiMBO_3 可能具有更高的比容量, 例如 LiFeBO_3 、 LiMnBO_3 、 LiCoBO_3 的理论比容量分别为 220、222、215 mAh/g, 比 LiFePO_4 约高出 50 mAh/g。这表明 LiMBO_3 有可能发展成为高比容量的锂离子电池新型正极材料。再加上其热稳定性和安全性能方面的优势, 在锂离子动力电池中具有巨大的应用前景。尤其是 LiFeBO_3 , 它的电子电导率比 LiFePO_4 的更高^[2]。因此, 尽管 LiMBO_3 的平均电压比相应的磷酸盐正极材料低 0.4 V, 但由于其理论比容量比相应的磷酸盐材料约高 50 mAh/g, 理论能量密度比相应的磷酸盐材料

仍高出 10%。这些优点使得 LiMBO_3 作为新一代的锂离子电池正极材料逐步进入研究者的视野。

1 结构

单斜 LiMBO_3 具有与 LiZnBO_3 相似的晶体结构, 属 C2/c 空间群。在结构中, 过渡金属离子位于稍微偏离 MO_3 三角双锥中心的位置。每一个 MO_3 三角双锥与相邻的 MO_3 通过共边连接起来, 并沿 [-101] 方向形成 MO_3 一维链。 LiO_4 四面体与相邻的 LiO_4 四面体通过共边而形成双三棱锥。双三棱锥沿着 [001] 方向通过共边和共顶点连接起来, 从而形成一维锂离子路径。 LiO_4 、 MO_3 链均与相邻的 BO_3 平面共顶点相连。这三种硼酸盐结构上的差异仅仅是 MO_3 三角双锥的大小不同, 且通过它们的晶格参数的变化体现出来。图 1 为 LiMBO_3 的晶体结构示意图。从表 1 可以看出, 当 Mn^{2+} ($r_v = 0.075$ nm) 被 Fe^{2+} ($r_v = 0.071$ nm)、 Co^{2+} ($r_v = 0.067$ nm) 取代时, LiMBO_3 的晶格参数和晶胞体积不断减小。

除单斜结构外, LiMnBO_3 还有与 LiCdBO_3 同型的六方结构 (图 2)。在结构中, Mn 与 5 个氧原子配位形成 MnO_5 正四面体, Li 与 4 个氧原子配位形成 LiO_4 四面体。整个晶体由 MnO_5 正四面体、 BO_3 平面以及 LiO_4 四面体相连而构成。每个 MnO_5 正四面体通过正方形面的两个边相连形成边链, 这些链与 BO_3

收稿日期: 2014-12-07

基金项目: 湖南省自然科学基金 (12JJ2022); 湖南省教育厅资助科研项目 (14A052); 湖南省科技计划项目 (2012KW3066)

作者简介: 唐安平 (1969—), 男, 湖南省人, 副教授, 博士, 主要研究方向为新型化学电源与电池材料。

Indispensable substituent cross-interaction effect on ^{13}C NMR chemical shifts of carbonyl group for disubstituted phenyl benzoates

Chen Guanfan^{1,2,3}, Luo Qingqing¹, Cao Chenzhong^{1,2,3*}, Zeng Rongjin^{1,2,3} and Liu Wanqiang^{1,2,3}

(1. School of Chemistry and Chemical Engineering, Hunan University of Science and Technology, Xiangtan 411201, Hunan Province, China.) (2. Key Laboratory of Theoretical Organic Chemistry and Function Molecule of Ministry of Education, Hunan University of Science and Technology, Xiangtan 411201, Hunan Province, China.) (3. Hunan Provincial University Key Laboratory of QSAR/QSPR, Xiangtan 411201, Hunan Province, China)

Abstract: The substituent effects on ^{13}C NMR chemical shifts of carbonyl group ($\delta_{\text{C}}(\text{C}=\text{O})$) for a diverse set of the substituted phenyl benzoates were deeply investigated, and a quad-parameter correlation equation with correlation coefficient 0.9981 and standard error 0.057 was obtained for 42 samples. The electron-withdrawing groups (EWGs) on the benzoyl ring and the phenyl ring decreased the δ_{C} values; While electron-donating groups (EDGs) on the benzoyl ring and the phenyl ring increased the δ_{C} values. A new substituent specific cross-interaction $\Delta\sigma_{\text{m}}^2$ was recommended to scale the interaction between substituents for the titled compounds. The obtained correlation equation can be used to predict the $\delta_{\text{C}}(\text{C}=\text{O})$ values of corresponding compounds.

Keywords: disubstituted phenyl benzoate; ^{13}C NMR chemical shift; substituent specific cross-interaction

1 Introduction

In whatever form, the additive item of substituent parameters was found satisfactory in numerous QSPR/QSAR studies of multiple-substituent effect^[1]. However, Suresh and Gadre^[2] ever pointed out that the simple additivity rule of substituent parameters had serious drawbacks, and the substituent cross-interaction effect should not be neglected despite its remoteness. Therefore, several reasons, both experimental and theoretical, can be invoked to find the parameter form.

Palm *et al.*^[3] considered that properties of mono-substituted alkanes (RX) are not only related to molecular groups R and X themselves, but also related to the group-group interaction, which could be shown by the following equation.

$$f(RX) = \varphi(R) + \varphi(X) + \varphi(R)\varphi(X) \quad (1)$$

where $f(RX)$ represents a function of compound RX , $\varphi(R)$ and $\varphi(X)$ are the contribution of the function groups R and X to the molecular properties, respectively. $\varphi(R)\varphi(X)$ is the interaction of groups R and X . Unfortunately, the detailed form of $\varphi(R)\varphi(X)$ was not involved in his works. Dubois and Ruasse investigated substituent-substituent interaction by the interactive free energy relationship (IFER), and theoretically derived on the reasonable assumption that the cross term in $\sigma_X\sigma_Y$ was effective compared to the quadratic terms in σ_X^2 and σ_Y^2 ^[4]. Liu and Guo^[5] defined the substituent interaction energies (SIE), which was expressed effectively by the product of Hammett parameters ($\text{SIE}(X, Y) = -k\sigma_X\sigma_Y$), and was

applicable to disubstituted benzenes, and hexatrienes, and so on. Lee *et al.* studied the solvent effects on the cross-interaction constants in benzhydryl cation and anion formation with the similar form, and obtained good results^[6]. Cao and his group used this form as the item of substituent cross-interaction effect for disubstituted systems, and successfully investigated the substituent effect on the UV absorption wavenumbers of *para*-disubstituted benzenes, *para*-disubstituted stilbenes, and so on^[7]. Those works showed that the substituent cross-interaction effect is remote but indispensable, and it can be scaled by the cross term of substituents in $\sigma_X\sigma_Y$.

For any properties of any compounds, can the substituent cross-interaction effect be scaled by the same form of substituent parameters? In research of substituent effect on ^{13}C NMR chemical shifts of carbonyl group for *para*-disubstituted phenyl benzoates (XPhCO_2PhY , XPBY), Neuvonen and her co-workers tried to scale the substituent cross-interaction effect with the $\text{SIE}(X, Y)$ form^[8]. Unfortunately, they found that the cross term in $\sigma_X\sigma_Y$ was not suitable to be scaled the substituent cross-interaction effect. Therefore, when they next investigated the substituent effect on ^{13}C NMR chemical shifts of bridge group $\text{C}=\text{N}$ in disubstituted benzylidene anilines ($\text{XPhCH}=\text{NPhY}$, XBAY)^[9], the substituent cross-interaction effect was not further discussed. Cao *et al.*^[10] considered that the substituent cross-interaction effect should exist, but Neuvonen and her co-workers did not find the correct expressions of the substituent cross-interaction effect. They investigated further the research results of ^{13}C NMR chemical shifts of bridge

Received: 2014-04-23; Revised: 2014-09-07

Foundation item: Supported by the National Natural Science Foundation of China (No. 21202043, 21272063, 21172065), and the Scientific Research Fund of Hunan Provincial Education Department (11K024)

Author information: Chen Guanfan (1978-), Male, doctor, associate professor, Speciality: Physical Organic Chemistry E-mail: gfcchen@hust.edu.cn

*Corresponding author: Cao Chenzhong (1957-), Male, Professor, Ph.D. E-mail: czcao@hust.cn

桐酸单甘酯改性水性聚氨酯的制备及其性能*

周虎¹ 李宁¹ 余斌¹ 郭家旺¹ 孙汉洲² 吴科建¹

(1. 湖南科技大学化学化工学院 理论有机化学与功能分子教育部重点实验室 湖南湘潭 411201)

(2. 中南林业科技大学理学院 长沙 410004)

摘要: 以异佛尔酮二异氰酸酯、聚己内酯二醇、聚醚三醇和 2,2-二羟甲基丙酸等为基本原料,以桐酸单甘酯(EAM)为改性剂,制备了水性聚氨酯(WPU)乳液。利用红外光谱仪、激光粒度分析仪、离心机、硬度计、透水汽性测试、吸水率测试、抑菌试验,研究了EAM改性WPU材料的结构和性能。结果表明,当EAM质量分数 $\leq 10\%$ 时,WPU粒径小、稳定性好;随着EAM含量的增加,聚氨酯膜的硬度增加、透水汽率减小、耐水性增强;EAM的引入赋予了聚氨酯一定的抗菌性。

关键词: 桐油; 水性聚氨酯; 脂肪族; 抗菌性

中图分类号: TQ 323.8

文献标识码: A

文章编号: 1005-1902(2015)04-0029-04

与传统溶剂型聚氨酯(PU)相比,水性聚氨酯(WPU)具有无毒、不燃、对环境友好等优点^[1]。但WPU由于引入亲水性基团,其耐水性、耐化学品、机械强度等都不及溶剂型PU。可对WPU进行改性以提高其性能^[2-6]。环氧树脂改性、聚硅氧烷改性和丙烯酸复合改性WPU较常见。植物油来源广泛,价格低廉。桐油具有附着力强、光泽性好、抗腐蚀、抗菌、防渗透等优良性能,广泛应用于涂料、胶粘剂、医药工业和生物柴油等领域^[7-9],其主要成分是桐酸甘油酯,长链结构中含有羟基和双键等可反应基团,具有很好的反应活性。

本研究以异佛尔酮二异氰酸酯(IPDI)、聚己内酯二醇(PCL)、聚醚三醇、2,2-二羟甲基丙酸(DMPA)等为基本原料,以桐油的不完全水解产物桐酸单甘酯(EAM)为改性剂制备WPU乳液。EAM改性WPU材料不仅能克服普通WPU的一些不足,还有桐油的某些优良性能,将具有良好的应用前景。

1 实验部分

1.1 主要原料及预处理

IPDI,工业级,南京嘉翔化工有限公司;PCL($M_n=2000$),工业级,上海风标化学科技有限公司;

聚醚三醇($M_n=3000$),工业级,上海慈太龙实业有限公司;桐酸单甘酯(EAM,结构式见图1),中南林业科技大学;DMPA,工业级,成都市鑫达化工有限公司;二月桂酸二丁基锡(DBTDL),化学纯,成都金山化学试剂有限公司;三乙胺(TEA),分析纯,天津市富宇精细化工有限公司;*N,N*-二甲基甲酰胺(DMF),分析纯,广东光华科技股份有限公司;黄曲霉,湖南科技大学生命科学学院。其中,PCL、聚醚三醇、DMPA和EAM在使用前置于恒温真空干燥箱内,于110℃下干燥24h后冷却备用。

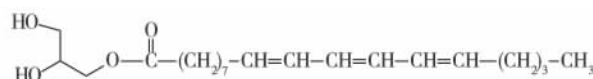


图1 EAM 结构式

1.2 EAM 改性 WPU 乳液的制备

在带有搅拌器、温度计、氮气通入装置的四口烧瓶中,加入一定比例的IPDI、PCL、1.5g聚醚三醇和EAM,升温至 $(80 \pm 2)^\circ\text{C}$,加入催化剂DBTDL反应2h;然后加入3.0gDMPA扩链反应2h,加18gDMF稀释反应物;再降温至 $40 \sim 50^\circ\text{C}$,加入2.3gTEA中和成盐,加160g水乳化,即得到固含量为26%的EAM改性WPU乳液。按乳化前原料的

* 基金项目: 国家科技部林业公益性行业科研专项(201304603); 国家自然科学基金(51443002); 湖南省自然科学基金(14JJ5013); 湖南省教育厅青年项目(14B064)。

LiFeBO₃ /LBO 复合材料的制备及其电化学性能

申洁,唐安平,贺冬华,刘立华,徐国荣

(湖南科技大学 化学化工学院 理论有机化学与功能分子教育部重点实验室 湖南 湘潭 411201)

摘要: 采用溶胶-凝胶法制备了单斜结构的 LiFeBO₃ /LBO 复合材料(C2/c 空间群)。通过 XRD、SEM、充放电测试、循环伏安、交流阻抗等手段分别对结构、形貌和电化学性能进行了研究。结果表明,与不含 LBO 的 LiFeBO₃ 相比,复合材料具有较高的放电比容量和良好的循环性能,尤其是当复合材料中含有 15.1% LBO 时,该材料在 C/20 倍率下获得了 194.6 mAh/g 的首次放电比容量,100 次循环后放电比容量仍维持在 137.0 mAh/g。循环伏安和交流阻抗测试结果也表明,LBO 含量为 15.1% 的复合材料中 LiFeBO₃ 粒子之间的导电性明显得到改善。

关键词: 正极材料; 硼酸铁锂; 溶胶-凝胶法; 锂离子电池

中图分类号: O646.2 文献标志码: A 文章编号: 1672 - 9102(2015)01 - 0110 - 06

Synthesis and electrochemical performance of LiFeBO₃ /LBO composite materials

Shen Jie, Tang Anping, He Donghua, Liu Lihua, Xu Guorong

(Key Laboratory of Theoretical Organic Chemistry and Function Molecule, Ministry of Education,
School of Chemistry and Chemical Engineering, Hunan University of Science and Technology, Xiangtan 411201)

Abstract: LiFeBO₃/lithium boron oxide (LBO) composites with single monoclinic phase (C2/c space group) were synthesized by sol-gel method. Structure and morphology of the samples were analyzed by X-ray diffraction and scanning electron microscopy, respectively. The electrochemical characteristics of samples were evaluated by means of the constant current charge-discharge, cyclic voltammetry (CV) and alternating current (AC) impedance. It is demonstrated that composites with LBO show higher discharge specific capacities and better cycling performance than bare LiFeBO₃, especially the sample with 15.1% LBO, which delivers an initial discharge specific capacity of 194.6 mAh/g and a discharge specific capacity of 137.0 mAh/g at the 100th cycle with a rate of C/20, respectively. The observation of CV and AC impedance also indicates that the composite with 15.1% LBO evidently increases the conductivity between LiFeBO₃ particles.

Keywords: cathode material; lithium iron borate; sol-gel method; lithium ion batteries

随着能源与环境问题的日益突出以及现代科技的高速发展,循环性能好、工作电压高、绿色环保的锂离子电池作为一种可重复使用的资源,逐渐进入人们的视野,成为人们关注的焦点,被研发用以缓解能源紧张和环保问题,并被广泛应用于便携式电子设备、储能设备以及电动车的驱动中。而锂离子电池电极材料的发展并不均衡,其中正极材料的发展相对滞后,成为制约锂离子电池整体性能进一步提高的关键因素之一。近年来报道的以橄榄石型 LiFePO₄ 为代表的聚阴离子型锂离子电池正极材料具有良好的性能,因而引起了人们的广泛关注^[1]。到目前为止,大部分研究聚焦在由 SO₄²⁻、PO₄³⁻ 或 SiO₄⁴⁻ 等聚阴离子组成的正极材料的电化学性能。最近, LiMBO₃ (M = Mn, Fe, Co) 硼酸盐作为锂离子电池正极材料也吸引了一定的

收稿日期: 2014 - 10 - 30

基金项目: 湖南省自然科学基金(12JJ2022); 湖南省教育厅资助科研项目(14A052)

通信作者: 唐安平(1969 -), 男, 湖南洞口人, 博士, 副教授, 主要从事新型化学电源及其电极材料研究。E-mail: anpingxt@126.com

PCL/MDI/DEG 体系聚氨酯水凝胶的 制备及其亲水性能

向柳姣, 周智华, 张金芝, 严 画, 黄慧华, 何思良

(湖南科技大学 化学化工学院, 理论有机化学与功能分子教育部重点实验室, 湘潭 411201)

摘 要: 以聚己内酯(PCL)和二苯基甲烷二异氰酸酯(MDI)等为主要原料, 分别采用二甘醇(DEG)、(2, 2-二羟甲基丙酸(DMPA)、N-甲基二乙醇胺(MDEA)作为扩链剂合成聚氨酯预聚体, 然后加入交联剂过氧化苯甲酰(BPO)进行自由基聚合, 制备 PCL/MDI/DEG 新型聚氨酯水凝胶。研究扩链剂种类以及扩链剂 DEG 用量对聚氨酯水凝胶接触角、溶胀度、形貌等的影响, 并研究扩链剂对聚氨酯水凝胶载氯霉素性能的影响。结果表明, 以 DEG 为扩链剂制备的聚氨酯水凝胶亲水性最差, 材料表面孔隙较少, 氯霉素载药量最小, 但前期药物释放速率比其它 2 种扩链剂制备的水凝胶更快。而以带有羧基的 DMPA 和带有叔氨基官能团的 MDEA 为扩链剂制备的聚氨酯水凝胶, 亲水性较强, 表面具有微孔结构, 氯霉素载药量较大。随扩链剂 DEG 用量增加, 聚氨酯水凝胶的溶胀度增大, 接触角逐渐减小, 表面形貌无明显变化。

关键词: 聚氨酯; 二苯基甲烷二异氰酸酯; 聚己内酯; 二甘醇; 亲水性; 药物释放

中图分类号: TQ 317.2

文献标识码: A

文章编号: 1673-0224(2015)5-788-07

Preparation and hydrophilicity of polyurethane hydrogel based on PCL/MDI/DEG

XIANG Liu-jiao, ZHOU Zhi-hua, ZHANG Jin-zhi, YAN Hua, HUANG Hui-hua, HE Si-liang

(The Key Laboratory of Theoretical Organic Chemistry and Function Molecule of Ministry of Education, School of Chemistry and Chemical Engineering, Hunan University of Science and Technology, Xiangtan 411201, China)

Abstract: A series of polyurethane (PU) prepolymers based on diphenyl-methane-diisocyanate (MDI) and polycaprolactam (PCL) were synthesized using diethylene glycol (DEG), dimethylolpropionic acid (DMPA) and methylolpropanolamine (MDEA), respectively, as the chain-extender, then the polyurethane hydrogels were obtained from the prepolymers using benzoyl peroxide (BPO) as crosslinking agent by free radical polymerization synthesis. The influences of the kind and the amount of chain-extender on the contact angle, swelling ratio and morphology of polyurethane hydrogel were investigated, and the influence of the kind of chain-extender on the release of chloramphenicol in polyurethane hydrogel were also studied. The results show that the polyurethane hydrogel, using DEG as chain-extender, is preferably hydrophobic with no micropore on its surface, and the loading efficiency of chloramphenicol is the lowest; However, the release speed of chloramphenicol is quicker than the hydrogel prepared by DMPA and MDEA. The polyurethane hydrogel, using DMPA and MDEA as chain-extenders, has higher hydrophilicity and microporous structure on their surfaces due to their functional groups, and the loading efficiencies of chloramphenicol are higher. The swelling ratio of PCL/MDI/DEG hydrogel increases and the contact angle decreases with increasing amount of DEG; however, the surface morphology has no obvious change.

Key words: polyurethane; diphenyl-methane; polycaprolactone; diglycol; hydrophilicity; drug release

基金项目: 国家自然科学基金资助项目(51273062); 湖南省自然科学基金青年人才培养重点联合基金资助项目(12JJA003); 湖南省教育厅青年项目(11B045); 湖南科技大学研究生创新基金资助项目(S140033)

收稿日期: 2014-10-14; 修订日期: 2014-12-11

通讯作者: 周智华, 教授, 博士。电话: 86-731-58291379; E-mail: zhou7381@126.com

电还原氧化石墨烯-铁氰化钴修饰电极对胍的测定

李春香, 邱喜阳, 周建红, 令玉林, 邓克勤*

(理论有机化学与功能分子教育部重点实验室, 湖南科技大学化学化工学院, 湖南湘潭 411201)

摘 要: 本文提出了一种新的水合胍的测定方法。利用静电作用, 在氧化石墨烯(GO)表面吸附一层均匀分散的 Co^{2+} 形成 GO-Co^{2+} 复合物, 通过恒电位法电还原复合物中的 GO, 再利用循环伏安法将吸附的 Co^{2+} 转化为铁氰化钴(CoHCF), 制得电还原的氧化石墨烯-铁氰化钴修饰玻碳电极(ERGO- CoHCF/GCE)。采用扫描电子显微镜(SEM)对修饰电极表面进行了表征。研究了水合胍在该修饰电极上的电化学反应及在不同电极上的电流响应。结果表明: ERGO- CoHCF/GCE 对胍具有很好的电催化氧化作用, 其浓度与氧化峰电流呈良好的线性关系。

关键词: 铁氰化钴; 氧化石墨烯; 胍; 电化学

中图分类号: O657.1

文献标识码: A

文章编号: 1006-6144(2015)04-475-04

胍又称联氨, 是一种强还原剂, 被广泛应用于化工、医药、航天和军事等领域。但胍对人体的血液及神经系统均有毒害, 为公认的致癌物质, 也是重要的环境污染物之一^[1]。因此, 建立胍的高灵敏测定方法十分重要。目前, 胍的检测方法主要有色谱法^[2]、流动注射分析法^[3]、分光光度法^[4]、化学发光法^[5]及电化学方法^[6,7]等。

金属铁氰化物(Metal Hexacyanoferrates, MHCF)是一类重要的混合价态金属化合物, 作为电子传递介质具有良好的电化学可逆性和高度的稳定性。胍在普通电极上的氧化过电位均较高, 而采用金属铁氰化物及其它过渡金属络合物修饰的电极, 均能不同程度地降低胍的氧化过电位, 提高检测的灵敏度^[7,8]。本文以氧化石墨烯(GO)作为电化学合成石墨烯的前驱体, 利用 GO 表面丰富的含氧基团, 通过静电作用在其表面吸附一层均匀分散的 Co^{2+} , 再通过恒电位法还原 GO, 然后利用循环伏安(CV)法, 把吸附的 Co^{2+} 转化为铁氰化钴(CoHCF), 制得电还原的氧化石墨烯-铁氰化钴修饰玻碳电极(ERGO- CoHCF/GCE), 并研究了胍在该修饰电极上的电化学反应及检测方法。

1 实验部分

1.1 仪器与试剂

CHI 760C 电化学工作站(上海辰华), 三电极系统: 修饰的玻碳电极(GCE)为工作电极, 饱和甘汞电极为参比电极, 铂电极为对电极。JSM-5610L 型扫描电子显微镜(SEM)(日本, JEOL 公司); KQ50E 型超声波清洗器(昆山市超声仪器有限公司)。

水合胍($\text{N}_2\text{H}_4 \cdot \text{H}_2\text{O}$), $\text{K}_3\text{Fe}(\text{CN})_6$, CoCl_2 , 高纯石墨粉, 均购于上海化学试剂厂。其他试剂均为分析纯, 实验用水为二次蒸馏水

1.2 GO 和吸附 Co^{2+} 的 GO-Co^{2+} 的合成

GO 采用 Hummers 和 Offeman 法^[9]制备, 然后将其分散于水中透析纯化 3 d, 超声处理 60 min, 取上

收稿日期: 2014-07-07 修回日期: 2014-09-17

基金项目: 国家自然科学基金(No. 21471052); 湖南省科技计划(No. 2014FJ3048); 湖南省教育厅资助项目(13C303); 教育部重点实验室开放课题(No. LKF1306)

* 通讯作者: 邓克勤, 男, 博士, 讲师, 研究方向: 分析化学。

文章编号: 1004-1656(2015)10-1531-08

One-pot synthesis and fungicidal activity of *N1,N3*-dialkylated 3,4-dihydropyrimidin-2(1*H*)-ones

ZENG Rong-jin^{1,2*}, LIU Chuan-lei^{1,2}, SHEN Peng-fei^{1,2,3}, TANG Sha^{1,2}, XIONG Chung-ang^{1,2}, WU Xiang-si^{1,2}

(1. School of Chemistry and Chemical Engineering, Hunan University of Science and Technology, Xiangtan 411201, China;

2. Key Laboratory of Theoretical Chemistry and Function Molecule of Ministry of Education, Hunan University of Science and Technology, Xiangtan 411201, China;

3. School of Chemistry and Chemical Engineering, Hunan Normal University, Changsha 410012, China.)

Abstract: A series of novel *N1,N3*-dialkylated 3,4-dihydropyrimidin-2(1*H*)-ones were synthesized under mild phase transfer catalyst (PTC). Their fungicidal activities against *Botrytis cinerea*, *Gibberella zeae*, *Phytophthora capsici*, *Sclerotinia sclerotiorum*, *Rhizoctonia solani* and *Pyricularia oryzae* were investigated. Most of the *N1,N3*-dialkylated DHPMs **4** had high fungicidal activities against the five latter, especially the compounds with the substituents ($R_3 = (CH_2)_nBr$) exhibited excellent fungicidal activities against *Sclerotinia sclerotiorum*, *Gibberella zeae* and *Phytophthora capsici*. The studies of all the compounds revealed the advantages of substituents on the pyrimidine and the ester group ($R_2 = CH_2CH_3$ and $R_3 = (CH_2)_nBr$) to the fungicidal activity.

Key words: *N1,N3*-dialkylation; 3,4-dihydropyrimidin-2(1*H*)-ones; solvent-free; phase transfer catalysis; fungicidal activity

一锅法合成 *N1,N3*-二烷基取代-3,4-二氢嘧啶-2(1*H*)-酮及其抗菌活性研究

曾荣今^{1,2*}, 刘传磊^{1,2}, 沈鹏飞^{1,2,3}, 唐沙^{1,2}, 熊春刚^{1,2}, 吴湘思^{1,2}

(1. 湖南科技大学化学化工学院, 湖南湘潭 411201,

2. 湖南科技大学理论有机化学与功能分子教育部重点实验室, 湖南湘潭 411201,

3. 湖南师范大学化学化工学院, 湖南长沙 410012)

摘要: 在温和的相转移催化剂存在下, 合成得到一系列 *N1,N3*-二烷基取代-3,4-二氢嘧啶-2(1*H*)-酮, 并测定了取代二氢嘧啶酮对灰霉菌、小麦赤霉菌、辣椒疫霉菌、油菜菌核病菌、水稻纹枯病菌、稻瘟病菌六种霉菌的抗菌活性。多数取代二氢嘧啶酮对后五种霉菌体现出不错的抗菌活性, 特别是 N 原子上被 $(CH_2)_nBr$ 取代的二烷基取代二氢嘧啶酮对于油菜菌核病菌、小麦赤霉菌以及辣椒疫霉菌表现出不错的抗菌活性。数据表明, 二氢嘧啶酮中嘧啶环和酯基上的取代基变化有助于改善嘧啶酮的抗菌活性。

关键词: *N1,N3*-二烷基取代; 3,4-二氢嘧啶-2(1*H*)-酮; 无溶剂; 相转移催化; 抗菌活性

中图分类号: O626.41 文献标志码: A

Over the past decades, the pyrimidine moiety had attracted immense attention of chemists because

收稿日期: 2015-03-11; 修回日期: 2015-06-08

基金项目: 国家自然科学基金项目(20942008, 21172065)资助; 湖南省高校创新平台开放基金项目(11K024)资助

联系人简介: 曾荣今(1963-), 男, 教授, 主要从事有机合成。E-mail address: rjzeng@hnust.cn